2021

Synthesis of Dual Small Molecule Hybrids to Probe the Synergy between DNA Repair Enzymes and IDO1

Nathaniel George
University of Kentucky, nathaniel.george2@gmail.com
Author ORCID Identifier:
https://orcid.org/0000-0002-3410-2799
Digital Object Identifier: https://doi.org/10.13023/etd.2021.174

STUDENT AGREEMENT:

I represent that my thesis or dissertation and abstract are my original work. Proper attribution has been given to all outside sources. I understand that I am solely responsible for obtaining any needed copyright permissions. I have obtained needed written permission statement(s) from the owner(s) of each third-party copyrighted matter to be included in my work, allowing electronic distribution (if such use is not permitted by the fair use doctrine) which will be submitted to UKnowledge as Additional File.

I hereby grant to The University of Kentucky and its agents the irrevocable, non-exclusive, and royalty-free license to archive and make accessible my work in whole or in part in all forms of media, now or hereafter known. I agree that the document mentioned above may be made available immediately for worldwide access unless an embargo applies.

I retain all other ownership rights to the copyright of my work. I also retain the right to use in future works (such as articles or books) all or part of my work. I understand that I am free to register the copyright to my work.

REVIEW, APPROVAL AND ACCEPTANCE

The document mentioned above has been reviewed and accepted by the student's advisor, on behalf of the advisory committee, and by the Director of Graduate Studies (DGS), on behalf of the program; we verify that this is the final, approved version of the student's thesis including all changes required by the advisory committee. The undersigned agree to abide by the statements above.

Nathaniel George, Student

Dr. Samuel G. Awuah, Major Professor

Dr. Yinan Wei, Director of Graduate Studies

Synthesis of Dual Small Molecule Hybrids to Probe the Synergy between DNA Repair Enzymes and IDO1

THESIS

A thesis submitted in partial fulfillment of the
requirements for the degree of Master of Science in the
College of Arts and Sciences
at the University of Kentucky

By

Nathaniel Hugh George

Lexington, Kentucky

Director: Dr. Samuel G. Awuah, Professor of Chemistry

Lexington, Kentucky

2021

https://orcid.org/0000-0002-3410-2799

ABSTRACT OF THESIS

Synthesis of Dual Small Molecule Hybrids to Probe the Synergy between DNA Repair Enzymes and IDO1

Indoleamine 2 3-dioxygenase (IDO) has recently been highlighted as a promising target for small molecule based immunotherapy. IDO is often coopted by various cancer cells to promote an immune-suppressive environment around tumors. DNA damage repair (DDR) enzymes have recently been targeted for inhibition to promote genetic instability and bolster immune recognition. DDR enzymes such as PARP and POLγ are common inhibition targets due to their direct effects on cellular function. In the process of designing conjugate inhibitors of IDO and DDR enzymes, novel synthetic methodology was developed for the mild deprotection of *N*-Tert-butyloxycarbonyl (N-BOC) group from various amines. Conjugate inhibitors of IDO and PARP were synthesized using the parent molecules 1-MLT and Olaparib. The conjugate molecules showed more potent cytotoxicity in various cancer cell lines than their precursor molecules. The novel conjugate inhibitors could be used as probes to explore interplay between the PARP and IDO signaling pathways and elucidate any synergy or dependency between the two enzymes.

KEYWORDS: Cancer, DNA Damage Repair, IDO, Inhibitors, Small Molecules, Synthetic Methodology

Nathaniel Hugh George
(Name of Student)

01/18/2021
Date

Synthesis of Dual Small Molecule Hybrids to Probe the Synergy between DNA Repair Enzymes and IDO1

By

Nathaniel Hugh George

Dr. Samuel G. Awuah

Director of Thesis

Dr. Yinan Wei

Director of Graduate Studies

01/18/2021

Date

DEDICATION

To *Gabriel George, Cheryl Page, and Charles George.*
Thank you for always believing in me!

ACKNOWLEDGMENTS

The following thesis, benefited from the insights and direction of several people. First, my Thesis Chair, Dr. Samuel G. Awuah, provided guidance, encouragement, and a level of scholarly acumen that I aspire to achieve. I would not have made it through this degree without his expert advice and direction. I would also like to thank Dr. Mark Watson, who constantly provided instructive comments and ideas throughout my research efforts. I would like to thank Dr. Sean Parkin, who provided expertise and assistance with obtaining crystallography data throughout my research project. I would also like to thank the UKY NMR center for NMR access and for their help throughout my degree. Next, I wish to thank the complete Thesis Committee: Dr. Samuel Awuah, Dr. Mark Watson, and Dr. Jason DeRouchey. Each member of my committee provided insights that guided and challenged my thinking.

I would like to thank my lab mate Sam Ofori. Sam provided a ton of support and advice for many of my synthetic and biological projects and I will be forever grateful. My other lab mates Sailajah Gukathasan and Tyler Mertens also played a large role in my success and were helpful throughout my time in the Awuah lab. I want to thank our postdoc, Dr. Jong Kim, who was a valuable source of knowledge, emotional, as well as academic support. My Friend Trever Ferguson was a constant source of support throughout my degree. I'd like to acknowledge my brother, Gabriel, and parents, Charles and Shelly, who always supported me and believed in me even when I barely believed in myself. Thanks to everyone else who supported me and encouraged me throughout my degree process.

TABLE OF CONTENTS

ACKNOWLEDGMENTS iii

TABLE OF CONTENTS iv

LIST OF TABLES vi

LIST OF FIGURES vii

LIST OF SCHEMES viii

CHAPTER 1. .....Indoleamine 2,3-dioxygenase as a target for Immunomodulation in the Tumor Micro-Environment 1

1.1 IDO and Cancer 1

1.2 IDO's multiple roles and effects 3

1.3 Effector Pathways 5

1.3.1 GCN2 6

1.3.2 MTORC1 7

1.3.3 AHr 8

1.4 Induction of IDO 9

1.5 Chemical Conversion of Tryptophan 10

1.6 IDO1 Inhibitors 11

1.7 IDO inhibition in the clinic 15

1.8 DNA Repair Mechanisms as targets for Immunotherapy. 16

1.9 Future Prospects and Experimental Aims 17

1.10 Experimental aims: Discovering the interplay between IDO and DNA Repair mechanisms 19

CHAPTER 2. ..... Mild Deprotection of N-tert-butyloxycarbonyl (N-Boc) Group Using Oxalyl Chloride 21

2.1 Rationale 21

2.2 Introduction 21

2.3 Results and Discussion 24

2.4 Determination of HCl effectiveness in Deprotection 30

2.5 Proposed Mechanism 32

2.6 Experimental Procedures 34

CHAPTER 3. .....Synthesis of small molecule inhibitors for novel immunotherapy treatments 47
3.1 Introduction..... 47
3.2 Synthetic Methodology..... 48
3.3 Future Directions 52
3.4 Experimental Procedures: 53
CHAPTER 4. ..... Cellular Analysis of Small molecule PARP-IDO inhibitors 58
4.1 Introduction..... 58
4.2 Results and Discussion 58
4.3 Future Directions 62
4.4 Experimental Procedures 63
APPENDIX : Selected spectra of Final Compounds 65
REFERENCES 73
Vita 89

LIST OF TABLES

TABLE 2.1 OPTIMIZATION OF DEPROTECTION USING N-BOC-1-NAPHTHYLAMINE-AMINE .. 25
TABLE 2.2 DEPROTECTION OF STRUCTURALLY DIVERSE N-BOC-AMINES 26
TABLE 4.1 CYTOXIC EFFICACY OF CONJUGATE INHIBITORS ON CELL VIABILITY OF OVCAR8 62

LIST OF FIGURES

FIGURE 2.1 CONJUGATE INHIBITOR OF IDO AND POLΓ (FC1) 21
FIGURE 3.1 TARGET INHIBITORS OF IDO, DNA POLYMERASE Γ, AND PARP 48
FIGURE 4.1 CYTOXIC EFFICACY OF CONJUGATE INHIBITORS ON CELL VIABILITY OF MDA-MB-231 59
FIGURE 4.2 CYTOXIC EFFICACY OF CONJUGATE INHIBITORS ON CELL VIABILITY OF HCC-1937 60
FIGURE 4.3 CYTOXIC EFFICACY OF CONJUGATE INHIBITORS ON CELL VIABILITY OF A549 . 60
FIGURE 4.4 CYTOXIC EFFICACY OF CONJUGATE INHIBITORS ON CELL VIABILITY OF OVCAR8 61

LIST OF SCHEMES

SCHEME 2.1 GENERAL DEPROTECTION REACTION SCHEME 25
SCHEME 2.2 SYNTHESIS OF 5 (FC1) VIA OXALYL CHLORIDE-MEDIATED DEPROTECTION OF 4 (EC1). THE X-RAY OF EC1 IS DRAWN AT 50% THERMAL ELLIPSOID. SOLVENT MOLECULES WERE REMOVED FOR CLARITY. 28
SCHEME 2.3 PROPOSED MECHANISM OF OXALYL-CHLORIDE MEDIATED DEPROTECTION OF N-BOC GROUP. 32
SCHEME 3.1 SYNTHESIS OF IDO-PARP CONJUGATE INHIBITOR MOLECULES 49
SCHEME 3.2 SYNTHESIS OF POLΓ-PARP CONJUGATE INHIBITOR MOLECULES 51
SCHEME 3.3 SYNTHESIS OF INCB14943 52

CHAPTER 1. INDOLEAMINE 2,3-DIOXYGENASE AS A TARGET FOR IMMUNOMODULATION IN THE TUMOR MICRO-ENVIRONMENT

1.1 IDO and Cancer

Indoleamine 2,3-dioxygenase (IDO) has recently become a high profile target for immunotherapy in the fight against multiple types of cancer. Though often viewed as an immunosuppressing enzyme that modulates the adaptive immune system, IDO has been shown to be involved in the early stages of inflammation[1]. IDO's immunomodulatory role varies between different types of cells, cancers, and pathogenic microenvironments, making it's eventual effects hard to predict as well as unique to that particular environment[1-3]. Recent clinical trials have aimed to use small molecule inhibitors as a monotherapy or coupled with immune checkpoint antibodies and vaccines to target tumors prone to immune escape[4]. Though initial trials showed tumor reduction and promising response to IDO inhibition and combination therapy, recent failures in stage III clinical trials of pioneering IDO small molecule inhibitor therapies have left the field second guessing the efficacy of targeting IDO[5, 6]. Despite recent setbacks, IDO remains a key immunomodulatory enzyme that with further research could become a very useful tool in the fight against cancer. This introduction aims to summarize the method of action, current clinical targets, and in particular the potential hurdles and difficulties involved with tuning the immune response via IDO inhibition.

IDO is an heme containing enzyme that catalyzes the rate limiting step in the conversion of cellular tryptophan to kyurenine[7]. Tryptophan catabolism was first observerd to be elevated in cancer patients as early as the 1950's. Munn, Mellor, and colleagues first described the active immune suppressive role of IDO in suppressing T-cell mediated

rejection of fetuses during pregnancy[8]. These discoveries led to the investigation of IDO's role in the immune escape of tumors as well as autoimmune disorders and graft tolerance following transplantation[9]. IDO was shown to be expressed within the tissue of multiple different types of cancers as early as 2003 and multiple subsequent studies found a correlation between poor patient prognosis and limited lymphocyte migration to and infiltration of the tumor microenvironment[10-13]. It's overexpression and activity have been studied in numerous types of gynecological cancers such as ovarian, vulvar, and cervical carcinomas[14].

IDO is commonly overexpressed in tumor milieu[15]. This overexpression characteristic varies between tissue and cell types and can cause varying outcomes[15, 16]. Overexpression of IDO has been correlated to a poor patient prognosis, indicating the large role IDO plays in tumor immune escape[17]. Within dendritic cells (DC), IDO has been found to be overexpressed near the edge of the inflammatory tissue microenvironment as well as within tumor draining lymph nodes (TDLN)[9, 18]. IDO is commonly found in multiple types of healthy epithelial cells as well as epithelial cells within the inflamed tumor milieu. Initial theories held that IDO was induced upon inflammation and acted as an adaptive immunosuppressive molecule. This theory is further supported by the fact that interferon gamma (INFγ), TGFβ, and various TLR ligands have been shown to upregulate IDO expression and activity with INFγ being the strongest inducer of IDO. Increased IDO expression within the tumor environment is also often due to mutations in the BIN-1 gene, a tumor suppressor gene that is commonly inactive or mutated in cancer cells[19]. Within the inflamed tumor environment IDO acts to suppress T-cell response and promote T-cell anergy through multiple methods. Downstream metabolites of IDO It

have been shown to inhibit the proliferation of NK cells as well as B cells[20]. Though it's role as an immunosuppressant enzyme has been studied in depth and confirmed, recent studies have shed light on the role of IDO in the early stages of tumor growth and suggest a role for the enzyme in the onset of inflammation, lymphocyte proliferation and angiogenesis within the tumor[1, 21]. A suggested role in the induction of inflammation was shown by the presence and activity of IDO in inflamed tissues in the absence of cancer cells[9]. IDO^{KO} cells also showed little response in terms of tumor formation in the absence of an inflammatory stimulant like INF-γ, showing that IDO has a multifunctional purpose in the growth and eventual immune escape of tumors[22].

1.2 IDO's multiple roles and effects

Outside of the cancer realm IDO is involved in immune system modulation throughout various organs. The complex signaling and effector pathways involving IDO often vary between different organ systems. In certain autoimmune diseases increased IDO function can promote tolerance and reduce inflammation. Peripheral autoreactive memory T cells show a decrease and eventual long-term cessation of multi-organ inflammation after INF-γ stimulated induction of IDO by host APC's[23]. In other autoimmune environments epithelial cells induce IDO to reign in autoreactivity. In allergic airway disease, inflammation triggered by activation of TLRs is suppressed by induction of IDO within the inflamed environment[24]. IDO has been implicated as a target for diseases such as Asthma, Atopy, and Graft verses Host Disease, in each case being induced to promote tolerance or reduce inflammatory cell functions[25-30]. Other scientist have explored inducing IDO overexpression or increasing IDO activity in an attempt to promote immune tolerance to various drugs[31, 32].

Aberrant function of IDO has been implicated in multiple forms of virus-derived inflammatory diseases. IDO activity has been shown to play a role in Hepatitis C mediated cirrhosis of the liver, though the exact mechanism is only partially understood. The critical role of CD4+ T cells in the removal of the virus is hindered by IDO overexpression within hepatic cells. Similar to its role in cancer progression and tumor immune escape, the concurrent blunting of CD4+ cells and proliferation of Treg cells produces and state of chronic infection leading to cirrhosis[33]. Hepatocellular carcinoma experiences a tolerance profile similar to that of HCV induced cirrhosis, and is often induced by chronic HCV and HCB infection[34]. IDO-KO mice further highlighted the tolerance promoting properties of IDO when it was observed that the IDO knockout mice fed a high fat diet experience higher infiltration of macrophages and T-lymphocytes into the white adipose tissue within the liver, eventually leading to fibrosis of the liver tissue[35]. Advanced human atherosclerotic plaque progression has also been linked to IDO mediated degradation of tryptophan with the root cause being and increase in macrophage infiltration of atheromatous core coupled with increased FOXp3 T-reg cell function and APC expression of more IDO[36].

A study in 2014 established a link between IDO and PARP in DNA repair and immune response to the tumor environment[37]. The researchers found that IDO mediated an immune independent tolerance to Oliparib, a small molecule PARP inhibitor, through modulation of downstream metabolites like NAD+[37, 38]. The kynurenine pathway is one of two mechanisms within the cell for production of NAD+, which is vital to PARP DNA repair activities[37].

Endometrial cancer patients with higher expression levels of IDO experienced greater tumor progression and poor clinical outcome[39]. In a clinical trial of colorectal cancer patients high IDO expression was linked with decreased tumor infiltration of CD3+ Tcells and poor survival rates[40].

1.3 Effector Pathways

IDO suppresses immune response and promotes immune escape of tumors through three main effector pathways[41, 42]. Depletion of cytosolic tryptophan leads to an increase in uncharged tRNA levels which begins a signaling pathway mediated by phosphorylation of the initiation factor EIF-2α by the stress response kinase GCN2[43]. mTORC1 mediates cellular transcription in response to stimulation by growth factors or critical amino acid concentration levels[1, 7, 44]. The AHr is activated by downstream metabolites of tryptophan as well as other substrates and initiates cell signaling pathways that either stimulate regulatory t-cell function or perturb cytoxic T-cell function proliferation within the tumor environment[45, 46]. These three pathways account for the most investigated modes of action of IDO. While IDO action has been shown to play a role in other immune system regulatory pathways, they have not been investigated in depth and usually have not been investigated in multiply types of cancer. All three of these regulatory pathways are also hijacked by tumors and exploited to achieve immune escape in the absence of IDO overexpression.

1.3.1 GCN2

The general control nonderepressible 2 kinase (GCN2) acts as an effector pathway for IDO by dampening the response of T cells within the tumor microenvironment. IDO, when active, reduces cellular tryptophan levels as well as tryptophan within the local tissue microenvironment. GCN2 primarily limits protein translation in nutrient deprived tissue but does upregulate the transcription factor LIP which in turn increases expression of NF-kβ, CHOP, and INFγ receptor while simultaneously decreasing production of IL-6, In a negative feedback loop fashion. GCN2 is activated by binding to uncharged tRNA in amino acid starved cells[47]. Upon activation, GCN2 phosphorylates serine 51 on eIF2α, restricting translation within the cell and leading to arrest, apoptosis and anergy of CD-8+ T-cells[48]. GCN2 activation leads to cell cycle arrest within CD-8^+ T cells[43, 49] while simultaneously promoting differentiation of immature CD-4^+ T-cells into regulatory T-cells[50] and activating immuno-suppressive activity in mature Treg cells[51]. IDO therefore causes suppression of the immune system when overexpressed by tumor cells. Though GCN2 blunts the translation of most mRNA it does increase the translation of others and leads to an increase in production of IL-6 the anti-inflammatory cytokine. Some have argued that GCN2 is not the predominate force driving effector T cell non-proliferation during amino acid starvation and is also dispensable in exocellular amino acid sensing by T-cells[47, 52]. Therefore there is disagreement in the literature on whether or not IDO actually suppresses immune response via GCN2 due to the fact that $GCN2^{KO}$ mice show no symptoms of autoimmunity[53]. These discrepancies could play a crucial role in why IDO inhibition does not always cause the intended effects on the tumor milieu.

1.3.2 MTORC1

The master metabolic regulator (mTORC1) works in an opposite mode of action to GCN2. While tryptophan depletion activates GCN2, mTORC1 normal cellular response is inhibited during cellular stress and lack of nutrients. Normally mTOR functions when amino acids are sufficient, phosphorylating transcription regulators like S6K1 and 4EBP1[54]. Depleting amino acids within the tumor milieu allows GCN2 and mTORC1 to work in concert, with GCN2 restricting transcription due to its activation and mTORC restricting transcription due to its deactivation. As tryptophan is depleted due to IDO function, mTOR is repressed which can lead to autophagy[55]. Some of the signaling pathways that report amino acid deficiency to mTOR also are involved in activation of and signaling to protein kinase C-θ (PKC-θ), which is involved in T cell receptor regulation[56].

mTORC1 and mTORC2's roles have been implicated in cancer apart from the downstream affects of IDO[57]. mTORC1 is unique in the sense that it receives nutrient level signals as well as growth factor signals whereas mTORC2 only receives growth factor signals[58, 59]. mTORC1 is constitutively expressed due to a multitude of different oncogenes in various cancers[59]. Deregulation of mTORC1 function is found in nearly 80% of cancers and the underlying cause often has nothing to do with increased IDO induction. That being said, inhibition of mTORC1 in multiple clinical trials by rapamycin or other inhibitors has not been shown to be effective in reducing tumor size. The findings of multiple studies show that while mTORC1 obviously plays a major role in Tumor immune escape and growth, it works in concert with other signaling pathways to exact this effect. The cross talk between the mTOR and GCN2 effector pathways of IDO

has not been studied in depth and continued investigation in this area could shed light other mechanisms of suppression as well as how tumor cells circumvent inhibition of IDO.

1.3.3 AHr

The aryl hydrocarbon receptor (AHr) is activated by Kynurenine, the product of IDO metabolization of tryptophan[46, 60]. AHr function promotes the differentiation of naïve CD4+ cells into forkhead box P3-positive ($FOXP3^{+}$) Tregs while simultaneously repressing the production of TH17 cells[61, 62]. Binding of Kynurenine to AHR also leads to anergy of other effector T cells[63]. Upon activation, AHR travels to the nucleus where it works as a transcription factor inducing multiple immune suppressing genes[63]. Increased activity of AHr reduces T cell migration to the tumor microenvironment as well as blunts T-cell proliferation[63]. AHr has been shown to be constitutively expressed in multiple tumor cells[64]. Combined with an increase in IDO function, this heightened expression causes strong modulation of immune response and suppression of effector cells[65]. AHr studies in mouse models revealed that an AhR deficiency often led to autoimmunity whereas the constitutive expression of AhR can promote tumorigenesis[66].

The role of AHr in cancer is not strictly confined to regulation of immune response, and has been implicated in tumor cell proliferation, angiogenesis and metastasis as well[66-68]. Kynurenine is not the only ligand that can activate the AHr's immune-modulatory functions and different types of cancers hijack the AHr's functions through various mutations[69]. Multiple other ligands such as 2,3,7,8-tetrachlorodibenzo-*p*-dioxin (TCDD), 6-formylindolo[3,2-b]carbazole (FICZ), and 2-(1′H-indole-3′-carbonyl)-thiazole-4-carboxylic acid methyl ester (ITE) also have strong affinity for AHr[66, 70]. A common

theme between all three effector pathways of IDO is the fact that different malignancies coopt the same immuno-regulatory pathways through different mechanisms. It is also not uncommon for a cancer cells to manipulate a specific cellular function through multiple mechanisms, making inhibition of a singular upstream pathway with the intended result being a loss of AHr function or upregulation ineffective.

1.4 Induction of IDO

IFN-γ is the most common inducer of IDO within antigen presenting cells (APC). IFN-γ mediates IDO expression through the Janus Kinase (JAK)/ signal transducer and activator of transcription (STAT) pathway[71]. The induction of IDO can be further potentiated by addition of other inflammatory cytokines and soluble molecules such as TNF-α, IL-10, and IL-1β[41, 71]. IDO has been shown to both increase production of IL-6 through an AHr mediated pathway, and be induced by IL-6 signaling within the cell, indicating a self-sustaining loop for IDO expression[69]. Different types of Dendritic cells and macrophages respond to different stimuli when it comes to the induction of IDO. For example, IFN-γ promotes CD8+ DC's mediated inhibition of CD8- DC antigen presentation and blocks it's response to IL-12 stimulation but has no effect on CD8- DCs in the absence of their CD8+ counterparts[72]. Because an assortment of genes commonly called IFN-stimulated genes(ISGs) can stimulate both immunity and tumor specific tolerance, IDO expression is often upregulated in response to beneficial inflammation[73] but can also be upregulated due to tumor promoting chronic inflammation[74]. Induction of IDO within the tumor environment can come from a plethora of different stimuli as well as cells. Within monocyte derived dendritic cells and some other APC's, PGE2 induces expression of IDO via a signaling pathway through the EP2 receptor which activates PKA[75]. This

signaling pathway is only efficient in inducing IDO expression when combined with a TLR antagonist or substrate binding to the TNF-R[75].

A few different IDO regulatory pathways have been investigated through the literature. iNOS which is also activated upon INF-γ stimulation, produces nitric oxide, a direct inhibitor of IDO[76]. NO not only inhibits IDO function but leads to degradation of cellular IDO through a proteasome mediated mechanism[76]. Intracellular SOCS3 has been shown to bind to IDO and signal the complex for ubiquitinization also resulting in proteasome mediated degradation[77]. SOCS3 also functions to limit the tolerogenic functions of IDO. In some cancers migration of lymphocytes to the tumor milieu can induce expression of IDO. INF-γ stimulates IDO upregulation, CTLA-4 expression, and recruitment of FOXP3 regulatory T-cells to the tumor environment after infiltration of cytoxic T-cells[78]. This event indicates a reactionary role of multiple immuno-suppressive effector molecules after an increase in inflammation mediated by normal immune system function as opposed to tumor cells coopting tolerogenic mechanism for immune escape[78]. Inhibition of IDO with 1-methyl-*D*-Tryptophan actually stimulates increased expression of IDO in an attempt to reduce chronic inflammation.

1.5 Chemical Conversion of Tryptophan

IDO is a monomeric heme-containing enzyme that catalyzes the oxidative cleavage of L-tryptophan to Kynurenine[60]. In 2006 the crystal structure of the IDO molecule complexed with its ligand was published and a mechanism of action was proposed[79]. Proton extraction by the dioxygen species attached to the iron center of the heme ring is followed by oxidative cleavage of the alkene located on the pyrole ring of

the indole moiety. IDO initially converts L-tryptophan into N-formal-L-kynurenine, while Formamidase then catalyzes the conversion of N-formal-L-kynurenine to L-kynurenine, which is the substrate molecule for multiple immunoregulatory pathways[79-81]. Kynurenine can then be further converted into multiple different downstream metabolites that each play important roles within the cell. The kynurenine pathway is the de-novo pathway for the production of NAD+ within the cell, which is a key metabolite involved in many redox reactions within the cell[61, 80]. Critical enzymes like PARP require NAD+ for its DNA damage repair mechanism[82].

The inhibition of IDO can be accomplished by either competitive inhibition of the IDO enzyme or inhibition of downstream enzymes within the kynurenine pathway. Though IDO1 and IDO2 catalyze the conversion of tryptophan, IDO2 is less active in tryptophan conversion and has tighter substrate restrictions[80, 83]. TDO is similar in activity to IDO[81], but lacks structural homology and is found primarily in the liver and brain whereas IDO1 is found in multiple different types of peripheral tissues and cells[80]. For the purposes of this review only inhibition of the IDO1 enzyme will be discussed.

1.6 IDO1 Inhibitors

In the past two decades, a host of different small molecule IDO1 inhibitors have been discovered with some compounds having IC_{50} values in the low nanomolar range[84]. Early inhibitors of IDO1 were derivations of tryptophan maintaining the indole core[85]. 1-methyl-L-Tryptophan and its enantiomer are probably the most studied tryptophan derivatives[54, 85, 86]. Though Its binding affinity to the IDO active site and inhibitory affects are relatively weak compared to some other inhibitors, Its binding modes were

characterized early and it has been used to probe IDO signaling through the AHr and the MTORc[54, 87]. While trying to inhibit IDO activity using 1MDT, researchers surprisingly discovered that 1MDT can stimulate expression of IDO, a counterproductive result that is particularly relevant to many other IDO inhibitors currently in clinical trials[88]. The IDO inhibitor 5-((1*H*-indol-3-yl)methyl)-3-methyl-2-thioximidazolidin-4-one (MTH-trp), commonly known as Necrostatin-1, has an inhibitory constant Ki of 12 μM and also exhibits pluralistic modes of action within the tumor microenvironment[19]. The compound was found to inhibit necroptosis, as well as IDO[19, 89]. Keto-indoles such as 1-(1*H*-Indol-2-yl)-2-pyridin-3-yl-ethanone produced lower micromolar IC50 values than 1MDT but have yet to be selected for clinical investigation[90]. Currently 1MDT is the only tryptophan derivative to be utilized as an IDO inhibitor in a clinical trial[91]. Many IDO inhibitors utilize the Indole core due to the fact that the natural substrate incorporates this frame[92], but lower IC50 values have been achieved through various screening methods and by utilizing different core molecules entirely[93-99].

Quinone based IDO inhibitors are another class of small molecule inhibitors that achieve low micromolar IC_{50} values. The simple quinone, menadione inhibits IDO with a K_i value of 0.58 μM, a major improvement on the inhibitory activity of all the tryptophan derivatives[100]. Further derivatization of the quinone scaffold decreased the IC_{50} values of these inhibitors, but selectivity issues plague this genre of compounds reducing their efficacy as potent IDO inhibitors[98, 101]. Simple functionalization of quinones was investigated by multiple groups with varying success. The quinone scaffold alone does not impart strong binding affinity to the IDO active site. Aminophenoxazinone derivatives seemed promising due to the reactive amino functionality added to these

analogs, but in assays, these molecules produced only modest μM inhibition of IDO[102]. Imidazole and triazole cores have also been investigated with most reaching low micromolar inhibition constants[96-98, 103, 104]. Recently, researchers have isolated some natural product inhibitors of IDO from surprising sources[101, 105, 106]. Xestolactone A, derived from the sea sponge *Xestospongia vansoesti* work as a competitive inhibitor to the IDO binding site and has acute potency. The catechin, epigallocatechin-3-gallate, inhibits IDO function by disrupting STAT1 signaling and blocking expression of IDO. Multiple groups have explored naphthoquinone and pyranonaphthoquinone derivatives as potent IDO inhibitors[107].Many of these derivatives utilize common functional groups and structural similarity to annulin B[108]. Annulin A and B were identified as natural product derived IDO inhibitors as early as 2009 and have activity on the nanomolar scale[109]. Pyranonaphthoquinone derivatives incorporating a carborane moiety were first introduced in 2014 with IC_{50} values as low as 0.78 μM[110]. Annulin A served as the parent molecule to a class of benzofuranquinone analogs. Though similar in structure to Annulin A, these derivatives exhibit surprisingly poor activity with IC50 values only reaching the millimolar range[111]. β-lapachone has been used in clinical trials as a cytoxic tumor targeting agent, but has recently been shown to be a potent IDO inhibitor as well[107].

Other IDO inhibitors incorporating varying cores have recently been identified and studied in various cell lines and assays[112]. A group of phenyl benzene-sulfonylhydrazides show high enzymatic affinity for IDO with IC_{50} values as low as 61nm in enzymatic assays and similarly low (nM range) EC50 values in HeLa cells[113]. Bromophenylhydrazinyl benzenesulfonylphenylurea derivatives were synthesized and tested within a murine CT26 model and yielded up to 30% tumor weight reduction and

25% tumor growth reduction[114]. The antihypertensive agent candesartan cilexetil was also found to potently inhibit IDO. Though candesartan is the active portion of the drug, when administered alone, it's inhibition activity was notably lower than that of candesartan cilexetil, indicating the entire structure plays a role in the inhibition of the active site[115].

Currently the most potent class of IDO inhibitors that have been studied in depth and utilized in clinical trials are the N-hydroxyamidine based inhibitors[116]. Using a high throughput screening process Incyte discovered the highly competitive inhibitor 4-amino-1,2,5-oxadiazole-3-carboximidamide, and optimized the molecule into the pharmacophore Epacadostat (INCB024360)[117-119].

Multiple groups have developed IDO targeting drugs that work in concert with other cancer drugs or DNA damaging agents. 1-methyl-*D*-tryptophan was conjugated to a platinum IV DNA damaging agent and was shown to have efficacy in cisplatin resistant cell lines[120]. The conjugate drug was more effective than solo therapy with either the DNA damage agent or the IDO inhibitor[120]. Platinum prodrugs have also been developed to target TDO, in an attempt to promote immune response within the tumor environment[121].

Tumor derived hypoxia has also been targeted by researchers looking to more selectively target cancer. Nakashima and company developed hypoxia targeting agents coupled with 1-methyl tryptophan derivatives and observed increased efficacy within multiple cell lines due to a coupling of the cytoxic activity of the hypoxic agents followed by the metabolization of the drug into potent IDO inhibitors[122].

1.7 IDO inhibition in the clinic

IDO inhibitors have routinely been tested in the clinic as a solo therapeutic, or in conjunction with or contrasted against PD1-PDL1 antibody inhibitors and/or various DNA damaging agents[123]. Table 1 summarizes the scope, drug combination, and target cancer type for most of the clinical trials investigating IDO inhibition. The three major small molecule inhibitors used in clinical trials are Indoximod, Epacadostat (incyte's N-hydroxyamidine inhibitor), and GDC-0919[98, 124]. Epacadostat has been tested in multiple phase I and II trials in combination with CTLA-4 and PD-1/PD-L1 inhibitors[124]. Epacadostat has been shown to promote CD-8+ T cell and NK-cell proliferation and migration to the tumor milieu as well as suppress conversion of naïve T-cells into Treg cells[117, 125, 126]. GDC-0919 in combination with chemotherapy promotes an increase in complement deposition due to upregulation of vascular cell adhesion molecule-1 (VCAM-1) on endothelial cells within the tumor[127]. It has also been investigated in combination therapy with the PD-L1 inhibitor atezolizumab[128]. GDC-0919 produced promising results in phase 1 trials with a high dosage tolerance but failed to effectively reduce tumor proliferation when used as single therapeutic[124]. Though incyte's epacadostat passed phased I and II trials with promising results, the phase III trials of epacadostat in combination with EGFR and PD-1 monoclonal antibodies have failed, showing no increased benefit over the monoclonal antibodies as a single treatment.

A few trials have also explored using IDO peptides or antibodies against IDO as a vaccine to promote immune response. A phase I clinical vaccination trial (NCT01219348) tested the efficacy of an IDO-derived peptide with montanide adjuvant on stage III and IV non-small cell lung cancer (NSCLC) patients. The investigators found

that the vaccine led to a decrease in Treg cell count as well as a possible increase in NK cells[129, 130]. Currently, there no clinical trials investigating the an IDO inhibitor with a PARP (DNA repair protein) inhibitor or any other high profile immuno-regulatory target outside of the Immune checkpoint inhibitors (i.e. PD-1 or CTLA-4 targeting inhibitors). While patient response IDO inhibitor immunotherapy has been compared to DNA damaging agent- immune checkpoint inhibitor cocktails, the three have only been used together in a few early phase clinical trials and with a scope limited to dose safety determination. Though the list of viable IDO small molecule inhibitors is growing steadily with the use of high throughput screening and intelligent design, only the major three IDO inhibitors above have been investigated in phase III trials. This lack of diversity in pharmacophores has somewhat stalled discovery of novel treatment combinations, and allowed phase III failures of the most utilized drugs to cast doubt on the feasibility of IDO inhibition as an effective Immunotherapeutic target.

1.8 DNA Repair Mechanisms as targets for Immunotherapy.

DNA repair enzymes have recently become a promising target for new cancer treatments. These treatments often utilize small molecule inhibitors and/or antibodies to perturb normal cellular DNA repair. Poly (ADP-ribose) polymerase (PARP), in particular has been explored in the clinic with multiple inhibitors being approved for monotherapy against MMRD breast cancer cell lines. PARP is recruited to the site of DNA damage where it specifically repairs single strand breaks. Without normal function of PARP these SSB's would lead to double strand breaks and stalled replication forks. The cell can still maintain genetic stability through other repair mechanisms such as homologous recombination or mismatch repair. In a method called synthetic lethality, PARP inhibitors

promote cell death only in cancer lines that are deficient in the back up repair mechanisms, while not having an effect on WT cells.

Another DNA repair enzyme recently highlighted as a target for inhibition is DNA Polymerase gamma (POLγ). POLγ is critical to mitochondrial DNA replication and repair. Though few inhibitors have been developed specifically for POLγ inhibition, multiple known small molecules have shown inhibition activity against POLγ. Multiple different types of cancers hijack the mitochondria to help produce an environment primed for rapid cellular division. The POLγ inhibitor Menadione (Vitamin K3) has been shown to disrupt redox shuttling and homeostasis and increase production of ROS which can subsequently lead to cell death via apoptosis.

Clinical researchers have utilized these inhibitors in conjunction with other chemotherapy drugs to selectively target cancer cells. Though some have proven effective, most combination therapies have not seen widespread use or FDA approval for multiple types of cancers.

1.9 Future Prospects and Experimental Aims

With the recent high profile phase III failures of Incyte's Epacadostat as well as other promising IDO small molecule inhibitors in late stage clinical trials, excitement over the possibilities of IDO inhibition has waned. These results do not prove that IDO is not a feasible or promising target but simply highlight a need for increased study into the feedback loops and induction of IDO within the tumor environment. Specifically, probes and methods are needed to delineate the downstream effects of IDO inhibition. IDO has been shown to experience an increase in expression due to inhibition of cellular IDO with

Indoximod, indicating the intended increase in inflammation due to suppressing IDO, in turn upregulates IDO. IDO also promotes and sustains function of PARP in the presence of PARP inhibitors[37]. While a host of studies have shown an increase in IDO expression in conjunction with overexpression of PD-1, attempts to combine IDO inhibitors with PD-1 specific monoclonal antibodies, does not increase overall survival rates of patients. This may be due to the fact that the tumor environment often utilizes multiple methods to exact the same immuno-suppressive environment, and inhibition of a single effector pathway can cause produce a heightened inflammation event that in turn activates other immune suppressive effector pathways that have been hijacked by the cancerous cells. The intricate and often obscure multifaceted suppression of the immune system by cancer cells can only elucidated by designing probes that exact multiple effects concurrently on the tumor environment.

Cancer immunologists might explore the role of IDO in other inflammatory diseases such as Crohn's disease or Diabetes for insight on ulterior functions of IDO. In other inflammatory diseases, IDO inhibition coupled with other treatments have produced beneficial results. Understanding how a blockade of IDO in other inflammation environments affects the immune system might provide critical insight on novel modes of action utilized by cancer cell when coopting IDO.

The focus on simply inhibiting IDO function or combining this inhibition with immune checkpoint inhibitors might also be hindering progress in the development of potent immunotherapeutic agents. Since the expression of multiple immune suppressive pathways are governed by common upstream transcription events, a focus on blocking the transcription of immune suppressors in conjunction with active inhibition immune

checkpoints might be more effective. In a similar fashion to method of broad neutralizing antibodies using three or more determinants to target the viral envelope in HIV infection, cancer immunologists could increase the amount of concomitantly targeted effector pathways in addition to shifting the focus from direct inhibition to transcription or expression inhibition. Even in the face of recent setbacks, IDO remains a promising therapeutic target. With an in-depth investigation of regulatory feedback loops, coupled with new multi-target inhibition strategies, IDO immunotherapy could one day represent the pinnacle of chemical immunology research and clinical success.

1.10 Experimental aims: Discovering the interplay between IDO and DNA Repair mechanisms

IDO is critically involved in the de novo synthesis of NAD+ within the cell. The conversion of tryptophan into kynurenine through the kynurenine pathway directly ends with a final oxidation into NAD+. This process is increased in the event of INFγ mediated inflammation, since INFγ promotes upregulation of IDO and increases its activity. NAD+/NADH ratios are critical to mitochondrial function and energy production. As previously discussed, POLγ is a DNA repair enzyme specific to the mitochondria. Inhibiting POLγ has direct consequences on cellular energy production and mitochondrial stability. PARP, while not specific to the mitochondria, relies on cellular NAD+ to function properly with a recognizable depletion of NAD+ levels whenever increased PARP activity is observed. PARP function also promotes a metabolic shift in dependency from glycolysis to oxidative phosphorylation.

On the surface, accumulation of DNA damage would theoretically promote immune recognition of cancer cells, especially if combined with inhibitors that block their

tolerogenic capabilities. Small molecule blockade of DNA damage repair (DDR) enzymes should increase antigen presentation and MHC expression on antigen presenting cells (APC), which would stimulate activation of cytoxic CD8 + T cells. Tumors often evade immunosurveillance by upregulating expression of immune checkpoint receptors such as CTLA-4 and PD-1/PDL-1 or through other immunomodulating enzymes like IDO. Currently CTLA-4 and PD-1/PDL-1 inhibitors are the main immunomodulatory inhibitors experiencing widespread use in the clinic. They have even seen success when combined with other DNA damaging agents or PARP inhibitors. While these effects have been promising, not all cancers are sensitized by PARP inhibition or contain genetic mutations that would make them particularly susceptible to immune checkpoint inhibitors. These inhibitors often have limited efficacy in a broad sense and are highly effective in a small subsection of cancers. Because of IDO's ability to potentiate immune response through multiple methods, regardless of genetic mutation, it would be plausible that a conjugate IDO and DDR inhibitor would be a potent immunotherapeutic to a wide range of cancer cells.

While the initial rationale is straightforward and could be explored in the clinic immediately, the underlying modes of action and synergies between these enzymes seem to depend on a few common metabolites and mechanisms that are not completely understood. Because IDO, PARP, and DNA POLγ are all critically involved in mitochondrial function and stability, we aimed to develop inhibitors that could also probe the interplay between the three enzymes. An in-depth analysis of these pathways with conjugate inhibitors, could lead to novel methods of immunotherapy that would specifically target cancer cells.

CHAPTER 2. MILD DEPROTECTION OF N-TERT-BUTYLOXYCARBONYL (N-BOC) GROUP USING OXALYL CHLORIDE

The contents of this chapter were previously published in RSC Advances.

2.1 Rationale

To explore the interplay between IDO and DNA POLγ, we aimed to develop a conjugate inhibitor of 1-MLT and Menadione (Figure 2.1). In the process of synthesizing FC1 we discovered a novel synthetic methodology for the deprotection of N-tert-butyloxycabonyl (N-BOC) group using oxalyl chloride. The (BOC) protected precursor was found to be unstable under classical TFA deprotections and would immediately hydrolyze and split into its precursor molecules upon addition of any TFA solution. The following chapter discusses the novel methodology and explores its applications across a broad spectrum of substrates.

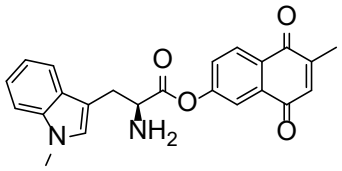

FC1

Figure 2.1 Conjugate inhibitor of IDO and POLγ (FC1)

2.2 Introduction

Synthetic organic transformations require the appropriate selection of reagents, catalysts, and most importantly, temporal masking and demasking agents. The objective for the deployment of relevant masking-demasking agents is to selectively form bonds of interest, whilst minimizing competing reactions with reactive functional groups. A good

protecting group will selectively block the functional group of interest, will be stable to the projected reactions, as well as being removed with readily available de-masking agents.[131]

The amino group is a key functionality that is present in several compounds: natural products, amino acids and peptides.[132] As such, there is an emergent need for its masking and demasking in forward synthesis. The *tert*-butyloxycarbonyl (Boc) group is one of the classical masking functionalities employed in organic synthesis for the protection of amino groups.[133-135] Boc fulfils this requirement of a 'good' protecting group, and is preferred in amino protection because of its stability to nucleophilic reagents, hydrogenolysis and base hydrolysis.[136, 137] The Boc- masking group is installed by reacting the amino-substrate with di-*tert*-butyl dicarbonate under basic conditions[138-140], or solvent free conditions[141-143].

Traditional approaches for N-Boc deprotection relies largely on TFA-induced cleavage.[144] Other strategies reported for the deprotection of N-Boc include the use of metal catalysts[145, 146], as well as acetylchloride in methanol[147], N-Boc removal with HCl in organic solvents: ethylacetate[148] , dioxane[149], in acetone.[150] Other N-Boc deprotection methodologies include aqueous phosphoric acid[151, 152], conc. sulfuric acid in tertbutylacetate[133], boiling water[153]; silica gel has also been reported to effect the deprotection of N-Boc from thermally-sensitive heterocycles including heterocondensed pyrroles.[154] Solvent free N-Boc deprotection strategies have been reported; Pal *et al.* reported the deprotection of several structurally diverse N-Boc substrates by using catalytic amounts of iodine.[155] Aouf and co-workers have also reported the selective cleavage of N-Boc from N-Boc Chiral cyclosulfamides by fusion: mixing N-Boc

substrates with catalytic amounts of iodine under reduced pressure.[156] Guillaumet and co-workers have developed the basic deprotection of N-Boc substrates - using sodium carbonate in refluxing DME.[157] Similar basic N-Boc deprotection has been reported by Ewing *et al.*, where sodium t-butoxide in slightly wet tetrahydrofuran was used to cleave off unactivated primary N-Boc from base stable substrates.[158] Microwave assisted basic deprotection of secondary N-Boc substrates have been reported by Williams & Dandepally.[159] Jia and co-workers have also developed a catalyst-free water-based deprotection of N-Boc aliphatic and aromatic substrates.[160]

Most recently, several N-Boc deprotection schemes have been reported. These include N-Boc deprotection via thermolysis[161, 162] and TMSI-mediated deprotection of N-Boc in zwiterrionic compounds[163].

In most cases, small molecules with sensitive functional groups or unique scaffolds are not compatible with these harsh deprotection conditions. Therefore, alternative reagents that orchestrate efficient deprotection, while providing functional group tolerance will be quintessential in the masking and unmasking of amines – a paradigm for broad utility.

Oxalyl chloride is a highly accessible organic reagent that has many applications: from the routine synthesis of acid chlorides to the preparation of dihydroquinolines via a modified Bischler-Napieralski ring closure.[164] The reactivity of oxalyl chloride with amides manifests in useful products through a typical imidoyl chloride intermediate when acetamide starting materials are used.[165]

2.3 Results and Discussion

In our effort to generate an acylchloride from the C-terminus of a N-Boc protected peptidomimetic using oxalyl chloride, we observed the concomitant formation of the deprotected N-Boc to form the peptidomimetic with a free amine. We therefore set out to investigate if oxalyl chloride can mildly promote the deprotection of N-Boc substrates. Using 1-napthylamine as a model compound, we screened oxalyl chloride with a host of organic solvents at varying temperature conditions and equivalence. We found that the deprotection reaction proceeds poorly in neat oxalyl chloride. In addition, the reaction proceeds to access deprotected amino substrates in $CHCl_3$ in moderate yields at room temperature over 24 – 48 h. However, under refluxing conditions in $CHCl_3$, *N*-chloroalkyl products formed, which were detected by GC-MS even after aqueous work-up. Further optimization led to the identification of a reaction condition that involved the use of five (5) equivalents of oxalyl chloride in methanol, which rapidly deprotects N-Boc substrates with respectable yields (Table 1). Ultimately, the use of three (3) equivalents of oxalyl chloride in MeOH achieved good-to-excellent yields of deprotected tert-butyl carbamates. Here, we report a mild, and selective deprotection of tert-butyl carbamates using oxalyl chloride in methanol. The approach is tolerant to several functional groups.

TABLE 2.1: OPTIMIZATION OF DEPROTECTION USING N-BOC-1-NAPHTHYLAMINE-AMINE

Entry	Reaction conditions	Time (h)	Yield (%)[a]
1	oxalyl chloride, neat, RT	72	0
2	oxalyl chloride, $CHCl_3$	24	23[b]
3	oxalyl chloride, $CHCl_3$, 50°C	24	12
4	oxalyl chloride, $CHCl_3$, 62°C	24	0
5	oxalyl chloride, MeOH, RT	0.5	80[b]

Conditions: (a) $(COCl)_2$ (1-3 equiv), (b) $(COCl)_2$ (3 equiv)

The general deprotection scheme is shown in Scheme 1. We then applied this deprotection strategy to a variety of aromatic, aliphatic, and heterocyclic substrates.

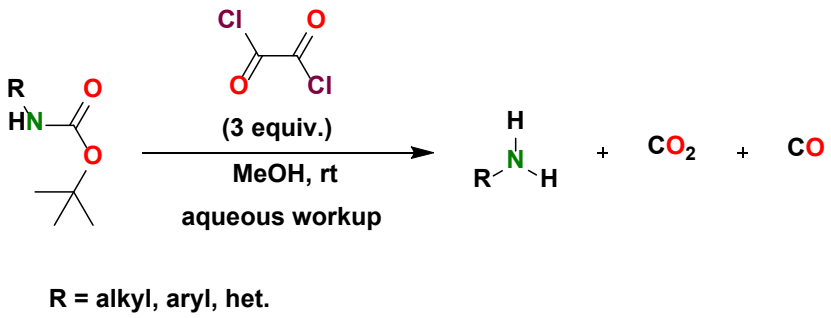

Scheme 2.1 General deprotection reaction scheme

Table 2.1 illustrates the wide substrate scope of the oxalyl chloride-methanol deprotection strategy. It was effective against structurally diverse N-Boc amines; from aromatics, heterocyclic, aliphatics to alicyclic systems.

Generally, the deprotection of N-Boc directly linked to aromatic moieties (Entry 1 - 9) were reasonably fast, occurring within 3 h and with high yields, >70%. Especially, compounds with electron withdrawing groups (EWG) including nitro, fluoro, chloro, iodo, or bromo display a faster response to the oxalyl chloride deprotection reagent with reactions in an hour.

Table 2.2 Deprotection of structurally diverse N-Boc-amines

Entry [a]	Substrate (a)	Time/ h	Product (b)	Yield (%)
1	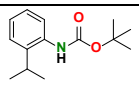	2		70
2	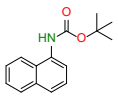	1.5		87
3	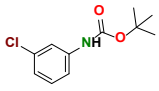	1.5	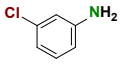	83
4	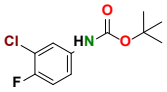	1	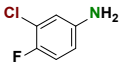	80
5	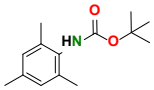	2		83
6	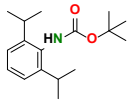	3	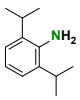	78

Table 2.2 (Cont.) Deprotection of structurally diverse N-Boc-amines

Entry [a]	Substrate (a)	Time/ h	Product (b)	Yield (%)
7	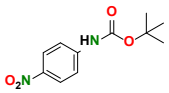	1.5	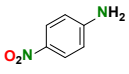	76
8	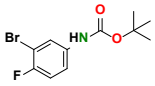	1.5	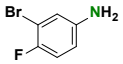	81
9	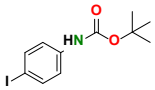	1	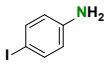	86
10	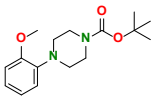	2.5	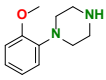	64
11	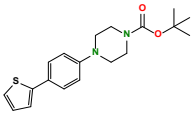	4	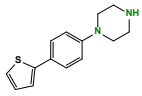	87
12	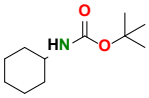	3.5		55
13	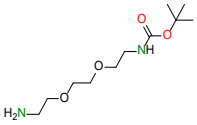	2	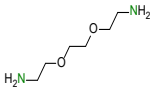	80

Conceivably, electronic destabilization of the aryl carbamate induced by EWG promotes its cleavage by oxalyl chloride. We further observed that steric hindrance of methyl or isopropyl units attached to the aromatic ring and adjacent to the N-Boc group slows the reaction as seen for entries 2, 5, and 6. Moreover, the deprotection reaction of heteroaromatics in entry 11 proceeded modestly in 4 h. Taken together, favorable

deprotection of aromatics by this deprotection strategy can be attributed to favorable electronic effects of these selected aromatic systems. The enhanced reactivity of the aromatic systems in contrast to their non-aromatic counterparts can be rationalized on the basis of the weakly nucleophilic oxygen atom of the carbonyl N-Boc atom. This oxygen is often stabilized or destabilized by the side group/chain directly connected to the N-Boc group. For entries possessing aromatics and electron-withdrawing groups, the pronounced ground-state destabilization of the carbonyl group caused by resonance or inductive effects, informs the increased O-atom reactivity to the electrophilic oxalyl chloride. This phenomenon could explain why the rate of reaction for alicyclic or heterocyclic systems were relatively slower.

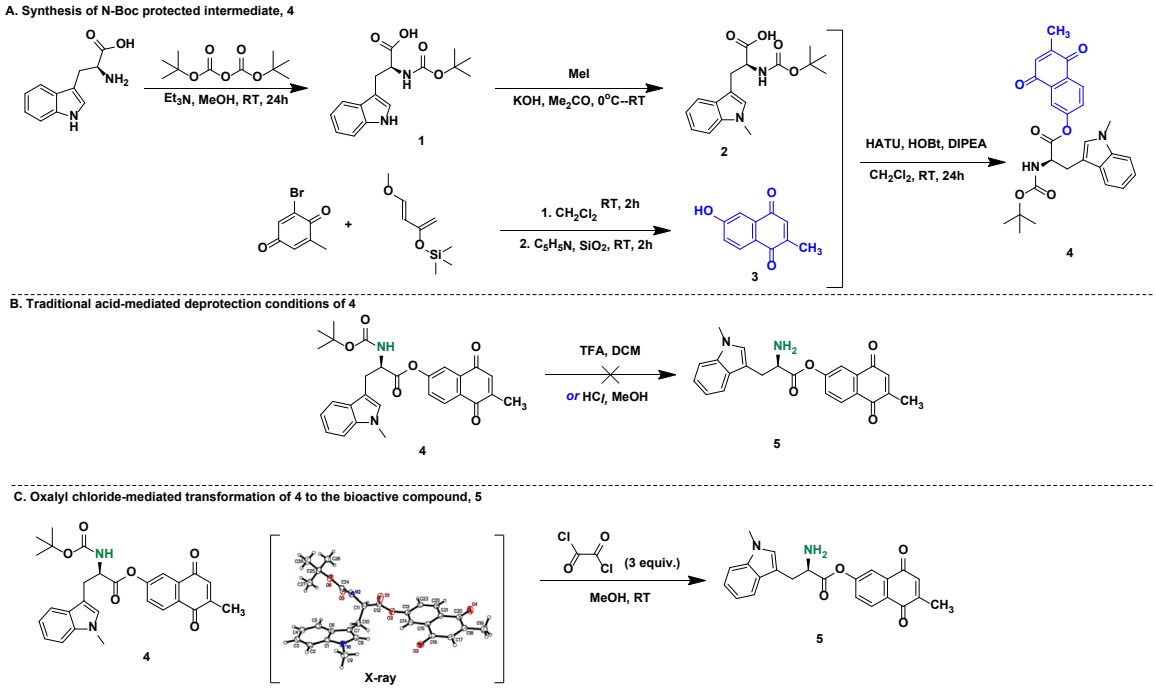

Scheme 2.2 Synthesis of 5 (FC1) via oxalyl chloride-mediated deprotection of 4 (EC1). The X-ray of EC1 is drawn at 50% thermal ellipsoid. Solvent molecules were removed for clarity.

Hybrid drugs possess multiple pharmacological activity[166]. These agents often have sensitive functional groups and their synthesis require protection and deprotection steps that are mild and of broad tolerance. One such molecule of interest in our laboratory is **5**, which is a dual inhibitor of indoleamine-2,3-dioxygenase 1 (IDO1) and DNA polymerase gamma.

Hybrid drugs possess multiple pharmacological activity. These agents often have sensitive functional groups and their synthesis require protection and deprotection steps that are mild and of broad tolerance. One such molecule of interest in our laboratory is **5**, which is a dual inhibitor of indoleamine-2,3-dioxygenase 1 (IDO1) and DNA polymerase gamma. To demonstrate the versatility of this deprotection strategy, we used the N-Boc protected small-molecule precursor of **5**, which possess acid-labile functionality. The synthesis of **4** was accomplished through, first, N-Boc protection of D-tryptophan, **1** and the subsequent N-methylation of the indole nitrogen to yield compound **2**. Second, hydroxymenadione, **3** , was synthesized from a derivatized quinone and a Danishefsky diene. Third, amide coupling of D-methyl tryptophan and hydroxymenadione afforded **4** in 10% yield. Initial attempts to convert **4** to **5** using traditional acid-mediated protocols were unsuccessful. For example, experiments with (1 - 60%) TFA in DCM, and HCl in dioxane/methanol did not yield FC1. However, products corresponding to the cleavage of the ester bond in EC1 were observed. We envisaged that the facile functional group tolerance of the described oxalyl chloride/MeOH methodology may work for our compound, **4**. We therefore applied our deprotection methodology to **5**. We observed a clean transformation of **4** to **5** (Scheme 2). Overall, oxalyl chloride is a worthy N-Boc

deprotection reagent for compounds with multiple functional groups and acid-labile groups.

2.4 Determination of HCl effectiveness in Deprotection

Considering that HCl/MeOH was incapable of deprotecting the N-Boc group in 4, we further explored the potential role of HCl to deepen our understanding of this reaction. One of the by-products of oxalyl chloride-alcohol reactions is the generation of HCl. Thus, the presumptive role of in-situ generated HCl in the deprotection of N-Boc substrates is reasonable. To examine this assertion, an equivalent mole of HCl generated in the oxalyl chloride-MeOH system was utilized in a model reaction as shown in Fig. 1. Specifically, N-Boc-L-Tryptophan was used as a model N-Boc amine. L-Tryptophan (0.657 mmol) in HCl (3.94 mmol) in MeOH, was compared to an equal mmol of N-Boc L-Tryptophan in oxalyl chloride (1.97 mmol) in MeOH system. After monitoring both reactions for 3 h, the N-Boc L-Tryptophan had been completely converted to L-Tryptophan in the oxalyl chloride-MeOH system, whereas the HCl-methanol system did not yield an observable deprotection of the N-Boc-L-tryptophan substrate. This suggests that the deprotection of N-Boc in oxalyl chloride-MeOH system involves a broader mechanism than simply in-situ generation of HCl.

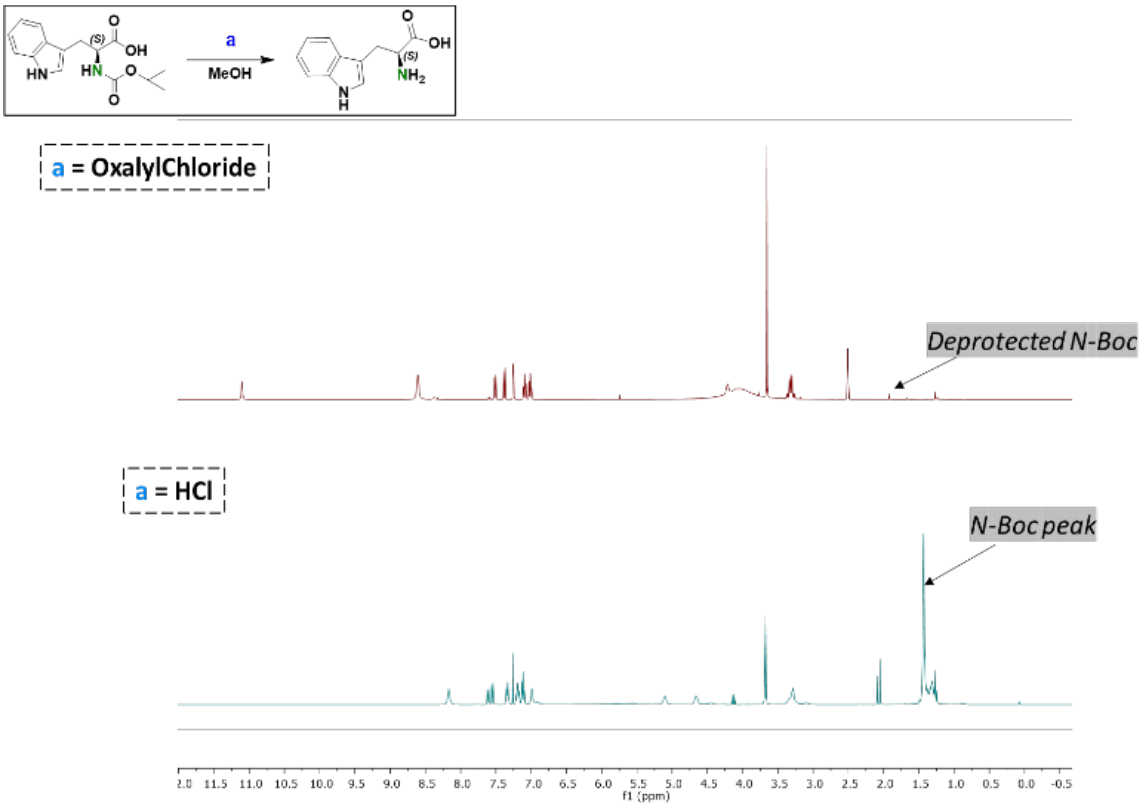

Figure 2.1 Comparative reaction conditions for the deprotection of N-Boc-L-Tryptophan (Methanol was used as the reaction solvent).

2.5 Proposed Mechanism

In the course of the reaction of the oxalylchloride-mediated deprotection of model compound, tert-butyl N-(1-naphthyl)carbamate, the GC-products, isocyanate ester, **II**.The *tert*-butanol as well as the hydroxy-oxazolidinedione, **IV** (scheme 3a) were observed.

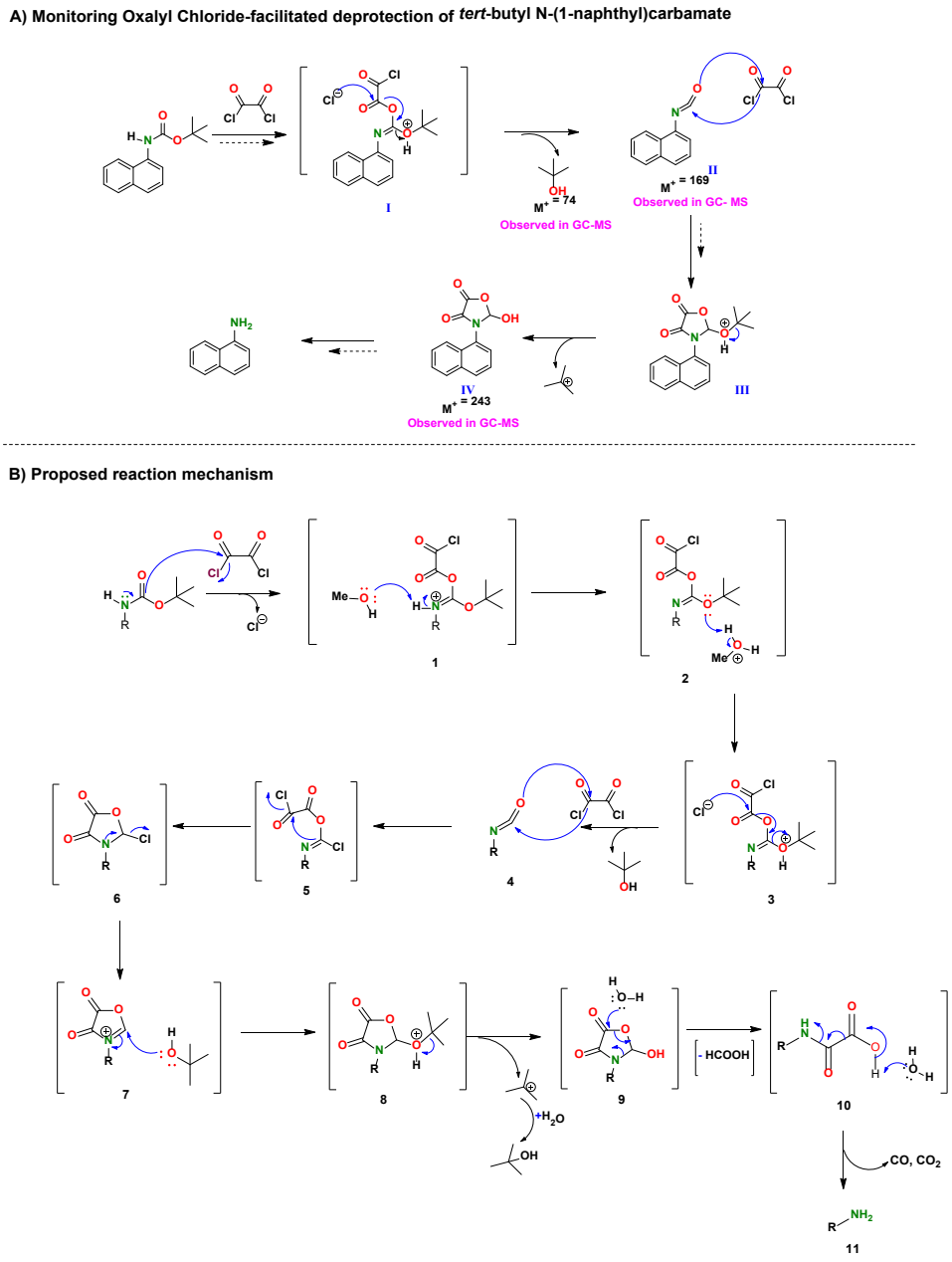

Scheme 2.3 Proposed mechanism of oxalyl-chloride mediated deprotection of N-Boc group.

It is important to note that the isocynate **II** could be hydrolyzed back to the free amine during a water work up. In practice, the final product was observed only after aqueous workup, making this theory plausible. However, the mechanistic analysis was carried out prior to aqueous workup and therefore all other proposed intermediates could be formed due to side reactions or thermally instability during GCMS aquistion.

We therefore propose a possible mechanism for the oxalyl chloride mediated deprotection of the N-Boc group (scheme 3b). The electrophilic character of oxalyl chloride present opportunities for unique reactivity. In this context, addition reactions of the carbonyl unit of the carbamate with oxalyl chloride is plausible. Therefore, it is possible that the intermediate, **1**, can be formed from such addition reactions. It has been shown that the oxalyl chloride mediated reactions with carboxylic acid derivates can yield isocyanate products .[167, 168] Therefore, It is not far-fetched that the removal of *tert*butanol, from intermediate, **3**, yields the isocyanate ester intermediate , **4**. The subsequent release of *tert*butyl ion from intermediate, **8** yields the oxazolidinedione-like intermediate, **9.** It has been shown that the oxazolidinedione scaffold undergoes hydrolysis and ring opening to release carbon dioxide and related products.[169, 170] It is therefore plausible that after the workup, the oxazolidinedione-like intermediate, **9** will undergo a ring opening and subsequently yield the amine product, **11**, by releasing carbon dioxide, carbon monoxide and possible formyl side products. It must be noted that the tertbutyl cation side-product produced from the conversion of **8** to **9**, will be transformed into isobutanol. This N-Boc deprotection methodology may have limited applications in large scale organic processes due to the possible formation of the carbon monoxide side-product.

Conclusion

In a nutshell, we have developed a simple method for the deprotection of N-Boc group under the mild conditions of oxalyl chloride and methanol. Our methodology should prove useful in total synthesis; for the deprotection of N-Boc of substrates in the presence of other functional groups. Also, we have the strongest conviction that this study will serve as a model for the subsequent method development for the oxalyl chloride-mediated direct transformation of N-Boc protected amines into amides.

2.6 Experimental Procedures

General procedure for N-Boc protection of amines

In a 100 ml round bottom flask equipped with a stirring bar, the starting amine (500 mg) and TEA (or DIPEA) (3 equiv.) was dissolved in 2:1 v/v mixture of H_2O/THF (45 ml) and allowed to stir at room temperature for 5 min. Once all starting materials were completely dissolved, the reaction mixture was cooled to 0 °C before di-*tert*-butyl dicarbonate (1.5 equiv.) was added to the solution in one portion. The reaction mixture was stirred at 0 °C for at least 2 h and then allowed to warm to room temperature over 4 h. The reaction was monitored via TLC. Upon complete conversion to the N-Boc-protected amine, THF was removed in vacuo and the crude material was subsequently extracted with dichloromethane (20 mL) , washed with deionized water twice (2 x 10 ml), and brine once (1 x 10 ml). The organic layer was dried over anhydrous $MgSO_4$, filtered, and concentrated under low vacuum on a rotary evaporator. Most products did not require further purification to yield the pure protected amine.

General procedure for the N-Boc deprotection:

In a dry 25 ml round bottom flask equipped with a stirring bar, the starting material (50 mg) was dissolved in MeOH (3 mL) and allowed to stir at room temperature for 5 min. Oxalyl chloride (3 equiv.) was then added to the solution (via syringe or micropipette) directly into the reaction solvent mixture. Sputtering and an increase in temperature of the reaction mixture were observed immediately upon addition of the oxalyl chloride. The reaction mixture was allowed to stir for up to 4 h depending on the starting material. The reaction was monitored via TLC. Upon complete conversion of the N-Boc-protected amine, deionized water (5 mL) was added to the flask slowly. The crude material was subsequently extracted with dichloromethane (5 mL) and washed with deionized water twice (2 x 5 ml). The organic layer was dried over anhydrous $MgSO_4$, filtered, and concentrated under low vacuum on a rotary evaporator. Some products required further purification via flash column chromatography to yield the pure deprotected amine.

Tert-butyl N-(2-isopropylphenyl)carbamate (Entry 1a)

Prepared according to general N-Boc procedure. Product : red liquid (870 mg, 3.69 mmol, 100%).

^{1}H NMR [$CDCl_3$, 400MHz]: δ 7.62 (d, 1H, CH, *J*=7.6 Hz), δ 7.17 (dd, 1H, CH, *J*= 8, 1.6 Hz), δ 7.11 (td, 1H, CH, *J*= 7.6, 1.2 Hz) δ 7.03 (td, 1H, CH, *J*= 7.6, 1.2 Hz), δ 6.22 (s, 1H, NH), δ 2.91(sep, 1H, CH, *J*=6.8 Hz), δ 1.44 (s, 9H, $(CH3)_3$), δ 1.17 (d, 6H, $(CH3)_2$, *J*=6.8Hz). ^{13}C NMR [$CDCl_3$, 101 MHz]: δ 153.6, 139.1, 134.7, 126.3, 125.4, 124.7,

123.1, 80.3, 28.4, 27.7, 23.0. The spectral data of the compound 1a was consistent with the values reported in the literature.[171]

2-isopropylaniline (Entry 1b)

Prepared according to general deprotection procedure. Product: Pale-yellow liquid (40 mg, 0.29 mmol, 70 %)

^{1}H NMR [$CDCl_3$, 400MHz]: δ 7.14 (dd, 1H, CH, *J*=7.6, 1.6 Hz), δ 7.02 (td, 1H, CH, *J*= 7.6, 1.2 Hz), δ 6.80 (td, 1H, CH, *J*= 7.6, 1.2 Hz), δ 6.71(dd, 1H, CH, *J*=7.6, 1.6 Hz), δ 3.96 (s, 2H, NH_2), δ 2.91(sep, 1H, CH, *J*=6.8 Hz), δ 1.25 (d, 6H, $(CH3)_2$, *J*=6.8 Hz). ^{13}C NMR [$CDCl_3$, 101 MHz]: δ 142.6, 133.2, 126.5, 125.5, 119.5, 116.3, 27.7, 22.3. The spectral data of the compound 1b was consistent with the values reported in the literature.[172]

tert-butyl *N*-(1-naphthyl)carbamate (Entry 2a)

Prepared according to general N-Boc procedure. Product: off-white solid (849 mg, 3.49 mmol, 100%)

^{1}H NMR [$CDCl_3$, 400MHz]: δ 7.89 (m, 3H, CH), δ 7.66 (d, 1H, CH, *J*= 8 Hz), δ 7.52 (m, 3H, CH), δ 6.93 (s, 1H, NH), δ 1.61 (s, 9H, $(CH3)_3$). ^{13}C NMR [$CDCl_3$, 101 MHz]: δ 153.6, 134.1, 133.0, 128.7 (2C), 126.0 (2C), 125.9, 125.8, 124.5, 120.5, 118.8 (2C), 80.7, 28.4. Melting point: 95-97 °C. The spectral data of the compound 2a was consistent with the values reported in the literature.[173]

Naphthylamine (Entry 2b)

Prepared according to general deprotection procedure. Product: Brown solid (51 mg, 0.35 mmol, 87 %)

^{1}H NMR [$CDCl_3$, 400MHz]: δ 7.92 (m, 1H, CH), δ 7.69 (m, 1H, CH), δ 7.36 (m, 2H, CH), δ 7.19 (d, 2H, CH, *J*=4.4 Hz), δ 6.77 (pen, 1H, CH, *J*=4.4 Hz), δ 4.81 (s, 2H, NH_2). **^{13}C NMR [CD_3OD, 101 MHz]:** δ 145.4, 137.0, 130.3 (2C), 128.4, 127.7, 123.6, 120.4, 111.8(2C). Melting point: 49-52 °C**.** The spectral data of the compound 2b was consistent with the values reported in the literature.[174]

***tert*-butyl *N*-(3-chlorophenyl)carbamate (Entry 3a)**

Prepared according to general N-Boc procedure. Product: White solid (892 mg, 3.9 mmol, 100%)

^{1}H NMR [$CDCl_3$, 400MHz]: δ 7.44 (singlet, 1H, CH), δ 7.09 (m, 2H, CH), δ 6.91 (dt, 1H, CH, *J*= 7.2, 1.6 Hz), δ 6.48 (s, 1H, NH), δ 1.44 (s, 9H, $(CH3)_3$). **^{13}C NMR [$CDCl_3$, 101 MHz]:** δ 152.5, 139.6, 134.7, 129.9, 123.0, 118.6, 116.5, 28.3. Melting point: 69-70 °C**.** The spectral data of the compound 3a was consistent with the values reported in the literature.[175]

3-chloroaniline (Entry 3b)

Prepared according to general deprotection procedure. Product: Yellow liquid (46 mg, 0.36 mmol, 83 %)

^{1}H NMR [$CDCl_3$, 400MHz]: δ 7.03 (t, 1H, CH, *J*= 8 Hz), δ 7.70 (ddd, 1H, CH, *J*= 8, 2, 0.8 Hz), δ 6.91 (t, 1H, CH, *J*= 2 Hz), δ 6.50 (ddd, 1H, CH, *J*= 8, 2, 0.8 Hz), δ 3.648 (s, 2H, NH_2)**. ^{13}C NMR [$CDCl_3$, 101 MHz]:** δ 147.7, 134.9, 130.3, 118.5, 115.0, 113.2**.** The spectral data of the compound 3b was consistent with the values reported in the literature.[176]

***tert*-butyl *N*-(3-chloro-4-fluorophenyl)carbamate (Entry 4a)**

Prepared according to general N-Boc procedure. Product: solid (843 mg, 3.4 mmol, 100%)

^{1}H NMR [$CDCl_3$, 400MHz]: δ 7.575 (dd, 1H, CH, *J*= 6.2, 2 Hz), δ 7.138 (ddd, 1H, CH, *J*= 8.8 , 4, 2.8 Hz), δ 7.047 (t, 1H, CH, *J*= 8.8 Hz), δ 6.554 (s, 1H, NH), δ 1.53 (s, 9H, $(CH3)_3$) **^{13}C NMR [$CDCl_3$, 101 MHz]:** δ 153.9, 136.4, 135.6, 131.5, 128.8, 79.7, 28.3, 20.9, 18.2. Melting point: 130-132 °C. The spectral data of the compound 4a was consistent with the values reported in the literature.[177]

3-chloro-4-flouroaniline (Entry 4b)

Prepared according to general deprotection procedure. Product: solid (47 mg, 0.32 mmol, 80%)

^{1}H NMR [$CDCl_3$, 400MHz]: δ 6.91 (t, 1H, CH, *J*= 8.8 Hz), δ 6.68 (dd, 1H, CH, *J*= 6.4, 2.8 Hz) δ 6.50 (ddd, 1H, CH, *J*= 8.8, 4, 2.8 Hz), δ 3.48 (s, 2H, NH_2). **^{13}C NMR [$CDCl_3$, 101 MHz]:** δ 152.8, 150.5, 143.2, 143.2, 121.1, 120.9, 116.9, 116.7, 116.4, 114.3, 114.2.

Melting point: 46-48 °C. The spectral data of the compound 4b was consistent with the values reported in the literature.[178]

***tert*-butyl *N*-(2,4,6-trimethylphenyl)carbamate (Entry 5a)**

Prepared according to general N-Boc procedure. Product: Off-white solid (870 mg, 3.69 mmol, 100%)

^{1}H NMR [$CDCl_3$, 400MHz]: δ 6.91 (t, 1H, CH, *J*= 8.8 Hz), δ 6.68 (dd, 1H, CH, *J*= 6.4, 2.8 Hz) δ 6.50 (ddd, 1H, CH, *J*= 8.8, 4, 2.8 Hz), δ 3.48 (s, 2H, NH_2)**. ^{13}C NMR [$CDCl_3$, 101 MHz]:** δ 153.9, 136.4, 135.6 (2C), 128.8, 79.7, 28.3, 20.9, 18.2. The spectral data of the compound 5a was consistent with the values reported in the literature.[179]

2,4,6-trimethylaniline (Entry 5b)

Prepared according to general deprotection procedure. Product: Pale yellow liquid (47 mg, 0.35 mmol, 83 %)

^{1}H NMR [$CDCl_3$, 400MHz]: δ 6.63 (s, 2H, CH), δ 2.10 (s, 3H, CH_3) δ 2.07 (s, 6H, CH_3)**. ^{13}C NMR [CD_3OD, 101 MHz]:** δ 142.3, 130.8, 129.5, 124.7, 21.7, 18.9. The spectral data of the compound 5b was consistent with the values reported in the literature.[180]

***tert*-butyl *N*-(2,6-diisopropylphenyl)carbamate (Entry 6a)**

Prepared according to general N-Boc procedure. Product: Pale red solid (782 mg, 2.82 mmol, 100%)

^{1}H NMR [$CDCl_3$, 400MHz]: δ 7.24 (t, 1H, CH, *J*=8 Hz), δ 7.107 (d, 1H, CH, *J*= 8 Hz), δ 5.82 (s, 1H, NH), δ 3.16 (s, 2H, 2(CH)), δ 1.505 (s, 9H, $(CH3)_3$), δ 1.17 (d, 12H, $2(CH3)_2$, *J*=6.8 Hz). **^{13}C NMR [$CDCl_3$, 101 MHz**]: δ 153.9, 136.4, 135.6, 131.5, 128.8, 79.7, 28.3, 20.9, 18.2. Melting point: 145-148 °C. The spectral data of the compound 6a was consistent with the values reported in the literature.[181]

2,6-diisopropylaniline (Entry 6b)

Prepared according to general deprotection procedure. Product: red liquid (49 mg, 0.28 mmol, 78 %)

^{1}H NMR [$CDCl_3$, 400MHz]: δ 7.06 (d, 2H, CH, *J*=8 Hz), δ 6.83 (t, 1H, CH, *J*= 7.6 Hz), δ 3.78 (s, 2H, NH_2), δ 2.97 (sep, 2H, 2(CH), *J*= 6.8 Hz), δ 1.30 (d, 12H, $2(CH3)_2$, *J*=6.8 Hz)**. ^{13}C NMR [$CDCl_3$, 101 MHz]:** δ 140.2, 132.5, 122.8, 118.6, 28.0, 22.5, 21.9. The spectral data of the compound 6b was consistent with the values reported in the literature.[182]

***tert*-butyl N-(4-nitrophenyl)carbamate (Entry 7a)**

Prepared according to general N-Boc procedure. Product: pale yellow solid (743.4 mg, 3.12 mmol, 86.2%)

^{1}H NMR [$CDCl_3$, 400MHz]: δ 7.15 (d, 2H, CH, J = 8.6 Hz), 6.71 (d, 2H, CH, J = 8.9 Hz), 1.48 (s, 9H, $(CH3)_3$). **^{13}C NMR [$CDCl_3$, 101 MHz]:** δ 153.4, 151.9, 131.2, 121.7, 115.7, 80.4, 28.3. Melting point: 112-113 °C. The spectral data of the compound 7a was consistent with the values reported in the literature.[183]

3-nitroaniline (Entry 7b)

Prepared according to general deprotection procedure. Product: yellow solid (22 mg, 0.16 mmol, 76 %)

^{1}H NMR [CD_3OD, 400MHz]: δ 7.92 (d, 2H, CH, J = 9.1 Hz), 6.71 (d, 2H, CH, J = 9.1 Hz). Melting point: 146-147 °C. The spectral data of the compound 7b was consistent with the values reported in the literature.[184]

***tert*-butyl *N*-(3-bromo-4-fluorophenyl)carbamate (Entry 8a)**

Prepared according to general N-Boc procedure. Product: pale yellow solid (763 mg, 2.63 mmol, 100%)

^{1}H NMR [$CDCl_3$, 400MHz]: δ 7.72 (dd, 1H, CH, *J*=5.8, 2.8 Hz), δ 7.202 (ddd, 1H, CH, *J*= 8.8, 4, 2.8 Hz), δ 7.045 (t, 1H, CH, *J*= 8.8 Hz), δ 6.456 (s, 1H, CH), δ 1.534 (s, 9H, $(CH3)_3$). **^{13}C NMR [$CDCl_3$, 101 MHz]:** δ 156.3, 152.5, 135.3, 123.4, 118.9, 116.4, 109.1, 81.1, 28.3.

3-bromo-4-fluoroaniline (Entry 8b)

Prepared according to general deprotection procedure. Product: Brown liquid (57 mg, 0.30 mmol, 88 %)

^{1}H NMR [$CDCl_3$, 400MHz]: δ 6.89 (t, 1H, CH, *J*= 8.8 Hz), δ 6.84 (dd, 1H, CH, *J*= 5.6, 2.8 Hz) δ 6.54 (ddd, 1H, CH, *J*= 8.8, 4, 2.8 Hz), δ 3.57 (s, 2H, NH_2)**. ^{13}C NMR [$CDCl_3$, 101 MHz]:** δ 13C NMR (101 MHz, CDCl3) δ 154.2, 151.8, 143.8, 119.5, 117.1, 115.4, 109.5. The spectral data of the compound 8b was consistent with the values reported in the literature.[185]

***tert*-Butyl (4-iodophenyl)carbamate (Entry 9a)**

Prepared according to general N-Boc procedure. Product: off-white solid (710.2mg, 2.22 mmol, 97.5 %)

^{1}H NMR [$CDCl_3$, 400MHz]: δ 7.56 (s, 1H), 7.54 (s, 1H), 7.12 (d, J = 8.7 Hz, 2H), 6.44 (s, 1H), 1.49 (d, J = 0.6 Hz, 9H). **^{13}C NMR [$CDCl_3$, 101 MHz]:** δ 152.5, 138.2, 120.4, 85.7, 80.9, 30.9, 28.3. The spectral data of the compound 9a was consistent with the values reported in the literature.[186] Melting point: 143.7-147 °C

4-Iodoaniline (Entry 9b)

Prepared according to general deprotection procedure. Product brown solid: (29.5 mg, 0.13 mmol, 86 %)

^{1}H NMR [$CDCl_3$, 400MHz]: δ 7.63 (d, J = 7.3 Hz, 2H), 6.71 (d, J = 7.4 Hz, 2H), 4.21 (s, 2H). Melting point: 67-68 °C. The spectral data of the compound 9b was consistent with the values reported in the literature.[187]

***tert*-butyl *N*-(*N*-(2-Methoxyphenyl)piperazine)carbamate (Entry 10a)**

Prepared according to general N-Boc protection procedure. Product: White solid (760 mg, 2.6 mmol, 100%)

^{1}H NMR [$CDCl_3$, 400MHz]: δ 7.11 (t, 1H, CH, *J*=7.4 Hz), δ 6.93 (m, 2H, CH), δ 3.90 (s, 3H, CH_3), δ 3.72 (s, 4H, $(CH_2)_2$), δ 3.15 (s, 4H, $(CH_2)_2$),δ 1.50 (s, 9H, $(CH3)_3$,). **^{13}C NMR [$CDCl_3$, 400 MHz]:** δ 154.7 (2C), 152.3, 121.3 (2C), 111.8 (2C), 79.9, 55.5, 50.9, 28.4. Melting point: 68-69 °C. The spectral data of the compound 10b was consistent with the values reported in the literature.[188]

***N*-(2-Methoxyphenyl)piperazine (Entry 10b)**

Prepared according to general deprotection procedure. Product: (42 mg, 0.21 mmol, 64 %)

^{1}H NMR [$CDCl_3$, 400MHz]: δ 6.89 (m, 1H, CH), δ 6.83 (m, 2H, CH) δ 6.77 (m, 1H, CH), δ 3.57 (s, 3H, CH_3), δ 2.94 (m, 8H, 4(CH_2)). **^{13}C NMR [$CDCl_3$, 101 MHz]:** δ 152.3, 141.8, 122.9, 121.0, 118.2, 111.4, 55.3, 52.0, 46.3. Melting point: 37-40 °C. The spectral data of the compound 10b was consistent with the values reported in the literature.[189]

***tert*-butyl *N*-(*N*-(4-thiophene-phenyl)piperazine)carbamate (Entry 11a)**

Prepared according to general N-Boc procedure. Yield: (704 mg, 2.04 mmol, 100%)

^{1}H NMR [$CDCl_3$, 400MHz]: δ 7.52 (d, 2H, CH, *J*= 8.8Hz), δ 7.18 (d, 2H, CH, *J*= 4.4 Hz), δ 7.04 (m, 1H, CH), δ 6.92 (d, 2H, CH, *J*= 9.2 Hz), δ 3.58 (t, 4H, CH_2, *J*= 5.2 Hz), δ 3.16 (t, 4H, CH_2, *J*= 5.2 Hz), δ 1.49 (s, 9H, $(CH3)_3$,). ^{13}C NMR [CD_3OD, 101 MHz]: 154.7, 150.5, 144.5, 127.9, 126.9, 126.4, 123.6, 121.8, 116.5, 79.9, 49.1, 28.4.

***N*-(4-thiophene-phenyl)piperazine (Entry 11b)**

Prepared according to general deprotection procedure. Product: off-white solid (61 mg, 0.25mmol, 87 %)

^{1}H NMR [$CDCl_3$, 400MHz]: δ 7.54 (d, 2H, CH, *J*= 9.2 Hz), δ 7.27 (m, 2H, CH) δ 7.02 (m, 3H, CH), δ 3.44 (m, 4H, CH_2), δ 3.38 (m, 4H, CH_2). **^{13}C NMR [CD_3OD, 101 MHz]:** δ 149.7, 143.9, 128.8, 126.7, 124.6, 122.6, 116.6, 45.7, 43.0

***tert*-butyl *N*-(cyclohexyl)carbamate (Entry 12a)**

Prepared according to general procedure. Product: colourless solid (1.0 g, 5.04 mmol, 100 %)

^{1}H NMR [$CDCl_3$, 400MHz]: δ 4.41 (s, 1H, CH), δ 3.43 (s, 1H, NH), δ 1.92 (m, 2H, CH), δ 1.69 (m, 3H, CH), δ 1.46 (s, 9H, $(CH3)_3$,)δ 1.36 (m, 2H, CH_2), δ 1.12 (m, 3H, CH). Melting point: 79-80 °C. The spectral data of the compound 12a was consistent with the values reported in the literature.[190]

Cyclohexylamine (Entry 12b)

Prepared according to general deprotection procedure. Product: colourless liquid (27 mg, 0.28 mmol, 55 %)

^{1}H NMR [$CDCl_3$, 400MHz]: δ 2.63 (s, 1H, CH), δ 1.93 (m, 2H, CH_2,), δ 1.70 (m, 3H, CH), δ 1.58 (d, 1H, CH, *J*= 12.4 Hz), δ 1.26 (q, 2H, CH_2, *J*=12.4 Hz), δ 1.11 (p, 3H, CH, *J*=12.4 Hz). The spectral data of the compound 12b was consistent with the values reported in the literature.[191]

***tert*-butyl *N*-(2-[2-(2-aminoethoxy)ethoxy]ethanamine)carbamate (Entry 13a)**

Prepared according to general procedure. Product: pale yellow liquid (318 mg, 1.2 mmol, 38 %)

^{1}H NMR [$CDCl_3$, 400MHz]: δ 4.13 (s, 1H, CH), δ 3.48 (s, 3H, CH), δ 3.41 (s, 3H, CH), δ 3.18 (s, 2H, CH_2), δ 2.74 (s, 1H, CH), δ 1.78 (s, 1H, CH_2), δ 1.31 (s, 9H, $(CH3)_3$,). The spectral data of the compound 13a was consistent with the values reported in the literature.[192]

2-[2-(2-aminoethoxy)ethoxy]ethanamine (Entry 13b)

Prepared according to general procedure. Product: colourless liquid (49 mg, 0.4 mmol, 90 %)

^{1}H NMR [$CDCl_3$, 400MHz]: δ 3.84 (m, 4H, CH_2), δ 3.73 (t, 2H, CH_2, *J*= 5.0 Hz), δ 3.70 (d, 2H, CH2, *J*= 1.2 Hz), δ 3.64 (s, 1H, CH), δ 3.32 (d, 1H, CH, *J*= 1.6 Hz), δ 3.14 (t, 2H, CH_2, *J*=4.6 Hz). The spectral data of the compound 13b was consistent with the values reported in the literature.[193]

EC1

1-methyl tryptophan was protected prior to synthesis of the conjugate molecule. Prepared according to general procedure.

^{1}H NMR [$(CD_3)_2CO$, 400MHz]: δ 8.06 (d, 1H, CH, *J*= 8.4 Hz), δ 7.65 (d, 1H, CH, *J*= 8 Hz), δ 7.55 (d, 1H, CH_2, *J*= 2.4 Hz), δ 7.38 (m, 2H, CH), δ 7.20 (m, 2H, CH), δ 7.07 (m, 1H, CH), δ 6.91 (s, 1H, CH), δ 4.73 (m, 1H, CH), δ 3.83 (s, 3H, CH_3), δ 3.77 (s, 1H, NH), δ 3.42 (m, 2H, CH_2), δ 2.16 (s, 3H, CH_3), δ 1.43 (s, 9H, $(CH_3)_3$). **^{13}C NMR [$(CD_3)_2CO$, 101MHz]:** δ 184.1, 183.6, 170.7, 155.6, 155.0, 148.4, 137.3, 135.3, 133.9, 129.9, 128.1, 126.8, 121.5, 118.9, 118.6, 118.6, 109.5, 108.9, 78.9, 55.3, 31.9, 27.7, 27.1, 15.4.

CHAPTER 3. SYNTHESIS OF SMALL MOLECULE INHIBITORS FOR NOVEL IMMUNOTHERAPY TREATMENTS

3.1 Introduction

Synthetic lethality has been utilized as an effective treatment to target mismatch repair deficient (MMRD) cancer cells. This perturbation of the stressed repair systems has not to our knowledge, previously been combined with inhibition of IDO. PARP and IDO both modulate cellular NAD/NADH ratios. PARP requires an abundance of NAD+ to function properly while IDO activation indirectly potentiates cellular NAD+ levels through the kynurenine pathway[194, 195]. Induction of IDO initially increases NAD+ synthesis but also has been shown to increase NAD+ catabolism[196]. IDO inhibitors have achieved limited success in the clinic when combined with other small molecule or antibody modulators of the immune response, but there have been very few studies probing the effect on of IDO inhibition on DNA damage repair[197]. We therefore aimed to synthesize conjugate inhibitors of 1-methyl -L-tryptophan (1-MLT) or INCB14943 (a potent IDO inhibitor), and Olaparib (a PARP inhibitor).

We also aimed to synthesize a small molecule probe to examine the effects of modulating redox homeostasis while concurrently inhibiting DNA repair mechanisms. Menadione, an analog of vitamin K, has been shown to trigger cell death by increasing the production of ROS. It is also known that menadione induced ROS promote the phosphorylation and subsequent activation of transducer kinases critical to DNA repair. The combination of an increase in ROS with the inhibition of PARP might increase PARPi effectiveness in MMRD cells and could help uncover new methods to target cancer cells that are highly

resistant to conventional chemotherapy. Menadione is has also been shown to inhibit DNA polymerase γ, which adds another complexity to our studies.

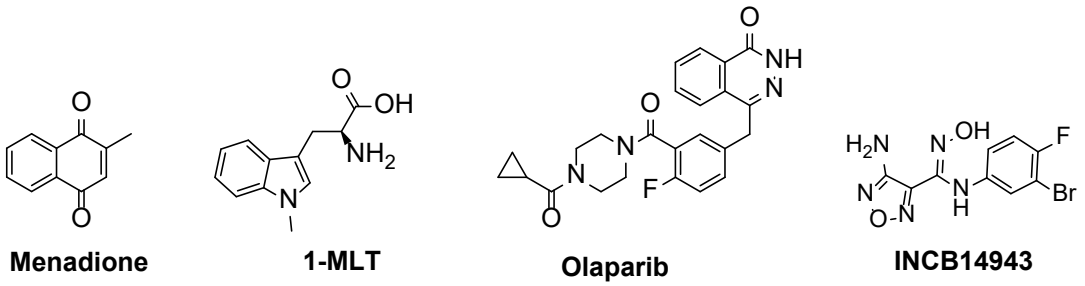

Figure 3.1 Target Inhibitors of IDO, DNA Polymerase γ, and PARP

3.2 Synthetic Methodology

1-MLT was synthesized by first BOC-protecting the free amine. The methylation of the indole amine was accomplished using the milder methylating agent dimethylcarbonate. The classical methylation utilizing methyl iodide could not be used because it was not selective for the indole position and produced multiple side products. 1-MLT(BOC) (**3**) was also synthesized by simply buying the methylated tryptophan and subsequently BOC-protecting the free amine. Olaparib was not used in it's complete form, but the core of the PARP inhibitor was retained in the PARPi analog compound (**4**). The PARPi (**4**) molecule would allow for direct coupling to the 1-MLT IDO inhibitor, but the conjugate would be an amide linker molecule, making it less likely to dissociate within the cell. The PARPi was therefore also converted into linker molecule (**5**) in order to form an ester version of the conjugate. Both final protected conjugates (**6**) and (**7**) were formed using an HATU coupling reaction from their necessary starting materials as shown in scheme 3.1. The final conjugates **(8) FC2** & (**9) FC3** were the only compounds used in subsequent biological assays.

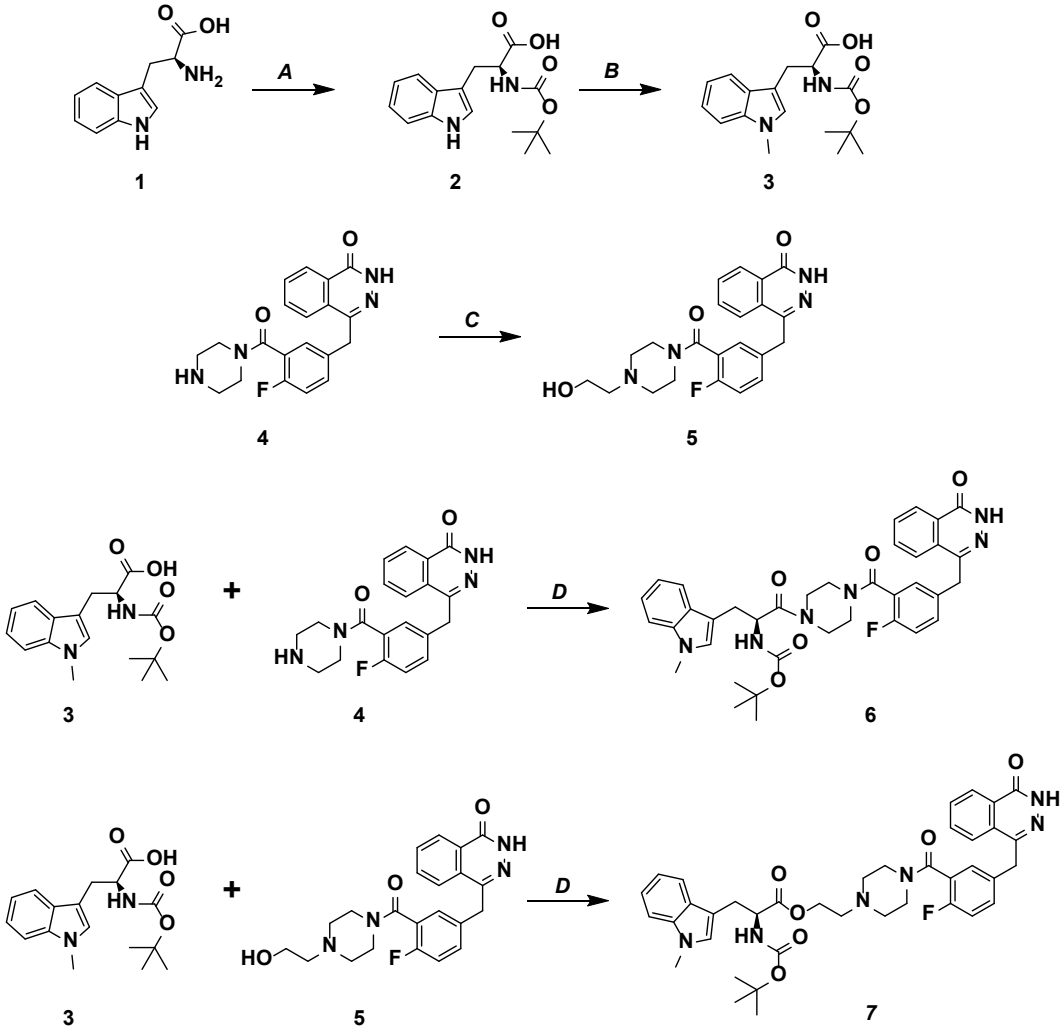

Scheme 3.1 Synthesis of IDO-PARP conjugate inhibitor molecules

A) $(BOC)_2O$, Na_2CO_3, H_2O, 0 °C, 12 h. B) DMC, TBAB, KOH, DMF, reflux, 3 h. C) BrEtOH, Na_2CO_3, ACN, reflux, 2 h. D) HATU, DIPEA, DMF, 22 °C, 48 h ,

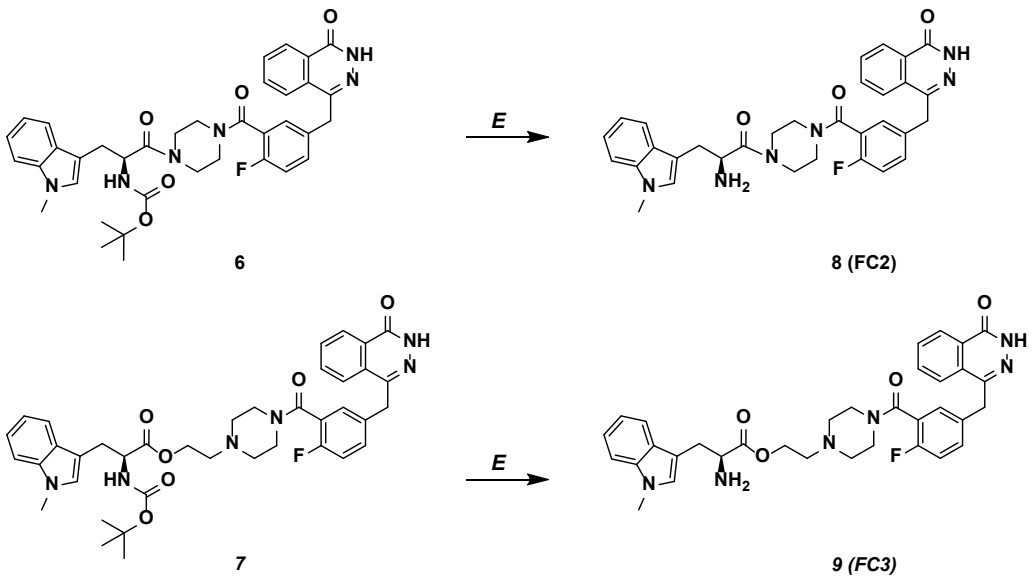

Scheme 3.1 (Cont.) Synthesis of IDO-PARP conjugate inhibitor molecules
E) 50% TFA, CH_2Cl_2, RT, 4 h.

The menadione inhibitor offered few sites favorable for functionalization in its current form, so the hydroxymenadione (**10**) version was synthesized using a diels alder reaction of Danishefsky's diene with 2-Bromo-5-methyl-1,4-benzoquinone. A second analog of the Menadione molecule was synthesized via allylic bromination of the methyl group. The menadione analog containing the primary bromine (**12**) could undergo a facile SN2 substitution with the PARPi linker **(5)** to produce the final conjugate (**14**). The PARPi **(4)** was combined with succinic anhydride in a ring opening amidation that would yield a new linker molecule capped with a free carboxylic acid (**13**). The carboxylic acid linker molecule was then coupled to the initial hydroxymenadione (**10**) via an EDC mediated esterification to yield the second conjugate inhibitor (**15**).

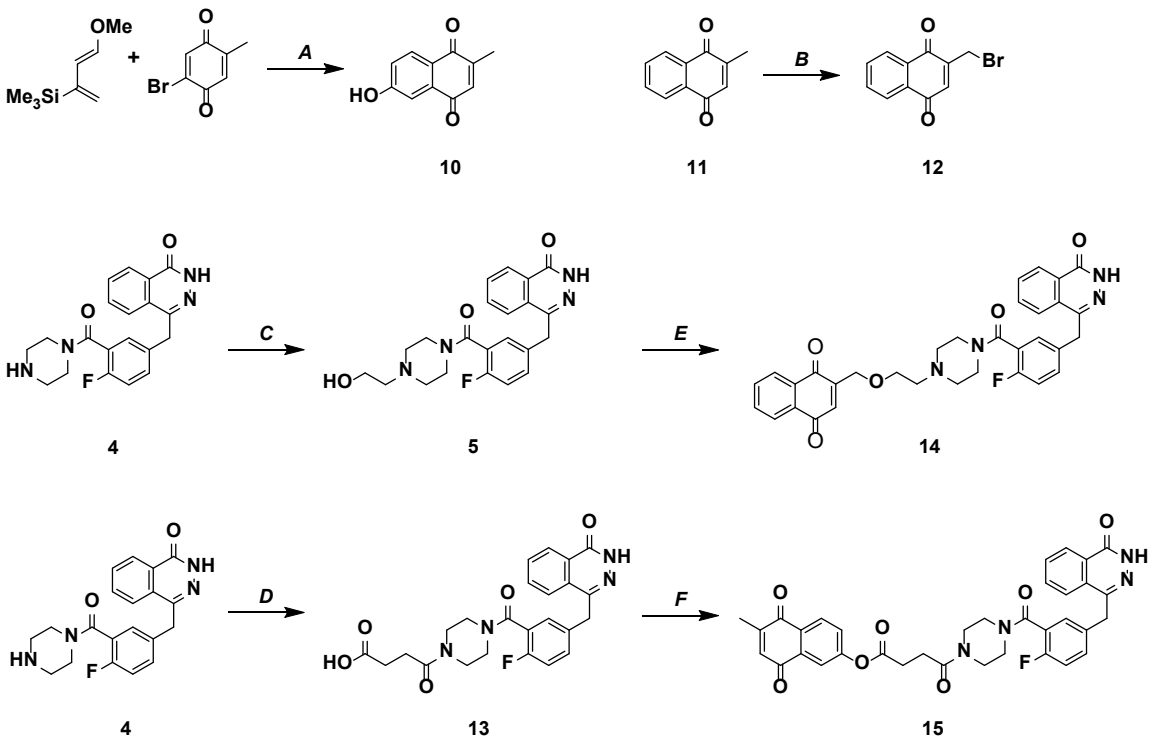

Scheme 3.2 Synthesis of POLγ-PARP conjugate inhibitor molecules

A) Pyridine, CH_2Cl_2, 0 °C, 8 h. B) NBS, hv, ACN, RT, 2-4 h. C) BrEtOH, Na_2CO_3, ACN, reflux, 2 h. D) Succinic Anhydride, DIPEA, DMF, reflux, 12 h, E) Na_2CO_3, ACN, reflux, 2 h, F) EDC, DMAP, CH_2Cl_2, 0 °C - RT, 24 h.

The hydroxyamidne INCB14943 molecule was synthesized using a 3 step process. The first reaction of malononitrile with sodium nitrate and hydroxylamine afforded the hydroxyamidine (**14**). Compound 14 was then converted into the imidoyl chloride (**15**), and then coupled with the target aniline to afford the IDO inhibitor INCB14943 (**16**).

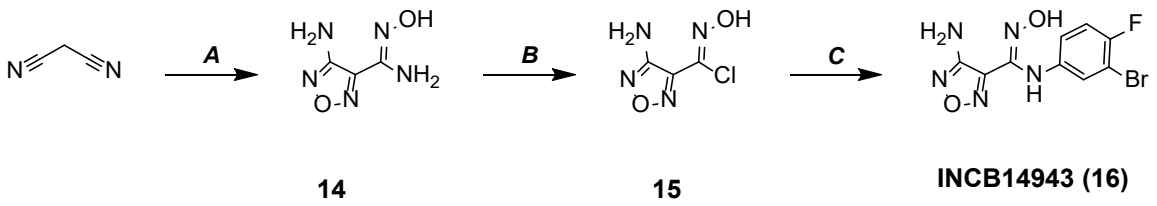

Scheme 3.3 Synthesis of INCB14943

A) $NaNH_2$, $NH_2OH(HCl)$,H_2O, 0 °C- 50 °C, 6 h, 10N NaOH; B) HCl, RT, 3 h; C) 4-fluoro-3-bromoaniline, TEA, CH_2Cl_2, RT, 3 h.

3.3 Future Directions

Conjugates 12 and 13 were never purified to above 95 % purity in quantitative amounts to be utilized in biological assays. The synthesis of molecules containing the hydroxymenadione scaffold were prone to hydrolysis once coupled as an ester due to the high electron density of the molecule. These conjugate molecules often split during purification due to the fairly acidic nature of silica. Alumina columns did not provide the necessary separation of the final conjugate from side products. C18 based columns were particularly useful in separating the menadione conjugates but poor yields in the coupling reactions made it difficult to even begin purification.

INCB14943 was never coupled to PARPi **(11)** as planned but would have theoretically offered the same effect as conjugate **(6)** or **(7)** with only a possible increase in inhibitory activity due to its potent activity as a single agent.

Though these compounds were never fully tested in vitro, they offer fascinating targets for delineating the synergy between redox homeostasis and DNA repair mechanisms. Initially , docking experiments were planned to discover novel POLγ inhibitors that could

be coupled to PARP inhibitors or IDO inhibitors. It would also be useful to couple more potent redox active molecules to IDO inhibitors. Metal complex molecules that perturb mitochondrial function conjugated with IDO inhibitors would offer clear insight into signaling pathways and immune response due to oxidative stress.

3.4 Experimental Procedures:

BOC-Tryptophan (2)

4 g of Tryptophan and 3 eq of DIPEA or Na_2CO_3 was added to a dry 250 ml RBF equipped with a stir bar and dissolved in 75 ml of of a 2:1 H_20/THF solution (v/v). The reaction mixture was cooled to 0 °C and stirred for 15 min. 1.2 eq of $(BOC)_2O$ was charged into the flask and the mixture was stirred at 0 °C for 6 h. The reaction mixture was monitored via TLC. After reaction completion, the reaction mixture was concentrated via rotary evaporator until all THF had been removed. The crude material was then extracted with DCM, washed with 2 ml of 0.2 N HCl followed by brine, then dried over Na_2SO_4. The solution was filtered and solvent removed in vacuo to afford the pure product. No further purification was necessary. White Powder. 100% yield.

^{1}H NMR [$CDCl_3$, 400MHz]: δ 10.04 (s, 1H, CH,), δ 7.27 (m, 2H, CH) δ 7.02 (m, 3H, CH), δ 3.44 (m, 4H, CH_2), δ 3.38 (m, 4H, CH_2). **^{13}C NMR [CD_3OD, 101 MHz]:** δ 149.7, 143.9, 128.8, 126.7, 124.6, 122.6, 116.6, 45.7, 43.0

BOC-1-MLT (3)

1 gram of BOC-TRP (2), 0.5 g of base (K2CO3/KOH/NaOH), 2 mL of dimethyl carbonate, 8 mL of dimethylformamide (DMF), and 0.2 g of catalyst (TBAB) were mixed together and heated to reflux. The reaction was monitored, and the products were identified by HPLC. The reaction (a mixture of N-methylated and N-,C-dimethylated products) was quenched by cooling the reaction mixture to room temperature and adding 16 mL of water. Then an extraction was carried out with 20 mL of EtOAc which was washed twice with 20 mL of water. EtOAc was concentrated under vacuum to about 5 mL. The resulting mixture was cooled and precipitated via slow addition of hexane. The suspension was filtered, washed with 50 mL of cold hexane, and dried under vacuum. The N-methylated product was isolated via flash column with a 25/75 (v/v) EtOAc/Hexane eluting solvent. Tan powder, 30% yield.

^{1}H NMR [$CDCl_3$, 400MHz]: δ 10.09 (s, 1H, OH), δ 7.59 (d, 1H, CH, *J*= Hz), δ 7.40 (d, 1H, CH, *J*= 7.6, 1.2 Hz), δ 7.22 (s, 1H, CH, *J*=7.6, 1.6 Hz), δ 7.08 (dt, 2H, CH , *J*= Hz), δ 5.99 (d, 1H, CH, *J*=Hz), δ 4.49 (d, 1H, CH), δ 3.67 (d, 1H, CH), δ 3.27 (d, 1H, CH), δ 1.38 (s, 9H, $(CH3)_3$,)

PARPi-Linker 1 (5)

500 mg of PARPi **(4)** was added to a dry 50 ml RBF equipped with a stir bar and dissolved in 10 ml of ACN. 2 eq of DIPEA was added to the reaction vessel and the mixture was heated to a mild reflux. 1.2 eq of 2-Bromoethanol was then charged into the flask and the mixture was refluxed vigorously at 100 °C for 2 hours. Upon completion of the reaction the ACN was completely removed and the crude material was dissolved in DCM and washed with 5, 5 ml DI H_2O. The product was isolated via flash column with a 7:93 (v/v) MeOH/DCM eluting solvent. White powder, 30 % yield.

^{1}H NMR [$CDCl_3$, 400MHz]: δ 11.52 (s, 1H, NH), δ 8.43 (s, 1H, CH), δ 7.75 (m, 3H, CH), δ 7.28 (m, 2H, CH), δ 7.00 (m, 1H, CH), δ 4.28 (s, 2H, CH_2), δ 3.8 (m, 2H, CH_2), δ 3.64 (m, 2H, CH_2), δ 3.31 (m, 2H, CH_2), δ 3.02 (s, 2H, CH_2), δ 2.59 (s, 2H, CH_2), δ 2.44 (s, 2H, CH_2).

FC2-BOC (6)

420 mg of 1MLT(BOC), 1.2 eq PARPi **(4)**, 2 eq of HATU and 3 eq of DIPEA. were added to a dry 50 ml rbf equipped with a stir bar and dried under vacuum for 30 min. The reagents were dissolved in 3 ml of DMF and the reaction mixture was allowed to stir at RT for 24-48 hours. Ice water was added to the reaction was to the reaction mixture and a white solid precipitate formed. The suspension was centrifuged and the solvent was decanted, revealing the crude product. The organic product washed with water and centrifuged 2 more times before being extracted with DCM. The product was isolated via flash column with a 100% EtOAc eluting solvent.. Pink powder, 43 % yield.

^{1}H NMR [$CDCl_3$, 400MHz]: δ 11.77 (s, 1H, NH), δ 8.34 (d, 1H, CH, *J*= 9.2 Hz), δ 7.83 (m, 4H, CH), δ 7.08 (m, 4H, CH), δ 6.13 (m, 3H, CH), δ 6.12 (s, 1H, NH), δ 4.35 (s, 2H, CH_2), δ 3.97 (m, 1H, CH), δ 3.77 (s, 3H, CH_3), δ 3.4 (m, 8H, CH), δ 2.74 (s, 2H, CH_3), δ 1.39 (s, 9H, CH_3).

FC3-BOC (7)

400 mg of 1MLT(BOC), 1.2 eq PARPiL1 **(5)**, 2 eq of HATU and 3 eq of DIPEA. were added to a dry 50 ml rbf equipped with a stir bar and dried under vacuum for 30 min. The reagents were dissolved in 3 ml of DMF and the reaction mixture was allowed to stir at RT for 24-48 hours. Ice water was added to the reaction was to the reaction mixture and a white solid precipitate formed. The suspension was centrifuged, and the solvent was decanted, revealing the crude product. The organic product washed with water and centrifuged 2 more times before being extracted with DCM. The product was isolated via flash column with a 7:93 (v/v) MeOH/DCM eluting solvent. Tan powder, 21 % yield.

^{1}H NMR [$CDCl_3$, 400MHz]: δ 8.63 (s, 1H, CH), δ 8.30 (m, 2H, CH), δ 7.78 (m, 4H, CH), δ 7.27 (m, 4H, CH), δ 6.94 (m, 1H, CH), δ 4.70 (s, 2H, CH_2), δ 4.28 (m, 2H, CH_2), δ 3.54 (s, 2H, CH_2), δ 3.38 (s, 1H, CH), δ 3.33 (s, 3H, CH_3), δ 3.11 (m, 2H, CH_2), δ 3.54 (m, 6H, CH_2), δ 1.39 (s, 9H, CH_3).

General BOC Deprotection Procedure

100 mg of BOC -protected compound was placed in a 20 ml scintillation vial equipped with a stir bar. 50 % TFA in DCM was added to the reaction vessel and the reaction mixture was allowed to stir at RT for 2 hours. The reaction mixture was concentrated in vacuo to afford the crude TFA salt. The salt was converted to the free amine with 2 M NaOH and was extracted with EtOAc.

FC2 (8)

Prepared according to general deprotection procedure. Product: Pink powder, 43 % yield.

^{1}H NMR [$CDCl_3$, 400MHz]: δ 8.35 (d, 1H, CH, *J*= 8.2 Hz), δ 7.86 (m, 3H, CH), δ 7.51 (m, 3H, CH), δ 7.09 (m, 4H, CH), δ 4.35 (s, 2H, CH_2), δ 3.79 (s, 1H, CH), δ 3.75 (s, 3H, CH_3), δ 3.28 (bm, 8H, CH), δ 2.73 (s, 2H, CH_2).

FC3 (9)

Prepared according to general deprotection procedure. Product: Pink powder, 43 % yield.

^{1}H NMR [$CDCl_3$, 400MHz]: δ 8.63 (s, 1H, CH), δ 8.30 (m, 2H, CH), δ 7.78 (m, 4H, CH), δ 7.27 (m, 4H, CH), δ 6.94 (m, 1H, CH), δ 4.70 (s, 2H, CH_2), δ 4.28 (m, 2H, CH_2),

δ 3.54 (s, 2H, CH_2), δ 3.38 (s, 1H, CH), δ 3.33 (s, 3H, CH_3), δ 3.11 (m, 2H, CH_2), δ 3.54

(m, 6H, CH_2).

2-methyl-7-hydroxy-1,4- naphthoquinone (10)

4-bromo-1-methylbenzoquinone was added to a dry 25 ml rbf, equipped with a stir bar, and dissolved in 10 ml of DCM. The flask was flushed with nitrogen and wrapped with foil before being cooled to 0 C. The diene was then added dropwise to the solution and the reaction mixture was allowed to warm to RT over 2 hours. 1.5 eq of Pyridine was then added to the reaction flask and the reaction mixture was allowed to stir for another 6 h. The crude residue was concentrated in vacuo and then dissolved in 15 ml of DCM. 3 ml of 2 M HCL was added to the solution and the organic layer was washed with 3, 10 ml portions of DI H_2O before being dried over $MgSO_4$. The pure product was isolated via flash column with a 33:66 (v/v) EtOAc/toluene eluting solvent. Tan powder, 21 % yield.

^{1}H NMR [$CDCl_3$, 400MHz]: δ 9.65 (s, 1H, OH), δ 7.97 (d, 1H, CH), δ 7.41 (d, 1H, CH), δ 7.23 (dd, 1H, CH), δ 6.83 (s, 1H, CH), δ 2.15 (s, 3H, CH).

(Bromo)-2-methyl- 1,4-naphthoquinone (12)

500 mg of menadione was added to a dry rbf equipped with a stir bar and dissolved in 12 ml of ACN. The starting material was cooled to 0 °C and 1.2 eq of NBS (dissolved in 4 ml of ACN) was added to the stirring mixture dropwise. The reaction flask was wrapped with foil and exposed to uv light for 2 h. The crude material was isolated via rotary evaporation. The pure product was isolated via flash column with a 30/70 (v/v) EtOAc/Hexane eluting solvent. Yellow powder, 30% yield.

^{1}H NMR [$CDCl_3$, 400MHz]: δ 8.05 (s, 1H, CH), δ 7.77 (m, 1H, CH) δ 6.83 (m, 2H, CH), δ 2.45 (s, 2H, CH_2).

PARPiL2 (13)

500 mg of PARPi and 1.2 eq of Succinic Anhydride was added to a dry 100 ml RBF equipped with a stir bar and dissolved in 30 ml of DMF. 2 eq of DIPEA was charged into the flask and the mixture was stirred at 100 °C for 24 h. The crude material was extracted with DCM and washed with 2, 2 ml portions of 2 N HCL and then with DI H2O. The crude material was purified via column chromatography with a 3.5% MeOH/DCM eluting solvent. 94% Yield (600 mg). Produced a yellow powder

^{1}H NMR [$CDCl_3$, 400MHz]: δ 11.52 (s, 1H, NH), δ 8.43 (s, 1H, CH), δ 7.75 (m, 3H,

CH), δ 7.28 (m, 2H, CH), δ 7.00 (m, 1H, CH), δ 4.28 (s, 2H, CH_2), δ 3.8 (m, 2H, CH_2), δ

3.64 (m, 2H, CH_2), δ 3.31 (m, 2H, CH_2), δ 3.02 (s, 2H, CH_2), δ 2.85 (m, 2H, CH_2), δ 2.75 (m, 2H, CH_2).

FC4 (14)

500 mg of PARPiL1 **(5)** was added to a dry 50 ml RBF equipped with a stir bar and dissolved in 10 ml of ACN. 2 eq of DIPEA was added to the reaction vessel and the mixture was heated to a mild reflux. 1.2 eq of (Bromo)-2-methyl- 1,4-naphthoquinone (12) was then charged into the flask and the mixture was refluxed vigorously at 100 °C for 6 hours. Upon completion of the reaction the ACN was completely removed and the crude material was dissolved in DCM and washed with 2, 5 ml DI H_2O. The product was isolated via flash column with a 5:95 (v/v) MeOH/DCM eluting solvent. White powder

FC5 (15)

100 mg of Hydroxymendadione **(10)** and 1.2 eq of PARPiL2 **(13)** was added to a dry 100 ml RBF equipped with a stir bar and dissolved in 10 ml of ACN. 0.01 eq of DMAP and 2 eq of EDC.HCl was charged into the flask simultaneously and the mixture was stirred at 0 °C for 2 h and then at RT for 12 h. The crude material was extracted with DCM and washed with 3, 5 ml portions of DI H_2O. Product was purified using flash column chromatography with an eluting solvent of 3.5 % MeOH in DCM.

CHAPTER 4. CELLULAR ANALYSIS OF SMALL MOLECULE PARP-IDO INHIBITORS

4.1 Introduction

As previously discussed, PARP and IDO are both commonly coopted by cancer cells to promote unchecked cell growth within the tumor microenvironment. The downstream metabolites and effector pathways of both enzymes are intertwined in ways that have not been thoroughly investigated. The conjugate inhibitors synthesized in chapter 3 were designed to target cells that over express one or both of the target enzymes. The selected cell lines were chosen by whether they had germline mutations to either BRC1 or BRC2, or if they endogenously expressed IDO. Within the tumor microenvironment, cancer cells themselves can express IDO upon stimulation by INFγ. or by mutations that cause constitutive expression. By synthesizing conjugate inhibitors that could target these cells, we aimed to highlight novel and synergistic effector pathways between the two enzymes.

4.2 Results and Discussion

The efficacy of FC2 and FC3 was first tested in MDA-MB-231, metastatic TNBC cells without germline BRCA mutations. After a 72 hour treatment with variable treatment concentrations, our data showed that FC2, the amide coupled conjugate had stronger inhibitory activity than the ester coupled conjugate. The IC50 values for both the FC2 and FC3 compound were 6.17 μM ± 0.09 and 13.48 μM ± 1.07 respectively.

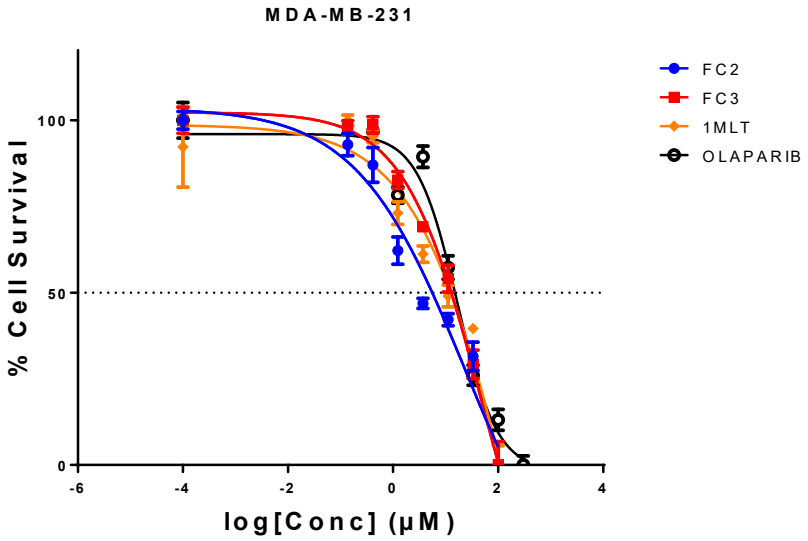

Figure 4.1 Cytoxic efficacy of conjugate inhibitors on cell viability of MDA-MB-231

The conjugate inhibitors were then tested in HCC-1937, a metastatic TNBC cell line with a germline BRCA1 mutation at nt5832insC. HCC-1937 endogenously expresses PARP and is particularly susceptible to monotherapy treatment of Olaparib with an IC_{50} of ~ 12 µM in literature. Upon 72 hour treatment with our conjugate inhibitors we obtained IC_{50} values of 3.63 µM ± 0.12 and 5.97 µM ± 0.46 for the FC2 and FC3 compounds respectively. The conjugate inhibitor FC2 was therefore found to be more potent than Olaparib in the BRCA deficient cell lines. In fact, FC2 was found to be most effective in the BRCA1 deficient cell lines, indicating a mechanism of action that directly affects PARP function. FC2 is unlikely to break apart upon entry into the cell due to the strong amide bond linkage, and therefore must be exerting its inhibitory effect on PARP regardless of the 1-MLT inhibitor moiety.

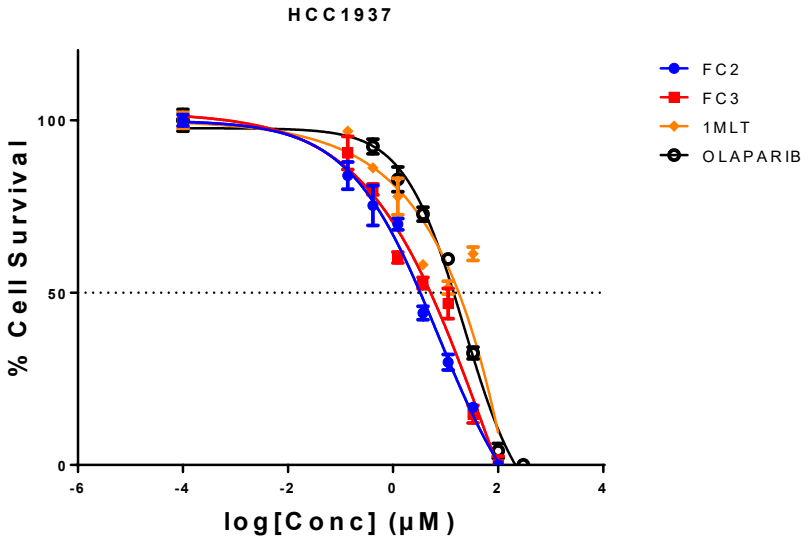

Figure 4.2 Cytoxic efficacy of conjugate inhibitors on cell viability of HCC-1937

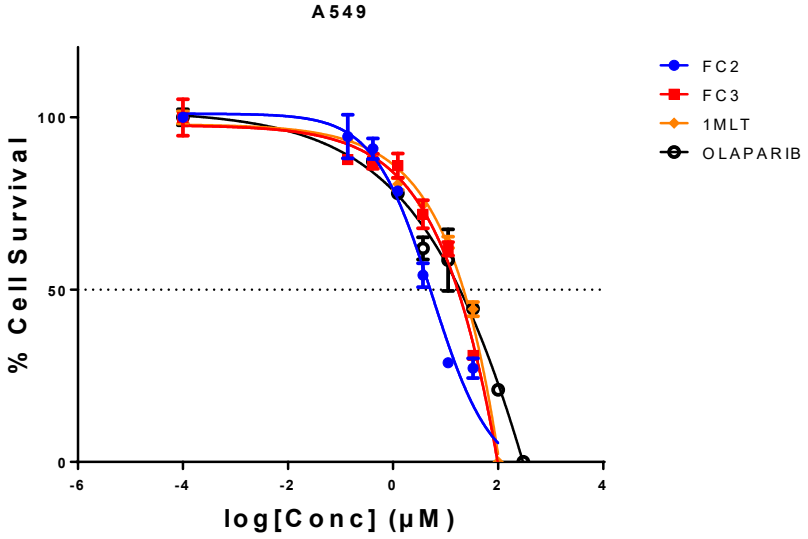

Figure 4.3 Cytoxic efficacy of conjugate inhibitors on cell viability of A549

A549 is a non-small cell lung carcinoma (NSCLC) cell line that does not have a germline BRCA mutation. Previous studies have shown that A549 is fairly resistant to Olaparib unless combined with concurrent radiation treatment. Our compounds were tested in this

cell line to determine efficacy in a lung cancer cell line since lung cancers are the most prevalent form of cancer. The previous trend continued with the conjugate inhibitors achieving much lower IC_{50} values than their parent inhibitor counterparts.

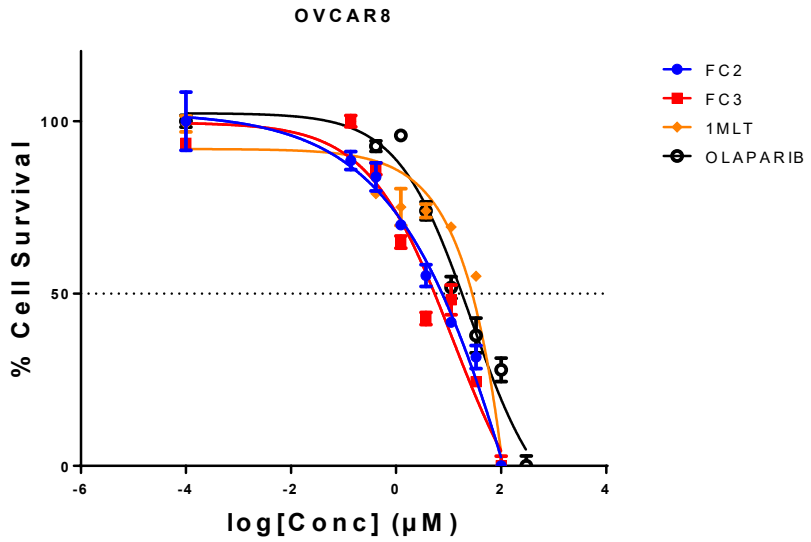

Figure 4.4 Cytoxic efficacy of conjugate inhibitors on cell viability of OVCAR8

We also tested our compounds in OVCAR8 cells, an ovarian cell line that is susceptible to multiple BRCA1 mutations. Our results showed FC2 and FC3 to be more toxic than monotreatment with the PARP inhibitor Olaparib or the IDO inhibitor 1-MLT.

FC2 in particular proved to be particularly cytoxic, even without an easily degradable linker joining the conjugates. FC3's ester linker could be responsible for the variance in potency between cell lines. The compound could be degrading upon entry into the cell and losing its effectiveness since it has been shown that Olaparib and 1-MLT both have much weaker IC_{50} values as monotherapies.

Table 4.1 Cytoxic efficacy of conjugate inhibitors on cell viability of OVCAR8

Cell Line	**IC_{50}**			
	FC2	FC3	OLAPARIB	1MLT
A549	5.37 ± 0.23	18.20 ± 0.18	19.95 ± 1.66	22.91 ± 2.67
HCC1937	3.63 ± 0.12	5.97± 0.46	14.79± 3.28	19.95± 1.07
MDA-MB-231	6.17 ± 0.09	13.48±1.07	16.59-± 2.07	12.30± 1.88
OVCAR8	5.62 ± 0.12	7.76 ± 0.16	18.20 ± 1.22	29.51 ± 3.27

1-MLT was not found to be particularly active in any of the tested cell lines. This is primarily due to the fact that none of the current cell lines endogenously express IDO. The effectiveness of the conjugate inhibitors compared to single treatment with 1-MLT and IDO are summarized in table 4.1. The compound FC2 shows promising cytotoxicity in all cell lines and could be utilized as a probe in future analysis.

4.3 Future Directions

While the cell viability data proves our conjugate compounds are much more potent than the small molecule inhibitors they were derived from, there is more work needed to fully characterize the relationship between PARP and IDO. No cell lines that endogenously express IDO were tested, depriving us of information on whether our conjugate inhibitors were affecting IDO as well. Kynurenine detection experiments in cell lines that over express IDO would shine light on whether our compound directly effects IDO or is exacting its effect through an alternate pathway. Measuring the level of DNA damage and

PARP expression upon treatment with the conjugate drugs would help determine if our compounds were perturbing the DNA damage response.

To fully understand the interplay between IDO and PARP, co-co culture experiments with activated macrophages and T-cells would need to be run. These multi-cell cultures would elucidate novel mechanisms of action and synergy between IDO and PARP since IDO production is often induced by signals from peripheral cells. The role of PARP in the recruitment, activation, and differentiation of peripheral cells could then be studied upon inhibition with conjugate inhibitors. NAD/NADH levels would also need to be monitored in these systems to look at energy usage and mitochondrial activity in the tumor micro environment. These tests would provide an in depth exploration of any synergy or interplay between IDO and PARP and could provide hints at new targets for small molecule immunotherapeutics.

4.4 Experimental Procedures

Cell Culture[198]

All human immortalized cell lines were obtained from the American Type Culture Collection (ATCC) and were cultured per ATCC propagation instructions; cells were routinely grown in a humidified incubator at 37 °C with 5% CO_2. H460, HCC1937 human cells were grown in RPMI containing 10% FBS, 1% Penicillin/ Streptomycin, 4mM glutamine. MDA-MB-231, A549 cells were grown in DMEM containing 10% FBS, 1% Penicillin/ Streptomycin, 4mM glutamine. All media and supplements were obtained from VWR, USA.

MTT Assay[198]

Cells were counted to make a solution of 20,000 cells/mL. 100 mL of the cell solution was transferred to the desired wells on a clear 96-well plate. Cells were incubated overnight at 37 ^{o}C to allow cells to adhere to the plate. After incubation solutions of the compounds to be tested were prepared in a minimal volume of DMSO. 1-MLT solutions were dissolved in 0.2 M NaOH in H20/DMSO to ensure complete dissolution.

Compound solutions were diluted to the appropriate volume with media, so that the highest concentration is 3x the desired maximum within the well plate

50 mL of the desired concentration was added to the top 3 consecutive vertical wells. A second compound was added to the bottom 3 consecutive vertical wells. The process was continued via serial dilution until all wells were filled. Cells were incubated for 72 h at 37 ^{o}C. A 2 mg/mL solution of MTT ((3-(4,5-Dimethylthiazol-2-yl)-2,5-Diphenyltetrazolium Bromide) dissolved in PBS was added (50 mL per well) to each of the test wells in the dark. The plates were wrapped in foil and incubated 4 hours at 37 ^{o}C. The plates were then removed from the incubator and all media was removed from the well plates via suctioning with the multichannel pipette. 100 mL of DMSO was then added to each well. A Magellan plate reader was used to read the plates using the MTT assay protocol: 570nm, 3 flashes, 5 second orbital rotation. Data was plotted in GraphPad Prism 6.

Crystal Violet Assay[198]

Follow MTT protocol for treatment of cells. After the 72 h incubation period, remove media from the wells. Wells were gently rinsed with 100 mL of PBS. The PBS was removed and 100 µL of 1% glutaraldehyde solution was added to each well. Plates were incubated 10 minutes in the incubator. The solution was removed and the plates were dipped in H_2O and then allowed to dry. 50 µL of Crystal violet staining solution was then added to each well the plates were incubated at room temp while rocking at 20 rpm for 20 minutes. Plates were inverted and gently tapped on a paper towel to eliminate excess water. Plates were then placed in a non-sterile incubator for 2 hours to accelerate drying. Upon completion of drying, 190 µL of methanol was added to each well. Plates were read using the same parameters as MTT assay. Data was plotted in GraphPad Prism 6.

FC2 (BOC)

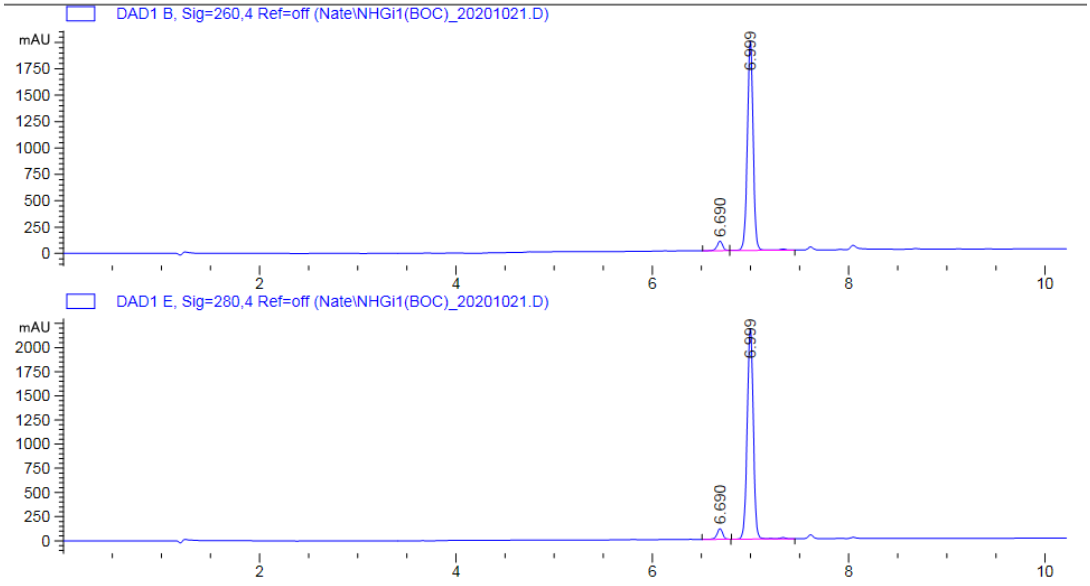

Signal 1: DAD1 B, Sig=260,4 Ref=off

Peak #	RetTime [min]	Type	Width [min]	Area [mAU*s]	Height [mAU]	Area %
1	6.690	BV	0.0627	357.45343	89.31129	4.1930
2	6.999	VV R	0.0637	8167.60156	1981.05688	95.8070
Totals :				8525.05499	2070.36818	

Signal 2: DAD1 E, Sig=280,4 Ref=off

Peak #	RetTime [min]	Type	Width [min]	Area [mAU*s]	Height [mAU]	Area %
1	6.690	BB	0.0617	432.01611	110.24840	4.3582
2	6.999	BV R	0.0685	9480.79199	2172.98584	95.6418
Totals :				9912.80811	2283.23424	

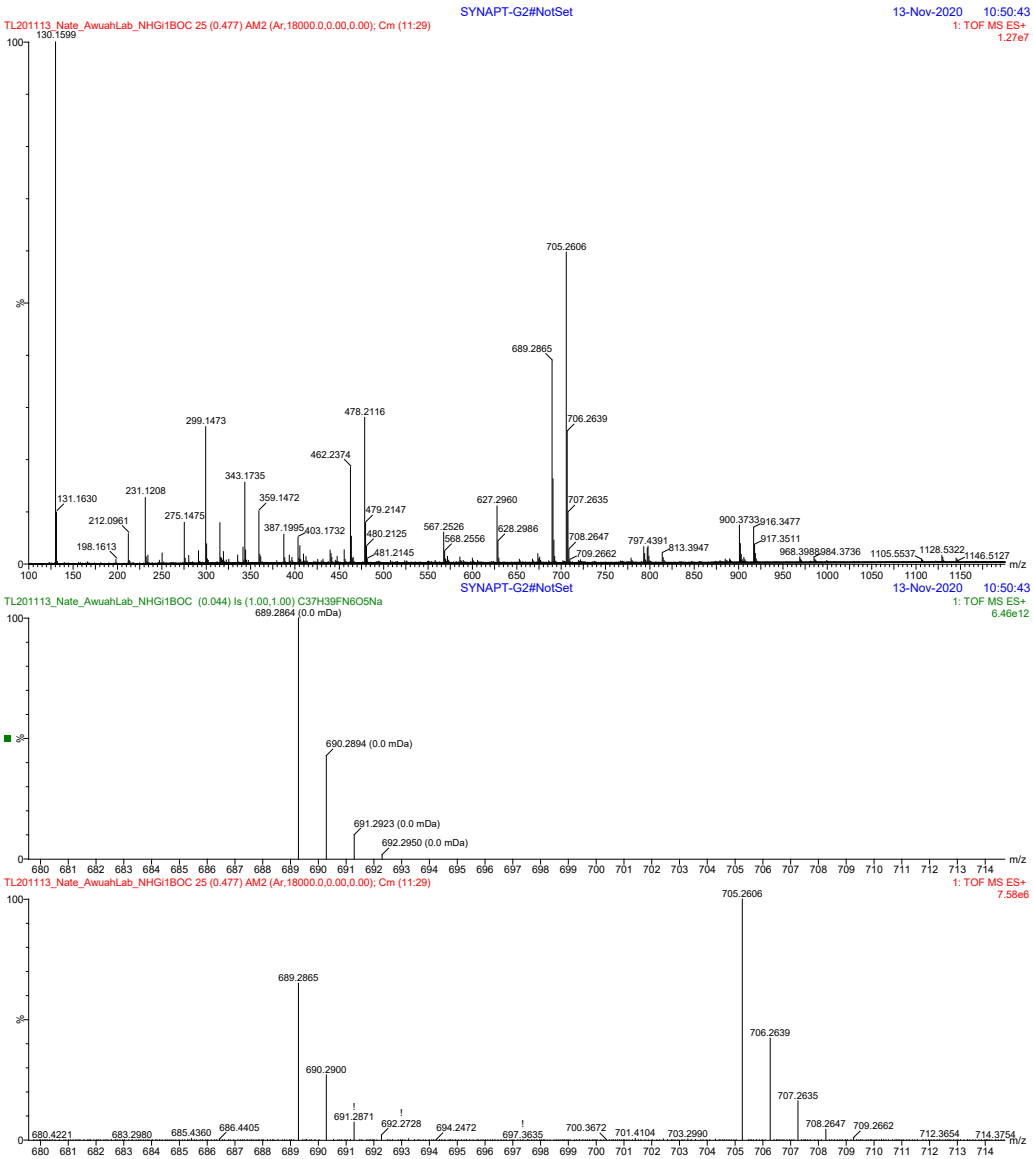
SYNAPT-G2#NotSet
13-Nov-2020 10:50:43
TL201113_Nate_AwuahLab_NHGi1BOC 25 (0.477) AM2 (Ar,18000.0,0.00,0.00); Cm (11:29)
1: TOF MS ES+
1.27e7
130.1599
705.2606
689.2865
706.2639
478.2116
299.1473
462.2374
343.1735
131.1630
231.1208
359.1472
479.2147
212.0961
275.1475
627.2960
707.2635
387.1995
403.1732
567.2526
480.2125
628.2986
198.1613
568.2556
481.2145
708.2647
797.4391
900.3733
916.3477
709.2662
813.3947
917.3511
968.3988
984.3736
1105.5537
1128.5322
1146.5127
m/z
SYNAPT-G2#NotSet
13-Nov-2020 10:50:43
TL201113_Nate_AwuahLab_NHGi1BOC (0.044) Is (1.00,1.00) C37H39FN6O5Na
1: TOF MS ES+
6.46e12
689.2864 (0.0 mDa)
690.2894 (0.0 mDa)
691.2923 (0.0 mDa)
692.2950 (0.0 mDa)
m/z
TL201113_Nate_AwuahLab_NHGi1BOC 25 (0.477) AM2 (Ar,18000.0,0.00,0.00); Cm (11:29)
1: TOF MS ES+
7.58e6
705.2606
689.2865
706.2639
690.2900
707.2635
691.2871
692.2728
708.2647
709.2662
694.2472
697.3635
700.3672
701.4104
703.2990
680.4221
683.2980
685.4360
686.4405
712.3654
714.3754
m/z

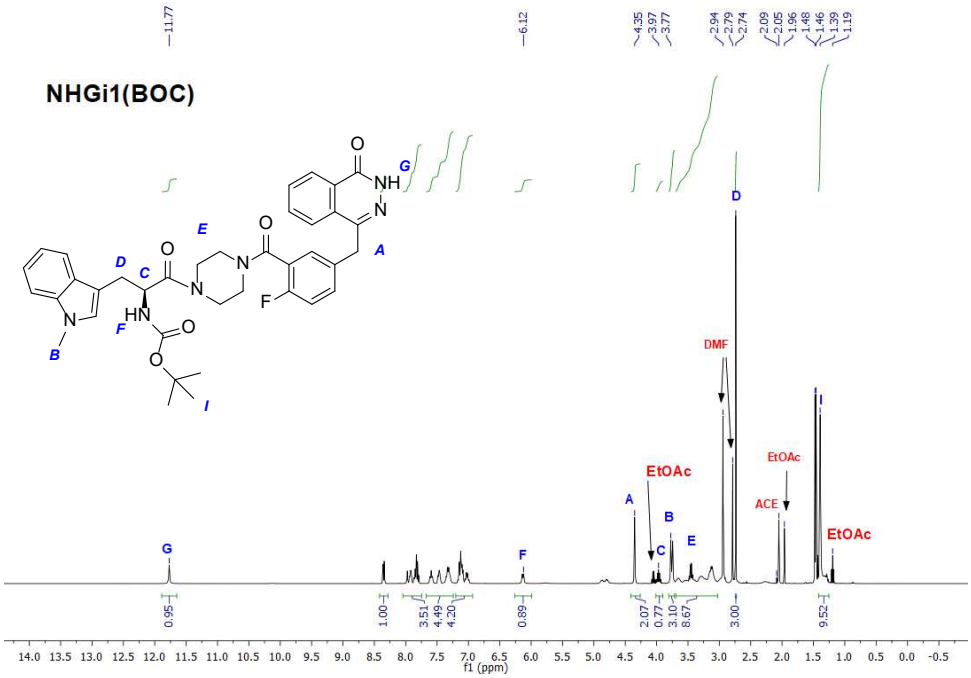
NHGi1(BOC)
11.77
6.12
4.35
3.97
3.77
2.94
2.79
2.74
2.09
2.05
1.96
1.48
1.46
1.39
1.19
G
E
D
C
A
F
B
I
DMF
EtOAc
EtOAc
ACE
EtOAc
0.95
1.00
3.51
4.49
4.20
0.89
2.07
0.77
3.10
8.67
3.00
9.52
f1 (ppm)

FC2

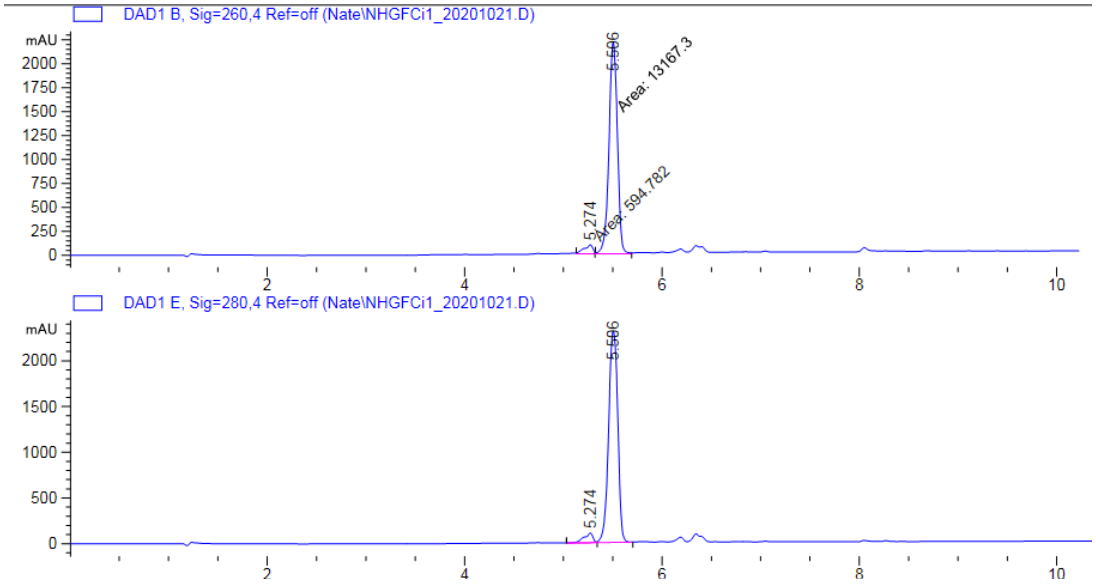

Signal 1: DAD1 B, Sig=260,4 Ref=off

Peak #	RetTime [min]	Type	Width [min]	Area [mAU*s]	Height [mAU]	Area %
1	5.274	MM T	0.1053	594.78174	94.13705	4.3219
2	5.506	MM T	0.1356	1.31673e4	2210.81567	95.6781
Totals :				1.37621e4	2304.95272	

Signal 2: DAD1 E, Sig=280,4 Ref=off

Peak #	RetTime [min]	Type	Width [min]	Area [mAU*s]	Height [mAU]	Area %
1	5.274	BV E	0.0865	661.12146	106.43625	4.2373
2	5.506	VB R	0.1035	1.49412e4	2307.83936	95.7627
Totals :				1.56024e4	2414.27560	

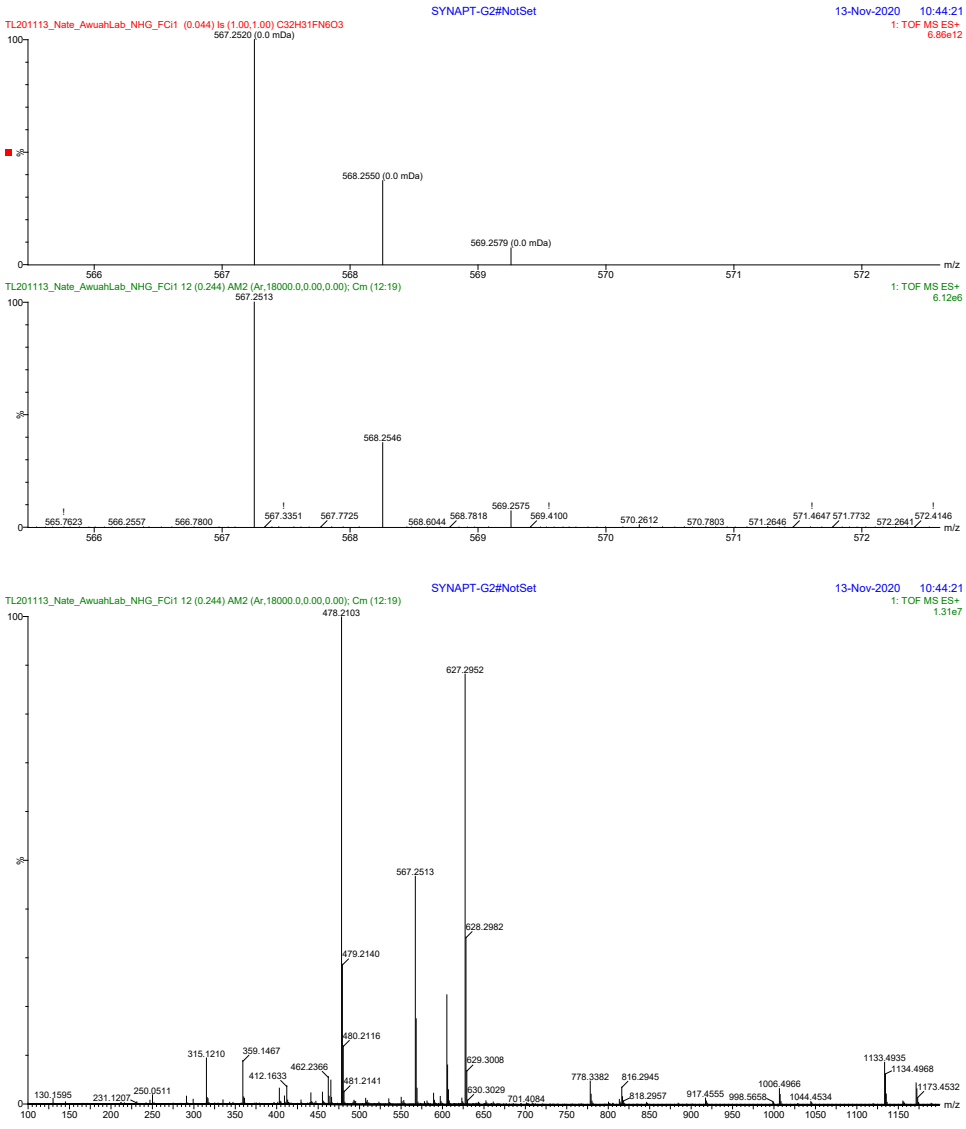
SYNAPT-G2#NotSet
13-Nov-2020 10:44:21
TL201113_Nate_AwuahLab_NHG_FCi1 (0.044) Is (1.00,1.00) C32H31FN6O3
1: TOF MS ES+
6.86e12
567.2520 (0.0 mDa)
568.2550 (0.0 mDa)
569.2579 (0.0 mDa)
TL201113_Nate_AwuahLab_NHG_FCi1 12 (0.244) AM2 (Ar,18000.0,0.00,0.00); Cm (12:19)
1: TOF MS ES+
6.12e6
567.2513
568.2546
569.2575
m/z
SYNAPT-G2#NotSet
13-Nov-2020 10:44:21
TL201113_Nate_AwuahLab_NHG_FCi1 12 (0.244) AM2 (Ar,18000.0,0.00,0.00); Cm (12:19)
1: TOF MS ES+
1.31e7
478.2103
627.2952
567.2513
628.2982
479.2140
480.2116
629.3008
315.1210
359.1467
462.2366
412.1633
481.2141
630.3029
778.3382
816.2945
818.2957
1133.4935
1134.4968
1173.4532
1006.4966
m/z

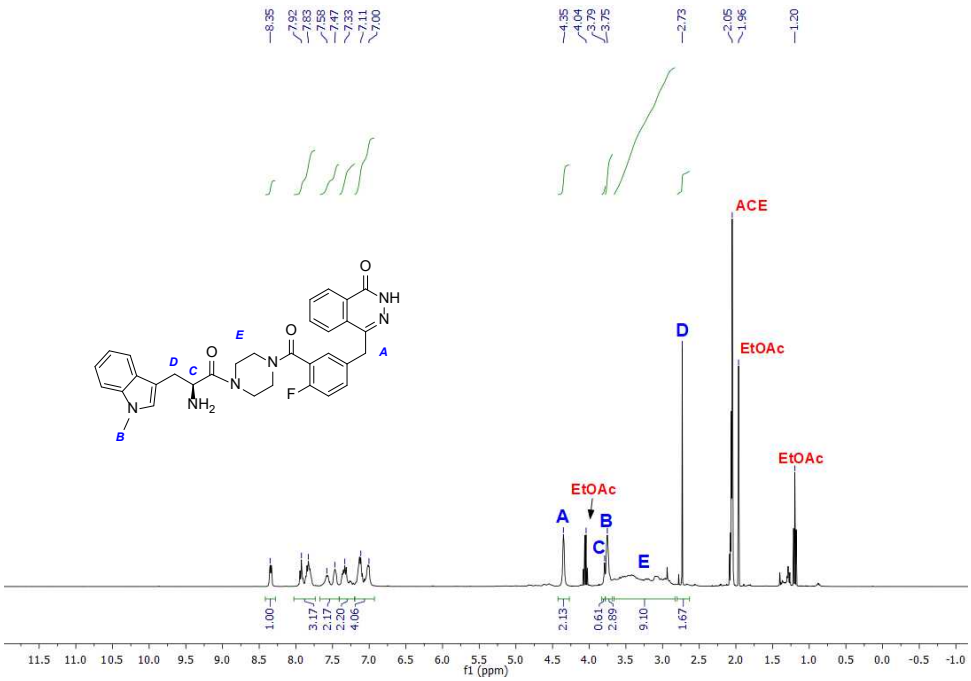
8.35
7.92
7.83
7.58
7.47
7.33
7.11
7.00
4.35
4.04
3.79
3.75
2.73
2.05
1.96
1.20
ACE
EtOAc
EtOAc
EtOAc
A
B
C
D
E
NH
N
O
F
NH2
1.00
3.17
2.17
2.20
4.06
2.13
0.61
2.89
9.10
1.67
f1 (ppm)

FC3

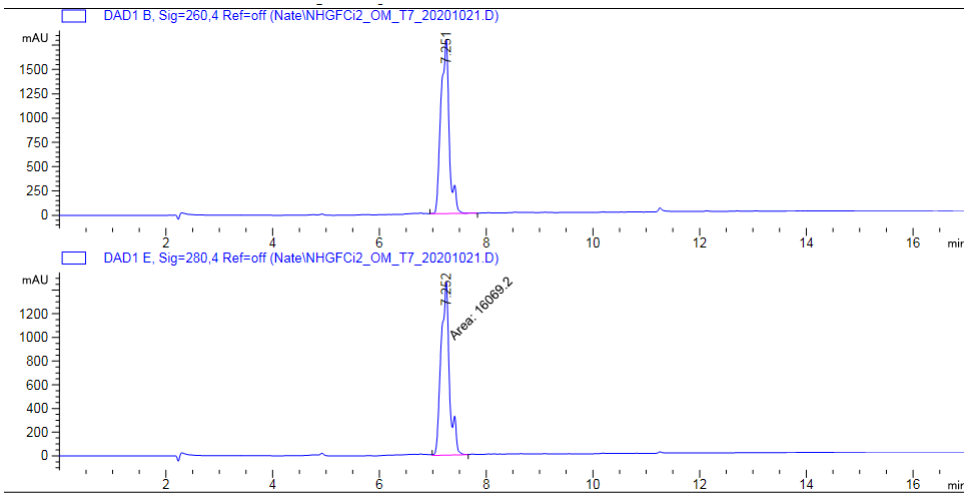

Signal 1: DAD1 B, Sig=260,4 Ref=off

Peak #	RetTime [min]	Type	Width [min]	Area [mAU*s]	Height [mAU]	Area %
1	7.251	BV R	0.1361	1.92990e4	1793.77527	100.0000
Totals :				1.92990e4	1793.77527	

Signal 2: DAD1 E, Sig=280,4 Ref=off

Peak #	RetTime [min]	Type	Width [min]	Area [mAU*s]	Height [mAU]	Area %
1	7.252	MM T	0.1821	1.60692e4	1470.73108	100.0000
Totals :				1.60692e4	1470.73108	

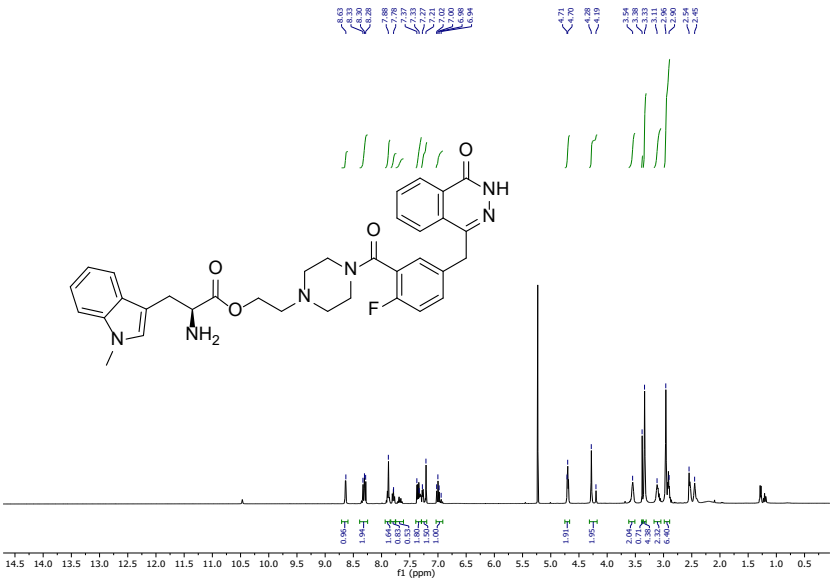
8.63
8.33
8.30
8.28
7.88
7.78
7.77
7.33
7.27
7.21
7.03
7.00
6.98
6.94
4.71
4.70
4.28
4.10
3.54
3.38
3.33
3.11
2.96
2.90
2.54
2.46
O
NH
N
O
N
O
O
N
F
NH2
N
0.96
1.94
1.64
0.83
0.83
0.97
1.90
1.00
1.91
1.95
3.04
2.71
4.38
2.10
6.64
14.5 14.0 13.5 13.0 12.5 12.0 11.5 11.0 10.5 10.0 9.5 9.0 8.5 8.0 7.5 7.0 6.5 6.0 5.5 5.0 4.5 4.0 3.5 3.0 2.5 2.0 1.5 1.0 0.5
f1 (ppm)

REFERENCES

1. Prendergast, G. C.; Smith, C.; Thomas, S.; Mandik-Nayak, L.; Laury-Kleintop, L.; Metz, R.; Muller, A. J., Indoleamine 2,3-dioxygenase pathways of pathgenic inflammation and immune escape in cancer. *Cancer immunology, immunotherapy : CII* **2014,** *63* (7), 721-735.
2. Prendergast, G. C., Immune escape as a fundamental trait of cancer: focus on IDO. *Oncogene* **2008,** *27*, 3889.
3. Soliman, H.; Mediavilla-Varela, M.; Antonia, S., Indoleamine 2,3-Dioxygenase: Is It an Immune Suppressor? *Cancer journal (Sudbury, Mass.)* **2010,** *16* (4), 10.1097/PPO.0b013e3181eb3343.
4. Interest in IDO inhibitors remains high. *C&EN Global Enterprise* **2018,** *96* (14), 12-12.
5. Incyte drug failure casts shadow on IDO class. *C&EN Global Enterprise* **2018,** *96* (16), 11-11.
6. Companies Scaling Back IDO1 Inhibitor Trials. *Cancer Discovery* **2018**.
7. Bilir, C.; Sarisozen, C., Indoleamine 2,3-dioxygenase (IDO): Only an enzyme or a checkpoint controller? *Journal of Oncological Sciences* **2017,** *3* (2), 52-56.
8. Munn, D. H.; Zhou, M.; Attwood, J. T.; Bondarev, I.; Conway, S. J.; Marshall, B.; Brown, C.; Mellor, A. L., Prevention of Allogeneic Fetal Rejection by Tryptophan Catabolism. *Science* **1998,** *281* (5380), 1191-1193.
9. Grohmann, U.; Fallarino, F.; Puccetti, P., Tolerance, DCs and tryptophan: much ado about IDO. *Trends in Immunology* **2003,** *24* (5), 242-248.
10. Uyttenhove, C.; Pilotte, L.; Théate, I.; Stroobant, V.; Colau, D.; Parmentier, N.; Boon, T.; Van den Eynde, B. J., Evidence for a tumoral immune resistance mechanism based on tryptophan degradation by indoleamine 2,3-dioxygenase. *Nature Medicine* **2003,** *9*, 1269.
11. Nelson, B. H., The impact of T-cell immunity on ovarian cancer outcomes. *Immunological Reviews* **2008,** *222* (1), 101-116.
12. Zhang, L.; Conejo-Garcia, J. R.; Katsaros, D.; Gimotty, P. A.; Massobrio, M.; Regnani, G.; Makrigiannakis, A.; Gray, H.; Schlienger, K.; Liebman, M. N.; Rubin, S. C.; Coukos, G., Intratumoral T Cells, Recurrence, and Survival in Epithelial Ovarian Cancer. *New England Journal of Medicine* **2003,** *348* (3), 203-213.
13. Zhao, Q.; Wang, P.-p.; Huang, Z.-l.; Peng, L.; Lin, C.; Gao, Z.; Su, S., Tumoral indoleamine 2, 3-dioxygenase 1 is regulated by monocytes and T lymphocytes collaboration in hepatocellular carcinoma. *Oncotarget* **2016,** *7* (12), 14781-14790.
14. Kazuhiko Ino, Y. T. A. K. S. T. Y. M.; Sawako, M., Role of the Immune Tolerance-Inducing Molecule Indoleamine 2,3-Dioxygenase in Gynecologic Cancers. *Journal of Cancer Science & Therapy* **2013,** *5* (8), -.
15. Vigneron, N.; van Baren, N.; Van den Eynde, B. J., Expression profile of the human IDO1 protein, a cancer drug target involved in tumoral immune resistance. *Oncoimmunology* **2015,** *4* (5), e1003012.
16. Yoshida, N.; Ino, K.; Ishida, Y.; Kajiyama, H.; Yamamoto, E.; Shibata, K.; Terauchi, M.; Nawa, A.; Akimoto, H.; Takikawa, O.; Isobe, K.-i.; Kikkawa, F., Overexpression of Indoleamine 2,3-Dioxygenase in Human Endometrial Carcinoma Cells

Induces Rapid Tumor Growth in a Mouse Xenograft Model. *Clinical Cancer Research* **2008,** *14* (22), 7251-7259.
17. Okamoto, A.; Nikaido, T.; Ochiai, K.; Takakura, S.; Saito, M.; Aoki, Y.; Ishii, N.; Yanaihara, N.; Yamada, K.; Takikawa, O.; Kawaguchi, R.; Isonishi, S.; Tanaka, T.; Urashima, M., Indoleamine 2,3-Dioxygenase Serves as a Marker of Poor Prognosis in Gene Expression Profiles of Serous Ovarian Cancer Cells. *Clinical Cancer Research* **2005,** *11* (16), 6030-6039.
18. Hornyák, L.; Dobos, N.; Koncz, G.; Karányi, Z.; Páll, D.; Szabó, Z.; Halmos, G.; Székvölgyi, L., The Role of Indoleamine-2,3-Dioxygenase in Cancer Development, Diagnostics, and Therapy. *Frontiers in Immunology* **2018,** *9* (151).
19. Muller, A. J.; DuHadaway, J. B.; Donover, P. S.; Sutanto-Ward, E.; Prendergast, G. C., Inhibition of indoleamine 2,3-dioxygenase, an immunoregulatory target of the cancer suppression gene Bin1, potentiates cancer chemotherapy. *Nature Medicine* **2005,** *11*, 312.
20. Frumento, G.; Rotondo, R.; Tonetti, M.; Damonte, G.; Benatti, U.; Ferrara, G. B., Tryptophan-derived Catabolites Are Responsible for Inhibition of T and Natural Killer Cell Proliferation Induced by Indoleamine 2,3-Dioxygenase. *The Journal of Experimental Medicine* **2002,** *196* (4), 459-468.
21. Smith, C.; Chang, M. Y.; Parker, K. H.; Beury, D. W.; DuHadaway, J. B.; Flick, H. E.; Boulden, J.; Sutanto-Ward, E.; Soler, A. P.; Laury-Kleintop, L. D.; Mandik-Nayak, L.; Metz, R.; Ostrand-Rosenberg, S.; Prendergast, G. C.; Muller, A. J., IDO Is a Nodal Pathogenic Driver of Lung Cancer and Metastasis Development. *Cancer Discovery* **2012,** *2* (8), 722-735.
22. Prendergast, G. C.; Jaffee, E. M., *Cancer Immunotherapy: Immune Suppression and Tumor Growth*. Elsevier Science: 2013.
23. O'Sullivan, B. J.; Pai, S.; Street, S.; An, X.; MacDonald, K. P. A.; Wong, M.; Strutton, G.; Gerondakis, S.; Steptoe, R. J.; Fazekas de St. Groth, B.; Hill, G. R.; Thomas, R., Immunotherapy with Costimulatory Dendritic Cells To Control Autoimmune Inflammation. *J. Immunol.* **2011,** *187* (8), 4018-4030.
24. Paveglio, S. A.; Allard, J.; Foster Hodgkins, S. R.; Ather, J. L.; Bevelander, M.; Campbell, J. M.; Whittaker LeClair, L. A.; McCarthy, S. M.; van der Vliet, A.; Suratt, B. T.; Boyson, J. E.; Uematsu, S.; Akira, S.; Poynter, M. E., Airway epithelial indoleamine 2,3-dioxygenase inhibits CD4+ T cells during Aspergillus fumigatus antigen exposure. *Am. J. Respir. Cell Mol. Biol.* **2011,** *44* (1), 11-23.
25. Koch, L. K.; Bucher, C.; Panoskaltsis-Mortari, A.; Mellor, A. L.; Munn, D. H.; Blazar, B. R., Inducing the tryptophan catabolic pathway, indoleamine 2,3-dioxygenase (IDO), for suppression of graft-versus-host disease (GVHD) lethality. *Blood* **2009,** *114* (24), 5062-5070.
26. Lin, Y. C.; Goto, S.; Tateno, C.; Nakano, T.; Cheng, Y. F.; Jawan, B.; Kao, Y. H.; Hsu, L. W.; Lai, C. Y.; Yoshizato, K.; Chen, C. L., Induction of Indoleamine 2,3-Dioxygenase in Livers Following Hepatectomy Prolongs Survival of Allogeneic Hepatocytes After Transplantation. *Transplant. Proc.* **2008,** *40* (8), 2706-2708.
27. Lin, Y.-C.; Chen, C.-L.; Nakano, T.; Goto, S.; Kao, Y.-H.; Hsu, L.-W.; Lai, C.-Y.; Jawan, B.; Cheng, Y.-F.; Tateno, C.; Yoshizato, K., Immunological role of indoleamine 2,3-dioxygenase in rat liver allograft rejection and tolerance. *J. Gastroenterol. Hepatol.* **2008,** *23* (7, Pt. 2), e243-e250.

28. Lu, A.; Zhang, J.; Wang, L.; Zhang, X.; Zhang, M., Role of indoleamine 2,3-dioxygenase in an animal asthma model. *Linchuang Erke Zazhi* **2011,** *29* (4), 301-306.
29. Jia, S.; Guo, P.; Ge, X.; Wu, H.; Lu, J.; Fan, X., Overexpression of indoleamine 2,3-dioxygenase contributes to the repair of human airway epithelial cells inhibited by dexamethasone via affecting the MAPK/ERK signaling pathway. *Exp. Ther. Med.* **2018,** *16* (1), 1-9.
30. Liu, H.-y.; Wang, F.-f.; Miao, W.-w.; Yin, K.-s.; Zhou, L.-f., Application of indoleamine 2,3-dioxygenase as new target for immunotherapy of bronchial asthma. *Zhonghua Weishengwuxue He Mianyixue Zazhi* **2012,** *32* (9), 831-834.
31. Ericsson, P.; Hedbys, L.; Salford, L.; Sjoegren, H.-O. Novel treatment method to induce immune tolerance to drugs. WO2016146842A1, 2016.
32. Ericsson, P.; Hedbys, L.; Salford, L.; Sjogren, H.-O. Novel treatment method to induce immune tolerance to drugs comprising ex-vivo treating antigen-presenting cells with an inducer of IDO (indolamine dioxygenase) and transferring those cells back to the mammal. US20170014499A1, 2017.
33. Asghar, K.; Ashiq, M. T.; Zulfiqar, B.; Mahroo, A.; Nasir, K.; Murad, S., Indoleamine 2,3-dioxygenase expression and activity in patients with hepatitis C virus-induced liver cirrhosis. *Exp Ther Med* **2015,** *9* (3), 901-904.
34. Asghar, K.; Farooq, A.; Zulfiqar, B.; Rashid, M. U., Indoleamine 2,3-dioxygenase: As a potential prognostic marker and immunotherapeutic target for hepatocellular carcinoma. *World Journal of Gastroenterology* **2017,** *23* (13), 2286-2293.
35. Nagano, J.; Shimizu, M.; Hara, T.; Shirakami, Y.; Kochi, T.; Nakamura, N.; Ohtaki, H.; Ito, H.; Tanaka, T.; Tsurumi, H.; Saito, K.; Seishima, M.; Moriwaki, H., Effects of Indoleamine 2,3-Dioxygenase Deficiency on High-Fat Diet-Induced Hepatic Inflammation. *PLoS ONE* **2013,** *8* (9), e73404.
36. Niinisalo, P.; Oksala, N.; Levula, M.; Pelto-Huikko, M.; Jaervinen, O.; Salenius, J.-P.; Kytoemaeki, L.; Soini, J. T.; Kaehoenen, M.; Laaksonen, R.; Hurme, M.; Lehtimaeki, T., Activation of indoleamine 2,3-dioxygenase-induced tryptophan degradation in advanced atherosclerotic plaques: Tampere Vascular Study. *Ann. Med. (London, U. K.)* **2010,** *42* (1), 55-63.
37. Vareki, S. M.; Rytelewski, M.; Figueredo, R.; Chen, D.; Ferguson, P. J.; Vincent, M.; Min, W.; Zheng, X.; Koropatnick, J., Indoleamine 2,3-dioxygenase mediates immune-independent human tumor cell resistance to olaparib, gamma radiation, and cisplatin. *Oncotarget* **2014,** *5* (9), 2778-2791.
38. Maleki Vareki, S.; Chen, D.; Di Cresce, C.; Ferguson, P. J.; Figueredo, R.; Pampillo, M.; Rytelewski, M.; Vincent, M.; Min, W.; Zheng, X.; Koropatnick, J., IDO Downregulation Induces Sensitivity to Pemetrexed, Gemcitabine, FK866, and Methoxyamine in Human Cancer Cells. *PLOS ONE* **2015,** *10* (11), e0143435.
39. Ino, K.; Yoshida, N.; Kajiyama, H.; Shibata, K.; Yamamoto, E.; Kidokoro, K.; Takahashi, N.; Terauchi, M.; Nawa, A.; Nomura, S.; Nagasaka, T.; Takikawa, O.; Kikkawa, F., Indoleamine 2,3-dioxygenase is a novel prognostic indicator for endometrial cancer. *British journal of cancer* **2006,** *95* (11), 1555-1561.
40. Brandacher, G.; Perathoner, A.; Ladurner, R.; Schneeberger, S.; Obrist, P.; Winkler, C.; Werner, E. R.; Werner-Felmayer, G.; Weiss, H. G.; G√∂bel, G.; Margreiter, R.; K√∂nigsrainer, A.; Fuchs, D.; Amberger, A., Prognostic value of indoleamine 2,3-

dioxygenase expression in colorectal cancer: effect on tumor-infiltrating T cells. *Clinical Cancer Research* **2006,** *12* (4), 1144-1151.
41. Munn, D. H.; Mellor, A. L., IDO in the Tumor Microenvironment: Inflammation, Counter-Regulation, and Tolerance. *Trends in Immunology* **2016,** *37* (3), 193-207.
42. Munn, D. H.; Mellor, A. L., Indoleamine 2,3 dioxygenase and metabolic control of immune responses. *Trends in Immunology* **2013,** *34* (3), 137-143.
43. Munn, D. H.; Sharma, M. D.; Baban, B.; Harding, H. P.; Zhang, Y.; Ron, D.; Mellor, A. L., GCN2 Kinase in T Cells Mediates Proliferative Arrest and Anergy Induction in Response to Indoleamine 2,3-Dioxygenase. *Immunity* **2005,** *22* (5), 633-642.
44. Peter, C.; Waldmann, H.; Cobbold, S. P., mTOR signalling and metabolic regulation of T cell differentiation. *Current Opinion in Immunology* **2010,** *22* (5), 655-661.
45. Ninomiya, S.; Nakamura, N.; Kitagawa, J.; Hara, T.; Shimizu, M.; Tsurumi, H., The Roles of Aryl Hydrocarbon Receptor in T Cells at IDO-Positive Tumor Microenvironment. *Blood* **2016,** *128* (22), 3693-3693.
46. Cheong, J. E.; Sun, L., Targeting the IDO1/TDO2–KYN–AhR Pathway for Cancer Immunotherapy – Challenges and Opportunities. *Trends in Pharmacological Sciences* **2018,** *39* (3), 307-325.
47. Van de Velde, L.-A.; Guo, X.-Z. J.; Barbaric, L.; Smith, A. M.; Oguin, T. H., 3rd; Thomas, P. G.; Murray, P. J., Stress Kinase GCN2 Controls the Proliferative Fitness and Trafficking of Cytotoxic T Cells Independent of Environmental Amino Acid Sensing. *Cell reports* **2016,** *17* (9), 2247-2258.
48. Dong, J.; Qiu, H.; Garcia-Barrio, M.; Anderson, J.; Hinnebusch, A. G., Uncharged tRNA Activates GCN2 by Displacing the Protein Kinase Moiety from a Bipartite tRNA-Binding Domain. *Molecular Cell* **2000,** *6* (2), 269-279.
49. Rao, R. V.; Ellerby, H. M.; Bredesen, D. E., Coupling endoplasmic reticulum stress to the cell death program. *Cell Death And Differentiation* **2004,** *11*, 372.
50. Fallarino, F.; Grohmann, U.; You, S.; McGrath, B. C.; Cavener, D. R.; Vacca, C.; Orabona, C.; Bianchi, R.; Belladonna, M. L.; Volpi, C.; Santamaria, P.; Fioretti, M. C.; Puccetti, P., The Combined Effects of Tryptophan Starvation and Tryptophan Catabolites Down-Regulate T Cell Receptor ζ-Chain and Induce a Regulatory Phenotype in Naive T Cells. *The Journal of Immunology* **2006,** *176* (11), 6752-6761.
51. Sharma, M. D.; Baban, B.; Chandler, P.; Hou, D.-Y.; Singh, N.; Yagita, H.; Azuma, M.; Blazar, B. R.; Mellor, A. L.; Munn, D. H., Plasmacytoid dendritic cells from mouse tumor-draining lymph nodes directly activate mature Tregs via indoleamine 2,3-dioxygenase. *The Journal of clinical investigation* **2007,** *117* (9), 2570-2582.
52. Sonner, J. K.; Deumelandt, K.; Ott, M.; Thomé, C. M.; Rauschenbach, K. J.; Schulz, S.; Munteanu, B.; Mohapatra, S.; Adam, I.; Hofer, A.-C.; Feuerer, M.; Opitz, C. A.; Hopf, C.; Wick, W.; Platten, M., The stress kinase GCN2 does not mediate suppression of antitumor T cell responses by tryptophan catabolism in experimental melanomas. *Oncoimmunology* **2016,** *5* (12), e1240858.
53. Costa-Mattioli, M.; Gobert, D.; Harding, H.; Herdy, B.; Azzi, M.; Bruno, M.; Bidinosti, M.; Ben Mamou, C.; Marcinkiewicz, E.; Yoshida, M.; Imataka, H.; Cuello, A. C.; Seidah, N.; Sossin, W.; Lacaille, J.-C.; Ron, D.; Nader, K.; Sonenberg, N., Translational control of hippocampal synaptic plasticity and memory by the eIF2alpha kinase GCN2. *Nature* **2005,** *436* (7054), 1166-1173.

54. Metz, R.; Rust, S.; Duhadaway, J. B.; Mautino, M. R.; Munn, D. H.; Vahanian, N. N.; Link, C. J.; Prendergast, G. C., IDO inhibits a tryptophan sufficiency signal that stimulates mTOR: A novel IDO effector pathway targeted by D-1-methyl-tryptophan. *Oncoimmunology* **2012,** *1* (9), 1460-1468.
55. Johnson, T. S.; Munn, D. H., Host Indoleamine 2,3-Dioxygenase: Contribution to Systemic Acquired Tumor Tolerance. *Immunological Investigations* **2012,** *41* (6-7), 765-797.
56. Chuang, H.-C.; Lan, J.-L.; Chen, D.-Y.; Yang, C.-Y.; Chen, Y.-M.; Li, J.-P.; Huang, C.-Y.; Liu, P.-E.; Wang, X.; Tan, T.-H., The kinase GLK controls autoimmunity and NF-κB signaling by activating the kinase PKC-θ in T cells. *Nature Immunology* **2011,** *12*, 1113.
57. Kim, L. C.; Cook, R. S.; Chen, J., mTORC1 and mTORC2 in cancer and the tumor microenvironment. *Oncogene* **2017,** *36* (16), 2191-2201.
58. Paquette, M.; El-Houjeiri, L.; Pause, A., mTOR Pathways in Cancer and Autophagy. *Cancers* **2018,** *10* (1), 18.
59. Ilagan, E.; Manning, B. D., Emerging role of mTOR in the response to cancer therapeutics. *Trends in cancer* **2016,** *2* (5), 241-251.
60. Moon, Y. W.; Hajjar, J.; Hwu, P.; Naing, A., Targeting the indoleamine 2,3-dioxygenase pathway in cancer. *Journal for Immunotherapy of Cancer* **2015,** *3*, 51.
61. Nguyen, N. T.; Kimura, A.; Nakahama, T.; Chinen, I.; Masuda, K.; Nohara, K.; Fujii-Kuriyama, Y.; Kishimoto, T., Aryl hydrocarbon receptor negatively regulates dendritic cell immunogenicity via a kynurenine-dependent mechanism. *Proceedings of the National Academy of Sciences of the United States of America* **2010,** *107* (46), 19961-19966.
62. Munn, D. H.; Mellor, A. L., Chapter 33 - IDO Pathway: Effect on Foxp3+ Tregs and Cancer. In *Cancer Immunotherapy (Second Edition)*, Prendergast, G. C.; Jaffee, E. M., Eds. Academic Press: San Diego, 2013; pp 583-596.
63. Opitz, C. A.; Litzenburger, U. M.; Sahm, F.; Ott, M.; Tritschler, I.; Trump, S.; Schumacher, T.; Jestaedt, L.; Schrenk, D.; Weller, M.; Jugold, M.; Guillemin, G. J.; Miller, C. L.; Lutz, C.; Radlwimmer, B.; Lehmann, I.; von Deimling, A.; Wick, W.; Platten, M., An endogenous tumour-promoting ligand of the human aryl hydrocarbon receptor. *Nature* **2011,** *478*, 197.
64. Gramatzki, D.; Pantazis, G.; Schittenhelm, J.; Tabatabai, G.; Köhle, C.; Wick, W.; Schwarz, M.; Weller, M.; Tritschler, I., Aryl hydrocarbon receptor inhibition downregulates the TGF-β/Smad pathway in human glioblastoma cells. *Oncogene* **2009,** *28*, 2593.
65. Vacher, S.; Castagnet, P.; Chemlali, W.; Lallemand, F.; Meseure, D.; Pocard, M.; Bieche, I.; Perrot-Applanat, M., High AHR expression in breast tumors correlates with expression of genes from several signaling pathways namely inflammation and endogenous tryptophan metabolism. *PLOS ONE* **2018,** *13* (1), e0190619.
66. Xue, P.; Fu, J.; Zhou, Y., The Aryl Hydrocarbon Receptor and Tumor Immunity. *Frontiers in immunology* **2018,** *9*, 286-286.
67. Murray, I. A.; Patterson, A. D.; Perdew, G. H., Aryl hydrocarbon receptor ligands in cancer: friend and foe. *Nature reviews. Cancer* **2014,** *14* (12), 801-814.

68. Maltepe, E.; Schmidt, J. V.; Baunoch, D.; Bradfield, C. A.; Simon, M. C., Abnormal angiogenesis and responses to glucose and oxygen deprivation in mice lacking the protein ARNT. *Nature* **1997,** *386*, 403.
69. Litzenburger, U. M.; Opitz, C. A.; Sahm, F.; Rauschenbach, K. J.; Trump, S.; Winter, M.; Ott, M.; Ochs, K.; Lutz, C.; Liu, X.; Anastasov, N.; Lehmann, I.; Höfer, T.; von Deimling, A.; Wick, W.; Platten, M., Constitutive IDO expression in human cancer is sustained by an autocrine signaling loop involving IL-6, STAT3 and the AHR. *Oncotarget* **2014,** *5* (4), 1038-1051.
70. Schlezinger Jennifer, J.; Liu, D.; Farago, M.; Seldin David, C.; Belguise, K.; Sonenshein Gail, E.; Sherr David, H., A role for the aryl hydrocarbon receptor in mammary gland tumorigenesis. In *Biological Chemistry*, 2006; Vol. 387, p 1175.
71. Sarkar, S. A.; Wong, R.; Hackl, S. I.; Moua, O.; Gill, R. G.; Wiseman, A.; Davidson, H. W.; Hutton, J. C., Induction of Indoleamine 2,3-Dioxygenase by Interferon-γ in Human Islets. *Diabetes* **2007,** *56* (1), 72-79.
72. Grohmann, U.; Bianchi, R.; Belladonna, M. L.; Silla, S.; Fallarino, F.; Fioretti, M. C.; Puccetti, P., IFN-γ Inhibits Presentation of a Tumor/Self Peptide by CD8α[−] Dendritic Cells Via Potentiation of the CD8α⁺ Subset. *The Journal of Immunology* **2000,** *165* (3), 1357-1363.
73. Mellor, A. L.; Lemos, H.; Huang, L., Indoleamine 2,3-Dioxygenase and Tolerance: Where Are We Now? *Frontiers in Immunology* **2017,** *8* (1360).
74. Muller, A. J.; Sharma, M. D.; Chandler, P. R.; DuHadaway, J. B.; Everhart, M. E.; Johnson, B. A.; Kahler, D. J.; Pihkala, J.; Soler, A. P.; Munn, D. H.; Prendergast, G. C.; Mellor, A. L., Chronic inflammation that facilitates tumor progression creates local immune suppression by inducing indoleamine 2,3 dioxygenase. *Proceedings of the National Academy of Sciences* **2008,** *105* (44), 17073-17078.
75. Braun, D.; Longman, R. S.; Albert, M. L., A two-step induction of indoleamine 2,3 dioxygenase (IDO) activity during dendritic-cell maturation. *Blood* **2005,** *106* (7), 2375-2381.
76. Samelson-Jones, B. J.; Yeh, S.-R., Interactions between Nitric Oxide and Indoleamine 2,3-Dioxygenase. *Biochemistry* **2006,** *45* (28), 8527-8538.
77. Orabona, C.; Pallotta, M. T.; Volpi, C.; Fallarino, F.; Vacca, C.; Bianchi, R.; Belladonna, M. L.; Fioretti, M. C.; Grohmann, U.; Puccetti, P., SOCS3 drives proteasomal degradation of indoleamine 2,3-dioxygenase (IDO) and antagonizes IDO-dependent tolerogenesis. *Proceedings of the National Academy of Sciences of the United States of America* **2008,** *105* (52), 20828-20833.
78. Spranger, S.; Spaapen, R. M.; Zha, Y.; Williams, J.; Meng, Y.; Ha, T. T.; Gajewski, T. F., Up-regulation of PD-L1, IDO, and T(regs) in the melanoma tumor microenvironment is driven by CD8(+) T cells. *Science translational medicine* **2013,** *5* (200), 200ra116-200ra116.
79. Sugimoto, H.; Oda, S.-i.; Otsuki, T.; Hino, T.; Yoshida, T.; Shiro, Y., Crystal structure of human indoleamine 2,3-dioxygenase: Catalytic mechanism of O₂ incorporation by a heme-containing dioxygenase. *Proceedings of the National Academy of Sciences of the United States of America* **2006,** *103* (8), 2611-2616.
80. Dounay, A. B.; Tuttle, J. B.; Verhoest, P. R., Challenges and Opportunities in the Discovery of New Therapeutics Targeting the Kynurenine Pathway. *Journal of Medicinal Chemistry* **2015,** *58* (22), 8762-8782.

81. Basran, J.; Booth, E. S.; Lee, M.; Handa, S.; Raven, E. L., Analysis of Reaction Intermediates in Tryptophan 2,3-Dioxygenase: A Comparison with Indoleamine 2,3-Dioxygenase. *Biochemistry* **2016,** *55* (49), 6743-6750.
82. Srivastava, S., Emerging therapeutic roles for NAD(+) metabolism in mitochondrial and age-related disorders. *Clinical and Translational Medicine* **2016,** *5*, 25.
83. Efimov, I.; Basran, J.; Sun, X.; Chauhan, N.; Chapman, S. K.; Mowat, C. G.; Raven, E. L., The Mechanism of Substrate Inhibition in Human Indoleamine 2,3-Dioxygenase. *Journal of the American Chemical Society* **2012,** *134* (6), 3034-3041.
84. Fang, K.; Dong, G.; Li, Y.; He, S.; Wu, Y.; Wu, S.; Wang, W.; Sheng, C., Discovery of Novel Indoleamine 2,3-Dioxygenase 1 (IDO1) and Histone Deacetylase (HDAC) Dual Inhibitors. *ACS Medicinal Chemistry Letters* **2018,** *9* (4), 312-317.
85. Yang, S.; Li, X.; Hu, F.; Li, Y.; Yang, Y.; Yan, J.; Kuang, C.; Yang, Q., Discovery of Tryptanthrin Derivatives as Potent Inhibitors of Indoleamine 2,3-Dioxygenase with Therapeutic Activity in Lewis Lung Cancer (LLC) Tumor-Bearing Mice. *Journal of Medicinal Chemistry* **2013,** *56* (21), 8321-8331.
86. Cady, S. G.; Sono, M., 1-Methyl-DL-tryptophan, beta-(3-benzofuranyl)-DL-alanine (the oxygen analog of tryptophan), and beta-[3-benzo(b)thienyl]-DL-alanine (the sulfur analog of tryptophan) are competitive inhibitors for indoleamine 2,3-dioxygenase. *Arch Biochem Biophys* **1991,** *291* (2), 326-333.
87. Lewis, H. C.; Chinnadurai, R.; Bosinger, S. E.; Galipeau, J., The IDO inhibitor 1-methyl tryptophan activates the aryl hydrocarbon receptor response in mesenchymal stromal cells. *Oncotarget* **2017,** *8* (54), 91914-91927.
88. Opitz, C. A.; Litzenburger, U. M.; Opitz, U.; Sahm, F.; Ochs, K.; Lutz, C.; Wick, W.; Platten, M., The indoleamine-2,3-dioxygenase (IDO) inhibitor 1-methyl-D-tryptophan upregulates IDO1 in human cancer cells. *PloS one* **2011,** *6* (5), e19823-e19823.
89. Degterev, A.; Huang, Z.; Boyce, M.; Li, Y.; Jagtap, P.; Mizushima, N.; Cuny, G. D.; Mitchison, T. J.; Moskowitz, M. A.; Yuan, J., Chemical inhibitor of nonapoptotic cell death with therapeutic potential for ischemic brain injury. *Nature Chemical Biology* **2005,** *1*, 112.
90. Dolušić, E.; Larrieu, P.; Blanc, S.; Sapunaric, F.; Norberg, B.; Moineaux, L.; Colette, D.; Stroobant, V.; Pilotte, L.; Colau, D.; Ferain, T.; Fraser, G.; Galleni, M.; Frère, J.-M.; Masereel, B.; Van den Eynde, B.; Wouters, J.; Frédérick, R., Indol-2-yl ethanones as novel indoleamine 2,3-dioxygenase (IDO) inhibitors. *Bioorg Med Chem* **2011,** *19* (4), 1550-1561.
91. Ino, K., Indoleamine 2,3-dioxygenase and immune tolerance in ovarian cancer. *Current Opinion in Obstetrics and Gynecology* **2011,** *23* (1), 13-18.
92. Crosignani, S.; Bingham, P.; Bottemanne, P.; Cannelle, H.; Cauwenberghs, S.; Cordonnier, M.; Dalvie, D.; Deroose, F.; Feng, J. L.; Gomes, B.; Greasley, S.; Kaiser, S. E.; Kraus, M.; Négrerie, M.; Maegley, K.; Miller, N.; Murray, B. W.; Schneider, M.; Soloweij, J.; Stewart, A. E.; Tumang, J.; Torti, V. R.; Van Den Eynde, B.; Wythes, M., Discovery of a Novel and Selective Indoleamine 2,3-Dioxygenase (IDO-1) Inhibitor 3-(5-Fluoro-1H-indol-3-yl)pyrrolidine-2,5-dione (EOS200271/PF-06840003) and Its Characterization as a Potential Clinical Candidate. *Journal of Medicinal Chemistry* **2017,** *60* (23), 9617-9629.
93. Coluccia, A.; Passacantilli, S.; Famiglini, V.; Sabatino, M.; Patsilinakos, A.; Ragno, R.; Mazzoccoli, C.; Sisinni, L.; Okuno, A.; Takikawa, O.; Silvestri, R.; La

Regina, G., New Inhibitors of Indoleamine 2,3-Dioxygenase 1: Molecular Modeling Studies, Synthesis, and Biological Evaluation. *Journal of Medicinal Chemistry* **2016,** *59* (21), 9760-9773.
94. Prendergast, G. C.; Malachowski, W. P.; DuHadaway, J. B.; Muller, A. J., Discovery of IDO1 Inhibitors: From Bench to Bedside. *Cancer Research* **2017,** *77* (24), 6795-6811.
95. Röhrig, U. F.; Awad, L.; Grosdidier, A.; Larrieu, P.; Stroobant, V.; Colau, D.; Cerundolo, V.; Simpson, A. J. G.; Vogel, P.; Van den Eynde, B. J.; Zoete, V.; Michielin, O., Rational Design of Indoleamine 2,3-Dioxygenase Inhibitors. *Journal of Medicinal Chemistry* **2010,** *53* (3), 1172-1189.
96. Röhrig, U. F.; Majjigapu, S. R.; Grosdidier, A.; Bron, S.; Stroobant, V.; Pilotte, L.; Colau, D.; Vogel, P.; Van den Eynde, B. J.; Zoete, V.; Michielin, O., Rational Design of 4-Aryl-1,2,3-Triazoles for Indoleamine 2,3-Dioxygenase 1 Inhibition. *Journal of Medicinal Chemistry* **2012,** *55* (11), 5270-5290.
97. Röhrig, U. F.; Majjigapu, S. R.; Chambon, M.; Bron, S.; Pilotte, L.; Colau, D.; Van den Eynde, B. J.; Turcatti, G.; Vogel, P.; Zoete, V.; Michielin, O., Detailed analysis and follow-up studies of a high-throughput screening for indoleamine 2,3-dioxygenase 1 (IDO1) inhibitors. *European Journal of Medicinal Chemistry* **2014,** *84*, 284-301.
98. Röhrig, U. F.; Majjigapu, S. R.; Vogel, P.; Zoete, V.; Michielin, O., Challenges in the Discovery of Indoleamine 2,3-Dioxygenase 1 (IDO1) Inhibitors. *Journal of Medicinal Chemistry* **2015,** *58* (24), 9421-9437.
99. Röhrig, U. F.; Zoete, V.; Michielin, O., The Binding Mode of N-Hydroxyamidines to Indoleamine 2,3-Dioxygenase 1 (IDO1). *Biochemistry* **2017,** *56* (33), 4323-4325.
100. Kumar, S.; Malachowski, W. P.; DuHadaway, J. B.; LaLonde, J. M.; Carroll, P. J.; Jaller, D.; Metz, R.; Prendergast, G. C.; Muller, A. J., Indoleamine 2,3-Dioxygenase Is the Anticancer Target for a Novel Series of Potent Naphthoquinone-Based Inhibitors. *Journal of Medicinal Chemistry* **2008,** *51* (6), 1706-1718.
101. Centko, R. M.; Steinø, A.; Rosell, F. I.; Patrick, B. O.; de Voogd, N.; Mauk, A. G.; Andersen, R. J., Indoleamine 2,3-Dioxygenase Inhibitors Isolated from the Sponge Xestospongia vansoesti: Structure Elucidation, Analogue Synthesis, and Biological Activity. *Organic Letters* **2014,** *16* (24), 6480-6483.
102. Pasceri, R.; Siegel, D.; Ross, D.; Moody, C. J., Aminophenoxazinones as Inhibitors of Indoleamine 2,3-Dioxygenase (IDO). Synthesis of Exfoliazone and Chandrananimycin A. *Journal of Medicinal Chemistry* **2013,** *56* (8), 3310-3317.
103. Sono, M.; Cady, S. G., Enzyme kinetic and spectroscopic studies of inhibitor and effector interactions with indoleamine 2,3-dioxygenase. 1. Norharman and 4-phenylimidazole binding to the enzyme as inhibitors and heme ligands. *Biochemistry* **1989,** *28* (13), 5392-5399.
104. Kumar, S.; Jaller, D.; Patel, B.; LaLonde, J. M.; DuHadaway, J. B.; Malachowski, W. P.; Prendergast, G. C.; Muller, A. J., Structure Based Development of Phenylimidazole-Derived Inhibitors of Indoleamine 2,3-Dioxygenase. *Journal of Medicinal Chemistry* **2008,** *51* (16), 4968-4977.
105. Carr, G.; Chung, M. K. W.; Mauk, A. G.; Andersen, R. J., Synthesis of Indoleamine 2,3-Dioxygenase Inhibitory Analogues of the Sponge Alkaloid Exiguamine A. *Journal of Medicinal Chemistry* **2008,** *51* (9), 2634-2637.

106. Pereira, A.; Vottero, E.; Roberge, M.; Mauk, A. G.; Andersen, R. J., Indoleamine 2,3-Dioxygenase Inhibitors from the Northeastern Pacific Marine Hydroid Garveia annulata. *Journal of Natural Products* **2006,** *69* (10), 1496-1499.
107. Flick, H. E.; Lalonde, J. M.; Malachowski, W. P.; Muller, A. J., The Tumor-Selective Cytotoxic Agent β-Lapachone is a Potent Inhibitor of IDO1. *International journal of tryptophan research : IJTR* **2013,** *6*, 35-45.
108. Bridewell, D. J. A.; Sperry, J.; Smith, J. R.; Kosim-Satyaputra, P.; Ching, L.-M.; Jamie, J. F.; Brimble, M. A., Natural Product-Inspired Pyranonaphthoquinone Inhibitors of Indoleamine 2,3-Dioxygenase-1 (IDO-1)*. *Australian Journal of Chemistry* **2013,** *66* (1), 40-49.
109. Carr, G.; Tay, W.; Bottriell, H.; Andersen, S. K.; Mauk, A. G.; Andersen, R. J., Plectosphaeroic Acids A, B, and C, Indoleamine 2,3-Dioxygenase Inhibitors Produced in Culture by a Marine Isolate of the Fungus Plectosphaerella cucumerina. *Organic Letters* **2009,** *11* (14), 2996-2999.
110. Austin, C. J. D.; Kahlert, J.; Issa, F.; Reed, J. H.; Smith, J. R.; Ioppolo, J. A.; Ong, J. A.; Jamie, J. F.; Hibbs, D.; Rendina, L. M., The first indoleamine-2,3-dioxygenase-1 (IDO1) inhibitors containing carborane. *Dalton Transactions* **2014,** *43* (28), 10719-10724.
111. Carvalho, C.; Siegel, D.; Inman, M.; Xiong, R.; Ross, D.; Moody, C. J., Benzofuranquinones as inhibitors of indoleamine 2,3-dioxygenase (IDO). Synthesis and biological evaluation. *Organic & Biomolecular Chemistry* **2014,** *12* (17), 2663-2674.
112. Tourino, M. C.; de Oliveira, E. M.; Bellé, L. P.; Knebel, F. H.; Albuquerque, R. C.; Dörr, F. A.; Okada, S. S.; Migliorini, S.; Soares, I. S.; Campa, A., Tryptamine and dimethyltryptamine inhibit indoleamine 2,3 dioxygenase and increase the tumor-reactive effect of peripheral blood mononuclear cells. *Cell Biochemistry and Function* **2013,** *31* (5), 361-364.
113. Cheng, M.-F.; Hung, M.-S.; Song, J.-S.; Lin, S.-Y.; Liao, F.-Y.; Wu, M.-H.; Hsiao, W.; Hsieh, C.-L.; Wu, J.-S.; Chao, Y.-S.; Shih, C.; Wu, S.-Y.; Ueng, S.-H., Discovery and structure-activity relationships of phenyl benzenesulfonylhydrazides as novel indoleamine 2,3-dioxygenase inhibitors. *Bioorg Med Chem Lett* **2014,** *24* (15), 3403-3406.
114. Lin, S.-Y.; Yeh, T.-K.; Song, J.-S.; Hung, M.-S.; Cheng, M.-F.; Liao, F.-Y.; Li, A.-S.; Cheng, S.-Y.; Lin, L.-M.; Chiu, C.-H.; Wu, M.-H.; Lin, Y.-J.; Hsiao, W.; Sun, M.; Wang, Y.-H.; Huang, C.-H.; Tang, Y.-C.; Chang, H.-H.; Huang, Z.-T.; Chao, Y.-S.; Shih, C.; Pan, S.-L.; Wu, S.-Y.; Kuo, C.-C.; Ueng, S.-H., 4-Bromophenylhydrazinyl benzenesulfonylphenylureas as indoleamine 2,3-dioxygenase inhibitors with in vivo target inhibition and anti-tumor efficacy. *Bioorganic Chemistry* **2018,** *77*, 600-607.
115. Matsuno, K.; Yamazaki, H.; Isaka, Y.; Takai, K.; Unno, Y.; Ogo, N.; Ishikawa, Y.; Fujii, S.; Takikawa, O.; Asai, A., Novel candesartan derivatives as indoleamine 2,3-dioxygenase inhibitors. *MedChemComm* **2012,** *3* (4), 475-479.
116. Wu, Y.; Xu, T.; Liu, J.; Ding, K.; Xu, J., Structural insights into the binding mechanism of IDO1 with hydroxylamidine based inhibitor INCB14943. *Biochemical and Biophysical Research Communications* **2017,** *487* (2), 339-343.
117. Koblish, H. K.; Hansbury, M. J.; Bowman, K. J.; Yang, G.; Neilan, C. L.; Haley, P. J.; Burn, T. C.; Waeltz, P.; Sparks, R. B.; Yue, E. W.; Combs, A. P.; Scherle, P. A.; Vaddi, K.; Fridman, J. S., Hydroxyamidine Inhibitors of Indoleamine-2,3-dioxygenase

Potently Suppress Systemic Tryptophan Catabolism and the Growth of IDO-Expressing Tumors. *Molecular Cancer Therapeutics* **2010,** *9* (2), 489-498.
118. Yue, E. W.; Douty, B.; Wayland, B.; Bower, M.; Liu, X.; Leffet, L.; Wang, Q.; Bowman, K. J.; Hansbury, M. J.; Liu, C.; Wei, M.; Li, Y.; Wynn, R.; Burn, T. C.; Koblish, H. K.; Fridman, J. S.; Metcalf, B.; Scherle, P. A.; Combs, A. P., Discovery of Potent Competitive Inhibitors of Indoleamine 2,3-Dioxygenase with in Vivo Pharmacodynamic Activity and Efficacy in a Mouse Melanoma Model. *Journal of Medicinal Chemistry* **2009,** *52* (23), 7364-7367.
119. Jochems, C.; Fantini, M.; Fernando, R. I.; Kwilas, A. R.; Donahue, R. N.; Lepone, L. M.; Grenga, I.; Kim, Y.-S.; Brechbiel, M. W.; Gulley, J. L.; Madan, R. A.; Heery, C. R.; Hodge, J. W.; Newton, R.; Schlom, J.; Tsang, K. Y., The IDO1 selective inhibitor epacadostat enhances dendritic cell immunogenicity and lytic ability of tumor antigen-specific T cells. *Oncotarget* **2016,** *7* (25), 37762-37772.
120. Awuah, S. G.; Zheng, Y.-R.; Bruno, P. M.; Hemann, M. T.; Lippard, S. J., A Pt(IV) Pro-drug Preferentially Targets Indoleamine-2,3-dioxygenase, Providing Enhanced Ovarian Cancer Immuno-Chemotherapy. *Journal of the American Chemical Society* **2015,** *137* (47), 14854-14857.
121. Hua, S.; Chen, F.; Xu, G.; Gou, S., Multifunctional platinum(IV) complexes as immunostimulatory agents to promote cancer immunochemotherapy by inhibiting tryptophan-2,3-dioxygenase. *European Journal of Medicinal Chemistry* **2019,** *169*, 29-41.
122. Nakashima, H.; Uto, Y.; Nakata, E.; Nagasawa, H.; Ikkyu, K.; Hiraoka, N.; Nakashima, K.; Sasaki, Y.; Sugimoto, H.; Shiro, Y.; Hashimoto, T.; Okamoto, Y.; Asakawa, Y.; Hori, H., Synthesis and biological activity of 1-methyl-tryptophan-tirapazamine hybrids as hypoxia-targeting indoleamine 2,3-dioxygenase inhibitors. *Bioorg Med Chem* **2008,** *16* (18), 8661-8669.
123. Godin-Ethier, J.; Hanafi, L.-A.; Piccirillo, C. A.; Lapointe, R., Indoleamine 2,3-Dioxygenase Expression in Human Cancers: Clinical and Immunologic Perspectives. *Clinical Cancer Research* **2011,** *17* (22), 6985-6991.
124. Qian, S.; Zhang, M.; Chen, Q.; He, Y.; Wang, W.; Wang, Z., IDO as a drug target for cancer immunotherapy: recent developments in IDO inhibitors discovery. *RSC Advances* **2016,** *6* (9), 7575-7581.
125. Yue, E. W.; Sparks, R.; Polam, P.; Modi, D.; Douty, B.; Wayland, B.; Glass, B.; Takvorian, A.; Glenn, J.; Zhu, W.; Bower, M.; Liu, X.; Leffet, L.; Wang, Q.; Bowman, K. J.; Hansbury, M. J.; Wei, M.; Li, Y.; Wynn, R.; Burn, T. C.; Koblish, H. K.; Fridman, J. S.; Emm, T.; Scherle, P. A.; Metcalf, B.; Combs, A. P., INCB24360 (Epacadostat), a Highly Potent and Selective Indoleamine-2,3-dioxygenase 1 (IDO1) Inhibitor for Immuno-oncology. *ACS Medicinal Chemistry Letters* **2017,** *8* (5), 486-491.
126. Liu, X.; Shin, N.; Koblish, H. K.; Yang, G.; Wang, Q.; Wang, K.; Leffet, L.; Hansbury, M. J.; Thomas, B.; Rupar, M.; Waeltz, P.; Bowman, K. J.; Polam, P.; Sparks, R. B.; Yue, E. W.; Li, Y.; Wynn, R.; Fridman, J. S.; Burn, T. C.; Combs, A. P.; Newton, R. C.; Scherle, P. A., Selective inhibition of IDO1 effectively regulates mediators of antitumor immunity. *Blood* **2010,** *115* (17), 3520-3530.
127. Li, M.; Bolduc, A. R.; Hoda, M. N.; Gamble, D. N.; Dolisca, S.-B.; Bolduc, A. K.; Hoang, K.; Ashley, C.; McCall, D.; Rojiani, A. M.; Maria, B. L.; Rixe, O.; MacDonald, T. J.; Heeger, P. S.; Mellor, A. L.; Munn, D. H.; Johnson, T. S., The indoleamine 2,3-dioxygenase pathway controls complement-dependent enhancement of

chemo-radiation therapy against murine glioblastoma. *Journal for ImmunoTherapy of Cancer* **2014,** *2* (1), 21.
128. Z. H. A. Nayak, R. S., R. Dobbins, L. Marshall, N. N. Vahanian, W. J. Ramsey, E. Kennedy, M. Mautino, C. Link, R. Lin, S. Royer-Joo, K. Morrissey, S. Mahrus, B. McCall, A. Pirzkall, J. E. J. D. H. Munn and S. N. Khleif, European Society for Medical Oncology, 2015; pp 25–29.
129. Iversen, T. Z.; Engell-Noerregaard, L.; Ellebaek, E.; Andersen, R.; Larsen, S. K.; Bjoern, J.; Zeyher, C.; Gouttefangeas, C.; Thomsen, B. M.; Holm, B.; thor Straten, P.; Mellemgaard, A.; Andersen, M. H.; Svane, I. M., Long-lasting Disease Stabilization in the Absence of Toxicity in Metastatic Lung Cancer Patients Vaccinated with an Epitope Derived from Indoleamine 2,3 Dioxygenase. *Clinical Cancer Research* **2014,** *20* (1), 221-232.
130. Kjeldsen, J. W.; Iversen, T. Z.; Noerregaard, L. E.; Mellemgaard, A.; Andersen, M. H.; Svane, I. M., 1326PLong-term follow-up results of stage III-IV non-small-cell lung cancer (NSCLC) patients treated with an epitope derived from Indoleamine 2,3 Dioxygenase (IDO) in a phase I study. *Annals of Oncology* **2017,** *28* (suppl_5), mdx380.028-mdx380.028.
131. Hyun Han, J.; Eun Kwon, Y.; Sohn, J.-H.; Hyun Ryu, D., *A facile method for the rapid and selective deprotection of methoxymethyl (MOM) ethers*. 2010; Vol. 66, p 1673-1677.
132. Isidro-Llobet, A.; Álvarez, M.; Albericio, F., Amino Acid-Protecting Groups. *Chemical Reviews* **2009,** *109* (6), 2455-2504.
133. S Lin, L.; Lanza, T.; E de Laszlo, S.; Truong, Q.; Kamenecka, T.; Hagmann, W., *Deprotection of N-tert-Butoxycarbonyl (Boc) Groups in the Presence of tert-Butyl Esters*. 2000; Vol. 41, p 7013-7016.
134. Curran, T. P.; Pollastri, M. P.; Abelleira, S. M.; Messier, R. J.; McCollum, T. A.; Rowe, C. G., Loss of the tert-butyloxycarbonyl (Boc) protecting group under basic conditions. *Tetrahedron Letters* **1994,** *35* (30), 5409-5412.
135. Ravinder, K.; Reddy, A. V.; Mahesh, K. C.; Narasimhulu, M.; Venkateswarlu, Y., Simple and Selective Removal of the t-Butyloxycarbonyl (Boc) Protecting Group on Indoles, Pyrroles, Indazoles, and Carbolines. *Synthetic Communications* **2007,** *37* (2), 281-287.
136. Neelarapu, R.; Petukhov, P. A., A one-pot selective synthesis of N-Boc protected secondary amines: tandem direct reductive amination/N-Boc protection. *Tetrahedron* **2012,** *68* (35), 7056-7062.
137. Liu, Y.-S.; Zhao, C.; Bergbreiter, D. E.; Romo, D., Simultaneous Deprotection and Purification of BOC-amines Based on Ionic Resin Capture. *The Journal of Organic Chemistry* **1998,** *63* (10), 3471-3473.
138. Jahani, F.; Tajbakhsh, M.; Khaksar, S.; Azizi, M. R., An efficient and highly chemoselective N-Boc protection of amines, amino acids, and peptides under heterogeneous conditions. *Monatshefte für Chemie - Chemical Monthly* **2011,** *142* (10), 1035.
139. Chankeshwara, S. V.; Chakraborti, A. K., Catalyst-Free Chemoselective N-tert-Butyloxycarbonylation of Amines in Water. *Organic Letters* **2006,** *8* (15), 3259-3262.

140. Heydari, A.; Khaksar, S.; Tajbakhsh, M., 1,1,1,3,3,3-Hexafluoroisopropanol: A Recyclable Organocatalyst for N-Boc Protection of Amines. *Synthesis* **2008,** *2008* (19), 3126-3130.
141. Majumdar, S.; De, J.; Chakraborty, A.; Maiti, D. K., General solvent-free highly selective N-tert-butyloxycarbonylation strategy using protic ionic liquid as an efficient catalyst. *RSC Advances* **2014,** *4* (47), 24544-24550.
142. Amira, A.; K'tir, H.; Berredjem, M.; Aouf, N.-E., A simple, rapid, and efficient N-Boc protection of amines under ultrasound irradiation and catalyst-free conditions. *Monatshefte für Chemie - Chemical Monthly* **2014,** *145* (3), 509-515.
143. Varala, R.; Nuvula, S.; Adapa, S. R., Molecular Iodine-Catalyzed Facile Procedure for N-Boc Protection of Amines. *The Journal of Organic Chemistry* **2006,** *71* (21), 8283-8286.
144. López-Soria, J. M.; Pérez, S. J.; Hernández, J. N.; Ramírez, M. A.; Martín, V. S.; Padrón, J. I., A practical, catalytic and selective deprotection of a Boc group in N,N′-diprotected amines using iron(iii)-catalysis. *RSC Advances* **2015,** *5* (9), 6647-6651.
145. Marcantoni, E.; Massaccesi, M.; Torregiani, E.; Bartoli, G.; Bosco, M.; Sambri, L., Selective Deprotection of N-Boc-Protected tert-Butyl Ester Amino Acids by the CeCl3·7H2O−NaI System in Acetonitrile. *The Journal of Organic Chemistry* **2001,** *66* (12), 4430-4432.
146. Subhas Bose, D.; Kiran Kumar, K.; Narsimha Reddy, A. V., A New Protocol for Selective Deprotection of N - tert -Butoxycarbonyl Protective Group (t -Boc) with Sn(OTf)2. *Synthetic Communications* **2003,** *33* (3), 445-450.
147. Nudelman, A.; Bechor, Y.; Falb, E.; Fischer, B.; Wexler, B.; Nudelman, A., Acetyl Chloride—Methanol as a Convenient Reagent for: A) Quantitative Formation of Amine Hydrochlorides, B) Carboxylate Ester Formation, C) Mild Removal of N-Boc-Protective Group. *Synthetic Communications* **1998,** *28*, 471-474.
148. Gibson, F. S.; Bergmeier, S. C.; Rapoport, H., Selective Removal of an N-BOC Protecting Group in the Presence of a tert-Butyl Ester and Other Acid-Sensitive Groups. *The Journal of Organic Chemistry* **1994,** *59* (11), 3216-3218.
149. Han, G.; Tamaki, M.; Hruby, V. J., Fast, efficient and selective deprotection of the tert-butoxycarbonyl (Boc) group using HCl/dioxane (4 m). *The Journal of Peptide Research* **2001,** *58* (4), 338-341.
150. Coffey, D. S.; Hawk, M. K. N.; Ghera, S. J.; Marler, P. G.; Dodson, P. N.; Lytle, M. L., Large Scale Deprotection of a tert-Butoxycarbonyl (Boc) Group Using Aqueous HCl and Acetone. *Organic Process Research & Development* **2004,** *8* (6), 945-947.
151. Li, B.; Berliner, M.; Buzon, R.; Chiu, C. K. F.; Colgan, S. T.; Kaneko, T.; Keene, N.; Kissel, W.; Le, T.; Leeman, K. R.; Marquez, B.; Morris, R.; Newell, L.; Wunderwald, S.; Witt, M.; Weaver, J.; Zhang, Z.; Zhang, Z., Aqueous Phosphoric Acid as a Mild Reagent for Deprotection of tert-Butyl Carbamates, Esters, and Ethers. *The Journal of Organic Chemistry* **2006,** *71* (24), 9045-9050.
152. Li, B.; Bemish, R.; Buzon, R. A.; Chiu, C. K. F.; Colgan, S. T.; Kissel, W.; Le, T.; Leeman, K. R.; Newell, L.; Roth, J., Aqueous phosphoric acid as a mild reagent for deprotection of the t-butoxycarbonyl group. *Tetrahedron Letters* **2003,** *44* (44), 8113-8115.
153. Wang, J.; Liang, Y.-L.; Qu, J., Boiling water-catalyzed neutral and selective N-Boc deprotection. *Chemical Communications* **2009,** (34), 5144-5146.

154. apelqvist, T.; Wensbo, D., Selective removal of the N-BOC protective group using silica gel at low pressure. *Tetrahedron Letters* **1996,** *37* (9), 1471-1472.
155. Pavan Kumar, G.; Rambabu, D.; Basaveswara Rao, M. V.; Pal, M., Iodine-Mediated Neutral and Selective N-Boc Deprotection. *Journal of Chemistry* **2013,** *2013*, 916960.
156. Nadia, K.; Malika, B.; Nawel, K.; Yazid, B. M.; Zine, R.; Aouf, N.-E., Simple and efficient cleavage reaction of the boc group in heterocyclic compounds. *Journal of Heterocyclic Chemistry* **2004,** *41* (1), 57-60.
157. El Kazzouli, S.; Koubachi, J.; Berteina-Raboin, S.; Mouaddib, A.; Guillaumet, G., A mild and selective method for the N-Boc deprotection by sodium carbonate. *Tetrahedron Letters* **2006,** *47* (48), 8575-8577.
158. Tom, N. J.; Simon, W. M.; Frost, H. N.; Ewing, M., Deprotection of a primary Boc group under basic conditions. *Tetrahedron Letters* **2004,** *45* (5), 905-906.
159. Dandepally, S. R.; Williams, A. L., Microwave-assisted N-Boc deprotection under mild basic conditions using K3PO4·H2O in MeOH. *Tetrahedron Letters* **2009,** *50* (9), 1071-1074.
160. Wang, G.; Li, C.; Li, J.; Jia, X., Catalyst-free water-mediated N-Boc deprotection. *Tetrahedron Letters* **2009,** *50* (13), 1438-1440.
161. Li, B.; Li, R.; Dorff, P.; McWilliams, J. C.; Guinn, R. M.; Guinness, S. M.; Han, L.; Wang, K.; Yu, S., Deprotection of N-Boc Groups under Continuous-Flow High-Temperature Conditions. *The Journal of Organic Chemistry* **2019,** *84* (8), 4846-4855.
162. Choy, J.; Jaime-Figueroa, S.; Jiang, L.; Wagner, P., Novel Practical Deprotection of N-Boc Compounds Using Fluorinated Alcohols. *Synthetic Communications* **2008,** *38* (21), 3840-3853.
163. Liu, Z.; Yasuda, N.; Simeone, M.; Reamer, R. A., N-Boc Deprotection and Isolation Method for Water-Soluble Zwitterionic Compounds. *The Journal of Organic Chemistry* **2014,** *79* (23), 11792-11796.
164. Larsen, R. D.; Reamer, R. A.; Corley, E. G.; Davis, P.; Grabowski, E. J. J.; Reider, P. J.; Shinkai, I., A modified Bischler-Napieralski procedure for the synthesis of 3-aryl-3,4-dihydroisoquinolines. *The Journal of Organic Chemistry* **1991,** *56* (21), 6034-6038.
165. Koenig, S. G.; Vandenbossche, C. P.; Zhao, H.; Mousaw, P.; Singh, S. P.; Bakale, R. P., A Facile Deprotection of Secondary Acetamides. *Organic Letters* **2009,** *11* (2), 433-436.
166. Ofori, S.; Awuah, S. G., Small-Molecule Poly(ADP-ribose) Polymerase and PD-L1 Inhibitor Conjugates as Dual-Action Anticancer Agents. *ACS Omega* **2019,** *4* (7), 12584-12597.
167. Flekhter, O. B.; Boreko, E. I.; Nigmatullina, L. R.; Tret'iakova, E. V.; Pavlova, N. I.; Baltina, L. A.; Nikolaeva, S. N.; Savinova, O. V.; Galin, F. Z.; Tolstikov, G. A., [Synthesis and antiviral activity of ureides and carbamates of betulinic acid and its derivatives]. *Bioorg Khim* **2003,** *29* (6), 655-61.
168. Finke, P. E.; Shah, S. K.; Fletcher, D. S.; Ashe, B. M.; Brause, K. A.; Chandler, G. O.; Dellea, P. S.; Hand, K. M.; Maycock, A. L., Orally Active .beta.-Lactam Inhibitors of Human Leukocyte Elastase. 3. Stereospecific Synthesis and Structure-Activity Relationships for 3,3-Dialkylazetidin-2-ones. *Journal of Medicinal Chemistry* **1995,** *38* (13), 2449-2462.

169. Rekker, R. F.; Nauta, W. T., The alkaline hydrolysis of oxazolidinediones-2,4. *Recueil des Travaux Chimiques des Pays-Bas* **1960,** *79* (8), 843-853.
170. Clark-Lewis, J. W., 2,4-Oxazolidinediones. *Chemical Reviews* **1958,** *58* (1), 63-99.
171. Ellames, G. J.; Gibson, J. S.; Herbert, J. M.; McNeill, A. H., The scope and limitations of deuteration mediated by Crabtree's catalyst. *Tetrahedron* **2001,** *57* (46), 9487-9497.
172. Voth, S.; Hollett, J. W.; McCubbin, J. A., Transition-Metal-Free Access to Primary Anilines from Boronic Acids and a Common +NH2 Equivalent. *The Journal of Organic Chemistry* **2015,** *80* (5), 2545-2553.
173. Deb, B.; Debnath, S.; Deb, A.; Maiti, D. K.; Majumdar, S., Copper nanoparticles catalyzed N-H functionalization: An efficient solvent-free N-tert-butyloxycarbonylation strategy. *Tetrahedron Letters* **2017,** *58* (7), 629-633.
174. Du, J.; Chen, J.; Xia, H.; Zhao, Y.; Wang, F.; Liu, H.; Zhou, W.; Wang, B., Commercially Available CuO Catalyzed Hydrogenation of Nitroarenes Using Ammonia Borane as a Hydrogen Source. *ChemCatChem* **2020,** *12* (9), 2426-2430.
175. Azizi, N.; Shirdel, F., Sustainable and chemoselective N-Boc protection of amines in biodegradable deep eutectic solvent. *Monatshefte für Chemie - Chemical Monthly* **2017,** *148* (6), 1069-1074.
176. Rai, R. K.; Mahata, A.; Mukhopadhyay, S.; Gupta, S.; Li, P.-Z.; Nguyen, K. T.; Zhao, Y.; Pathak, B.; Singh, S. K., Room-Temperature Chemoselective Reduction of Nitro Groups Using Non-noble Metal Nanocatalysts in Water. *Inorganic Chemistry* **2014,** *53* (6), 2904-2909.
177. Sarkar, A.; Roy, S. R.; Parikh, N.; Chakraborti, A. K., Nonsolvent Application of Ionic Liquids: Organo-Catalysis by 1-Alkyl-3-methylimidazolium Cation Based Room-Temperature Ionic Liquids for Chemoselective N-tert-Butyloxycarbonylation of Amines and the Influence of the C-2 Hydrogen on Catalytic Efficiency. *The Journal of Organic Chemistry* **2011,** *76* (17), 7132-7140.
178. Egbert, J. D.; Thomsen, E. C.; O'Neill-Slawecki, S. A.; Mans, D. M.; Leitch, D. C.; Edwards, L. J.; Wade, C. E.; Weber, R. S., Development and Scale-up of Continuous Electrocatalytic Hydrogenation of Functionalized Nitro Arenes, Nitriles, and Unsaturated Aldehydes. *Organic Process Research & Development* **2019,** *23* (9), 1803-1812.
179. Kumarasamy, E.; Raghunathan, R.; Kandappa, S. K.; Sreenithya, A.; Jockusch, S.; Sunoj, R. B.; Sivaguru, J., Transposed Paternò–Büchi Reaction. *Journal of the American Chemical Society* **2017,** *139* (2), 655-662.
180. Shuai, Q.; Li, J.; Zhao, F.; Su, W.; Deng, G., Metal-free chemoselective reduction of nitroaromatics to anilines via hydrogen transfer strategy. *Chemical Papers* **2019,** *73* (4), 965-975.
181. Lim, D. S. W.; Lew, T. T. S.; Zhang, Y., Direct Amidation of N-Boc- and N-Cbz-Protected Amines via Rhodium-Catalyzed Coupling of Arylboroxines and Carbamates. *Organic Letters* **2015,** *17* (24), 6054-6057.
182. Liu, L.; Wang, Q.; Liu, Y.; Zhang, X.; Lu, D.; Deng, S.; Gao, Y.; Chen, Y., Copper catalyzed reduction of azides with diboron under mild conditions. *Tetrahedron Letters* **2020,** *61* (14), 151702.
183. Mehndiratta, S.; Lin, M. H.; Wu, Y. W.; Chen, C. H.; Wu, T. Y.; Chuang, K. H.; Chao, M. W.; Chen, Y. Y.; Pan, S. L.; Chen, M. C.; Liou, J. P., N-alkyl-

hydroxybenzoyl anilide hydroxamates as dual inhibitors of HDAC and HSP90, downregulating IFN-γ induced PD-L1 expression. *Eur J Med Chem* **2020,** *185*, 111725.
184. Jiang, S.; Dong, X.; Qiu, Y.; Chen, D.; Wu, X.; Jiang, S., A new ligand for copper-catalyzed amination of aryl halides to primary(hetero)aryl amines. *Tetrahedron Letters* **2020,** *61* (13), 151683.
185. Zhang, D.; Raghavan, N.; Chen, S. Y.; Zhang, H.; Quan, M.; Lecureux, L.; Patrone, L. M.; Lam, P. Y.; Bonacorsi, S. J.; Knabb, R. M.; Skiles, G. L.; He, K., Reductive isoxazole ring opening of the anticoagulant razaxaban is the major metabolic clearance pathway in rats and dogs. *Drug Metab Dispos* **2008,** *36* (2), 303-15.
186. Malpani, Y. R.; Biswas, B. K.; Han, H. S.; Jung, Y.-S.; Han, S. B., Multicomponent Oxidative Trifluoromethylation of Alkynes with Photoredox Catalysis: Synthesis of α-Trifluoromethyl Ketones. *Organic Letters* **2018,** *20* (7), 1693-1697.
187. Ahmad, M. S.; He, H.; Nishina, Y., Selective Hydrogenation by Carbocatalyst: The Role of Radicals. *Organic Letters* **2019,** *21* (20), 8164-8168.
188. Yoon, H.; Lee, Y., Copper-Catalyzed Electrophilic Amination of Heteroarenes via C–H Alumination. *The Journal of Organic Chemistry* **2015,** *80* (20), 10244-10251.
189. Ageshina, A. A.; Sterligov, G. K.; Rzhevskiy, S. A.; Topchiy, M. A.; Chesnokov, G. A.; Gribanov, P. S.; Melnikova, E. K.; Nechaev, M. S.; Asachenko, A. F.; Bermeshev, M. V., Mixed er-NHC/phosphine Pd(ii) complexes and their catalytic activity in the Buchwald–Hartwig reaction under solvent-free conditions. *Dalton Transactions* **2019,** *48* (10), 3447-3452.
190. Hyodo, K.; Hasegawa, G.; Maki, H.; Uchida, K., Deacetylative Amination of Acetyl Arenes and Alkanes with C-C Bond Cleavage. *Org Lett* **2019,** *21* (8), 2818-2822.
191. Liu, Y.; Quan, Z.; He, S.; Zhao, Z.; Wang, J.; Wang, B., Heterogeneous palladium-based catalyst promoted reduction of oximes to amines: using H2 at 1 atm in H2O under mild conditions. *Reaction Chemistry & Engineering* **2019,** *4* (6), 1145-1152.
192. Uvyn, A.; De Coen, R.; Gruijs, M.; Tuk, C. W.; De Vrieze, J.; van Egmond, M.; De Geest, B. G., Efficient Innate Immune Killing of Cancer Cells Triggered by Cell-Surface Anchoring of Multivalent Antibody-Recruiting Polymers. *Angewandte Chemie International Edition* **2019,** *58* (37), 12988-12993.
193. Akine, S.; Onuma, T.; Nabeshima, T., A novel graphite-like stacking structure in a discrete molecule and its molecular recognition behavior. *New Journal of Chemistry* **2018,** *42* (12), 9369-9372.
194. Alano, C. C.; Garnier, P.; Ying, W.; Higashi, Y.; Kauppinen, T. M.; Swanson, R. A., NAD+ depletion is necessary and sufficient for poly(ADP-ribose) polymerase-1-mediated neuronal death. *J Neurosci* **2010,** *30* (8), 2967-2978.
195. Hurtado-Bagès, S.; Knobloch, G.; Ladurner, A. G.; Buschbeck, M., The taming of PARP1 and its impact on NAD+ metabolism. *Molecular Metabolism* **2020,** *38*, 100950.
196. Grant, R. S., Indoleamine 2,3-Dioxygenase Activity Increases NAD+ Production in IFN-γ–Stimulated Human Primary Mononuclear Cells. *International Journal of Tryptophan Research* **2018,** *11*, 1178646917751636.
197. Maleki Vareki, S.; Rytelewski, M.; Figueredo, R.; Chen, D.; Ferguson, P. J.; Vincent, M.; Min, W.; Zheng, X.; Koropatnick, J., Indoleamine 2,3-dioxygenase mediates immune-independent human tumor cell resistance to olaparib, gamma radiation, and cisplatin. *Oncotarget* **2014,** *5* (9), 2778-2791.

198. Kim, J. H.; Reeder, E.; Parkin, S.; Awuah, S. G., Gold(I/III)-Phosphine Complexes as Potent Antiproliferative Agents. *Scientific Reports* **2019,** *9* (1), 12335.

VITA

Place of birth:

San Juan, Trinidad & Tobago

Degrees

Master of Science in Chemistry – University of Kentucky, Lexington KY, May 2021 (expected)

Bachelor of Arts in Chemistry – Grinnell College, Grinnell, IA. May 2015

Professional positions held:

Quality Control Analyst – Catalent Pharma Solutions, Winchester KY. June 2018–May 2019

Chemist I – Piramal Pharma Solutions, Lexington KY. Jan 2021 – Present

Scholastic and professional honors:

Charles H.H. Griffith Outstanding General Chemistry Teaching Assistant Award May 2017

Professional publications:

"Mild deprotection of the N-tert-butyloxycarbonyl (N-Boc) group using oxalyl chloride" **RSC Adv.**, 2020,**10,** 24017-24026

Nathaniel Hugh George